

**A Dynamic Process Model of Palsa Genesis and Development
based on Geomorphologic Investigations at the Boundary Ridge Palsa Bog
near Schefferville, Québec**

David Alan Carlson
Department of Geography
McGill University
Montréal, Québec

A thesis submitted to McGill University
in partial fulfillment of the requirements of the degree of Master of Science
April 2005

Abstract

This original research of seasonal thermodynamic and dynamic geomorphologic processes at the Boundary Ridge palsa bog near Schefferville, Québec reports characteristic differences in heat flow (Q_H), and resulting permafrost mass aggradation/degradation behavior, between a mature-phase palsa (Palsa A) and young-phase palsa (Palsa B). Quantitative analysis of September 1976–August 1977 thermal data indicates how changing palsa material characteristics and bog thermodynamics affect palsa geomorphology.

Q_H patterns for Palsa A show greater amplitude, and shorter active-layer heat loss duration, at its center than along its periphery. Basal active-layer ice aggradation was more evident in Palsa A than Palsa B. Although Palsa A experienced lesser Q_H amplitudes than Palsa B, increased Q_H phase lag resulted in more heat loss and productive ice growth at depth.

Palsas A and B experienced permafrost-zone isothermal conditions just below 0°C for seven to eight months of the year, interrupted only by the winter frost season. The $\sqrt{\lambda \cdot \rho c_p}$ of palsa materials—especially peat, air, and peatland gases— influenced palsa thermodynamics by favoring heat loss during the winter frost season to heat gain during the summer thaw season. This thermodynamic characteristic is important to both young-phase and mature-phase palsa development.

The bog's submerged semi-confining peat layer partitioned hydrologic flow and attenuated Q_H between the overlying unconfined and lower semi-confined water-bearing zones. The peat layer perpetuated isothermal conditions in the lower water-bearing zone throughout the year, which favored

opportunistic frost front advance at depth. Study findings were incorporated into a conceptual model articulating palsa development from the point of antecedent ice nucleation onward and synthesizing key elements of previous conceptual models into a unified explanation of the palsa developmental sequence.

Résumé

Cette étude originale des processus thermodynamiques saisonniers et géomorphologiques dynamiques, conduite au marécage à pases de la chaîne de la Frontière à proximité de Schefferville (Québec) décrit les différences caractéristiques de flux de chaleur (Q_H) entre une palse de phase mature (Palse A) et une palse de phase jeune (Palse B) ainsi que les processus associés de dégradation ou d'aggradation du permafrost. Une analyse quantitative de données thermique de septembre 1976 et août 1977 montre de quelle manière des modifications du matériel ou des caractéristiques thermodynamiques des pases dans le marécage influencent leur géomorphologie.

Les mesures de Q_H dans la couche active à la palse A montrèrent une plus grande amplitude et une plus courte durée de perte de chaleur au centre de la palse plutôt qu'à sa périphérie. L'aggradation de glace basale dans la couche active fut par ailleurs plus évidente à la palse A qu'à la palse B. Bien que la palse A ait subi des amplitudes de Q_H plus faibles que celles subies par la palse B, le décalage de phase du cycle de Q_H y entraîna plus de perte de chaleur et de production de glace en profondeur.

Les pases A et B sont sujettes aux conditions isothermes de la zone de permafrost, à peine inférieures à 0°C pour sept à huit mois de l'année, et interrompues seulement par la période de gel de l'hiver. Le $\sqrt{\lambda \cdot \rho c_p}$ des matériaux de la palse —notamment la tourbe, l'air et les gaz de tourbière— influence les processus thermodynamiques inhérent à la palse en favorisant la perte de chaleur pendant la période de gel de l'hiver et le gain de chaleur

pendant la période de fonte de l'été. Ces caractéristiques thermodynamiques sont déterminantes pour les phases jeunes et matures des pases.

La couche semi-perméable de tourbe, immergée dans le marécage divisé le flux hydraulique et diminue Q_H entre la couche supérieure imperméable et la couche inférieure semi-perméable. La couche de tourbe induit des conditions isothermes dans la partie inférieure de la zone immergée du marécage tout le long de l'année favorisant ainsi l'avancée du front de gel en profondeur. Les résultats de cette étude ont été incorporés dans un modèle conceptuel marquant le début du développement des pases à partir du point précédant la nucléation de la glace et synthétisant les éléments clés empruntés à de précédents modèles en une explication unifiée de la séquence de développement des pases.

Dedication

This thesis is dedicated to my wife, Colleen,
whose deep devotion, boundless patience, and comic relief
were the source and origin of my inspiration.

Acknowledgements

Having spanned over 28 years, this academic odyssey owes much to the many people I came to know along the way. In recognizing and thanking those who inspired, supported, and collaborated in this research effort, my desire is that none are forgotten.

As accomplished teachers, dedicated mentors, and good friends, Drs. Rita M.L. Morris and George Downey kindled the spark in a young student that still burns today. I will be forever indebted to them.

By opening a door to a new world, my former graduate advisor, Frank Nicholson, deserves my sincere gratitude. His early guidance helped formulate the theoretical foundation of this thesis and develop the field techniques applied in this study of geomorphologic process at the Boundary Ridge site.

My deep appreciation goes to my current thesis supervisor, Wayne Pollard, for his persistent belief in this research's worth and his guidance toward final completion. Wayne reviewed and commented on the draft thesis, and suggested the possibility of transient clathrate occurrence under severe winter conditions at Boundary Ridge.

Thanks also to Hardy Granberg and Tim Moore for their ongoing support from the very beginning to today. Hardy offered helpful comments, references, and advice during the data analysis and thesis preparation phases of this research program. Tim provided much appreciated encouragement and insightful advice at key points along my path.

Many at the McGill Subarctic Research Station (MSARS) contributed greatly to this research, but none more than Richard Cossette, field assistant extraordinaire. Richard's innate inquisitiveness, boundless energy, and perpetual optimism, in the face of what at times were dire field conditions, invigorated me and all those who had the honor of knowing him. Merci beaucoup pour toutes les choses, Richard!

All those who resided at MSARS during my tenure there created a unique learning environment and intellectual dynamic rarely experienced, and for which I feel privileged to have shared. During this time, Garry Werren, Rick Wright, Doug Barr, and countless MSARS summer interns assisted with the plant survey, equipment installation, instrument upkeep, and field research program.

I extend my appreciation to those who have provided more recent assistance in completing this thesis. In particular, Mike Przybyla prepared the maps and plans that appear in Chapters 2-4. Thanks also to Nicole Couture for keeping the critical communication channels open and to Hugues Lantuit for the French translation of the thesis abstract.

Saving my dearest cheerleaders for last, the loving encouragement and understanding of my wife and soul mate, Colleen, and our children, Justin, Nicolette, and Zachary freed me to pursue this other love of my life. I am especially thankful to my parents, Joann and Torsten, for instilling in me a persevering nature and work ethic. My sincere gratitude is extended to my in-laws, Trudy and Pacho, for their backing along the way. None of what you read herein would have been possible without my family's unequivocal advocacy over these many years.

Contributions of Co-Authors

In compliance with McGill University requirements, I express my intention to publish both thesis manuscripts (*i.e.*, Chapters 3 and 4) in peer-reviewed technical journals. I attest to the originality of this thesis; to my role as its principal architect, researcher, analyst, and author; and to the contributions of the co-authors as outlined below.

Arguably the largest geomorphologic dataset on palsas ever assembled, this study represents one of the first year-round process investigations completed on palsas. As they relate to palsa genesis and development, the heretofore unrecognized behavior, fate, and transport characteristics of peat and peatland gas—particularly concerning their roles in the new dynamic conceptual model presented herein—constitute original contributions to periglacial geomorphology. The influence that the submerged semi-confining peat layer exerts in controlling seasonal thermodynamic and hydrogeologic flow through wetlands is also an original scientific finding.

Dr. Wayne H. Pollard will be listed as third co-author on Manuscript No. 1 and second co-author on Manuscript No. 2 (*i.e.*, Chapters 3 and 4). Dr. Pollard has reviewed and commented on my thesis outline and draft thesis. He has also suggested the possibility of transient clathrate occurrence under severe winter conditions at the Boundary Ridge site, which is mentioned in Chapter 5 as a future research topic.

It is my intention to include Dr. Frank H. Nicholson, my former advisor, as second co-author for Manuscript No. 1 if he agrees to this proposal. Dr. Nicholson offered me the opportunity to study palsas, helped me develop the theoretical

foundation and field techniques used in this research program, and helped fund my research through various governmental, private, and university grants.

Table of Contents

Abstract.....	i
Résumé.....	iii
Dedication.....	v
Acknowledgements.....	vi
Contributions of Co-Authors.....	viii
Table of Contents.....	x
List of Figures.....	xiii
List of Tables	xiv
List of Equations	xiv
 Chapter 1: Review of Published Palsa Literature and Thesis Research Focus	 1
1.1 Introduction.....	1
1.2 Literature Review	2
1.3 Descriptive Landform Assessments	3
1.31 Morphology.....	4
1.32 Constituent Earth Materials.....	7
1.33 Environmental Factors Influencing Distribution.....	10
1.34 Palsas as Indices of Global Climatic Change.....	13
1.4 Process-Focused Investigations.....	16
1.41 Processes Contributing to Palsa Aggradation.....	16
1.42 Processes Contributing to Palsa Degradation	21
1.5 Conceptual Models of Palsa Development.....	22
1.51 The “Buoyancy” Model	23
1.52 The “Ecocline” Model	24
1.53 The “Snowpack” Model	25
1.6 Data Gap Analysis of Published Research.....	26
1.7 Research Basis, Approach, and Goals.....	28
1.8 Initial Geomorphologic Hypotheses of Palsa Development.....	29

Chapter 2: Boundary Ridge Study Site and Research Methodology	30
2.1 Regional Background and Physical Setting	30
2.2 Regional Geology and Site Hydrogeology	31
2.3 Site Vegetation.....	33
2.4 Boundary Ridge Site as a Representative Palsa Bog.....	35
2.5 Methodology.....	37
2.51 Determination of Palsa Stratigraphy.....	37
2.52 Physical Properties of Palsa Materials	39
2.53 Preliminary Assessment of Peatland Gas Distribution	43
2.54 Temperature Measurements	44
2.6 Methodological Constraints	46
2.7 Research Introduction	49
 Chapter 3: Seasonal Thermodynamic and Dynamic Geomorphologic Processes Operating upon Palsas at Boundary Ridge near Schefferville, Québec	 50
Context in Thesis	50
Abstract.....	50
3.1 Introduction	51
3.2 Physical Setting	51
3.3 Methodology.....	53
3.31 Site Surveys.....	53
3.32 Subsurface Explorations and Sampling.....	54
3.33 Temperature Measurements	56
3.34 Annual Heat Flux Budgets	57
3.35 Heat Flux Budget Error Estimation.....	58
3.4 Results and Discussion.....	59
3.41 Spatial and Temporal Variations in Temperature.....	59
3.42 Palsa A Heat Flux Dynamics.....	65
3.43 Palsa B Heat Flux Dynamics.....	71
3.5 Survey Results	72
3.6 Discussion and Conclusions.....	74
Acknowledgements	77

Chapter 4: A Conceptual Model of Dynamic Geomorphologic Processes Acting on Palsas at Boundary Ridge near Schefferville, Québec	78
Context in Thesis	78
Abstract	79
4.1 Introduction.....	79
4.2 Physical Setting.....	80
4.3 Palsa Material Behavior, Fate, and Transport	82
4.31 Moisture Retention Hysteresis in Peat	83
4.32 Peatland Gas as a Key Palsa Material.....	85
4.33 Interaction of Peat and Peatland Gas in Palsa Development.....	87
4.4 Process-Focused Conceptual Model of Palsa Development	88
4.41 Embryonic Phase	88
4.42 Young Phase.....	92
4.43 Mature/Collapse Phase	94
4.44 Palsa Recurrence.....	96
4.5 Discussion and Conclusions	97
Acknowledgements.....	99
Chapter 5: Research Summary, Thesis Conclusions, and Future Research.....	100
5.1 Introduction.....	100
5.2 Research Summary and Thesis Conclusions.....	101
5.21 Hypothesis No. 1	101
5.22 Hypothesis No. 2	103
5.23 Hypothesis No. 3	106
5.3 Suggested Future Research	108
References	110

List of Figures

Figure 2.1: Boundary Ridge Site Map	30
Figure 2.2: Bedrock Geology Map	32
Figure 2.3: Vegetation Map	34
Figure 2.4: Equipment Installation Plan	45
Figure 3.1: Boundary Ridge Site Map	52
Figure 3.2: Equipment Installation Plan	55
Figure 3.3: Annual temperature variations near the center of Palsa A	60
Figure 3.4: Annual temperature variations near the southern periphery of Palsa A	62
Figure 3.5: Annual temperature variations near the center of Palsa B	63
Figure 3.6: Annual temperature variations at the background bog monitoring location	64
Figure 3.7: Monthly heat flux estimates for the Palsa A central monitoring location	68
Figure 3.8: Monthly heat flux estimates for the Palsa A southern peripheral monitoring location	69
Figure 3.9: Heat flux statistics for the Palsa A central monitoring location	70
Figure 3.10: Heat flux statistics for the Palsa A southern peripheral monitoring location	70
Figure 3.11: Monthly heat flux estimates for the Palsa B monitoring location	72
Figure 3.12: Heat flux statistics for the Palsa B	72
Figure 3.13: Representative survey results for Palsa A and Palsa B	73
Figure 4.1: Boundary Ridge Site Map	81
Figure 4.2: Bedrock Geology Map	82
Figure 4.3: Vegetation Map	83
Figure 4.4: Annual temperature variations at the background bog monitoring location	90
Figure 4.5: Representative survey results for Palsa A and Palsa B	91
Figure 4.6: Equipment Installation Plan	92
Figure 4.7: Monthly heat flux estimates for the Palsa B monitoring location	93

List of Figures (continued)

Figure 4.8: Monthly heat flux estimates for the Palsa A central monitoring location.....	96
Figure 4.9: Monthly heat flux estimates for the Palsa A southern peripheral monitoring location.....	96

List of Tables

Table 2.1: Comparative Summary of Key Climatic Data, Schefferville, Québec.....	36
Table 2.2: Palsa Material Properties.....	40
Table 2.3: Volumetric Fractions of Palsa Materials	41
Table 2.4: Descriptive Statistics for Cables 1–3 Q_H Parameters	47
Table 3.1: Thermal Properties of Palsa Materials.....	56
Table 3.2: Descriptive Statistics for Cables 1–3 Q_H Parameters	58
Table 3.3: Summary of Estimated Heat Flux for Palsa A Central Location.....	66
Table 3.4: Summary of Estimated Heat Flux for Palsa A Southern Periphery	66
Table 3.5: Summary of Estimated Heat Flux for Palsa B	71
Table 4.1: Palsa Material Properties.....	86

List of Equations

Equation 2.1: Effective thermal conductivity formula (unfrozen state)	41
Equation 2.2: Site-specific thermal conductivity of peat calculation	42
Equation 2.3: Effective thermal conductivity formula (frozen state)	42
Equation 2.4: Heat flux density formula	46
Equation 2.5: Heat flux error propagation.....	47
Equation 3.1: Heat flux density formula	57
Equation 3.2: Heat flux error propagation.....	59

Chapter 1:
Review of Published Palsa Literature and Thesis Research Focus

1.1 Introduction

The feedback between observation, experiment, and theory has been a hallmark of periglacial geomorphology. Through field investigations, hypotheses testing, and conceptual model development, the science of periglacial geomorphology has progressively advanced our understanding of geocryological phenomena. In the past, the lack of focus on and the paucity of quantitative analysis on the dynamic interaction between landforms, earth processes, and time in the creation of landscapes have kept periglacial geomorphology from fulfilling its potential as a scientific pursuit. In periglacial geomorphology, no more evident example has epitomized our pursuit of this deeper understanding than research on palsas.

This chapter begins by synthesizing basic literature on palsas and highlighting significant research that inspired this thesis. Chapter 2 presents background information about the Boundary Ridge study site and the methodology used to study the subject palsas and host bog. This overview serves as a springboard for discussing the research findings of this thesis in Chapters 3 and 4. Chapter 3 contains original research on the seasonal thermodynamic and dynamic geomorphologic processes observed during the 12-month term of this study extending from September 1976–August 1978. Based on Chapter 3 findings and ancillary biogeochemical research, Chapter 4 proposes a new conceptual model that unifies key elements of the three existing conceptual models of palsa development into a new geomorphologic process

model. This process model transcends prior models by explaining palsa development from nascent ice nucleation to ultimate landform decline and providing new insights into how palsa-constituent earth material behavior affects palsa development. Chapter 5 summarizes key investigation findings, evaluates this study's hypotheses, and offers suggestions for future geomorphologic and hydrogeologic research.

1.2 Literature Review

The pursuit of understanding palsa genesis, existence, and decline began over 200 years ago with Sveinn Pálsson's landmark observations of "rúst" in Iceland during the late 1700s (Thorarinsson, 1951). Fries and Bergström (1910) are credited with the first reference to "pals", a declension of the now familiar term palsa. With Scandinavian investigators dominating the authorship of early literature, the Lappish term "palsa" gained favor in describing a peat-covered hummock thrust above its surrounding bog or fen environment by an integral frozen core (Seppälä, 1972). Thereafter, the geomorphologic term "palsa" received universal acceptance as the landforms themselves attracted increasing attention from scientists throughout northern Europe, Russia, and eventually North America (Washburn, 1983).

Scientists actively undertook the systematic investigation of palsas as permafrost landforms from the mid-1900s onward (Lundqvist, 1951; Thorarinsson, 1951; Kudryavtsev, 1959; Tyrtikov, 1959). The transition in scientific focus from a preoccupation with what forms palsas take to more recent studies of how earth processes operate within palsas has itself progressed very slowly over the last 50 years. The study of palsas as periglacial landforms in many ways reflects an ongoing philosophical dialogue, which continues today

within geography, geology, and particularly geomorphology as reflected in the writings on palsas.

The discussion of palsa-related research in the following sections is broadly divided into three themes: (a) descriptive landform assessments, (b) process-focused investigations, and (c) conceptual models. By including studies within a certain category, it is acknowledged that the published works may indeed span more than one of these defined themes. For consistency, published works are included in the thematic category that most appropriately reflects the preponderance of scientific findings for each work.

1.3 Descriptive Landform Assessments

Intense economic interest in northern natural resources stimulated scientific and engineering studies seeking to identify and overcome physical obstacles to development. Among the many identified obstacles, the vast presence of wetlands (*i.e.*, variously fens, bogs, and peatlands) and permafrost across the Northern Hemisphere was acknowledged as a serious challenge to northern development (Brown, 1968).

As a conspicuous embodiment of both wetlands and permafrost, palsas soon gained recognition as key indicators not only of permafrost but also of constructability constraints posed by peatlands. Extensive research ensued as a natural outgrowth of the larger international economic interest in the Arctic and Subarctic (MacFarlane, 1959). Existing descriptive landform assessments focused on defining palsa morphology, distribution, and environmental settings; inferring relationships of palsas to other permafrost landforms; and

investigating them as indices of changing climatic conditions throughout the Northern Hemisphere.

1.31 Morphology

The interest in palsas as permafrost indicators began during the 1950s (Lundqvist, 1951; Thorarinsson, 1951; Kudryavtsev, 1959; Tyrtikov, 1959). Considerable effort was put forth to delineate the nature and extent of palsas as the Arctic and Subarctic were viewed as present-day corollaries to mid-latitude Pleistocene landscapes (French, 2003). Peat-covered palsas drew the early interest of investigators due to their predominant occurrence in Scandinavia and Eurasia. Typically recognized as circular mounds in paludal environments, peat-covered palsas were reported to also assume broad plateau, esker-like ridge, string, and complex hybrid forms. Many view palsas as one among various transitional permafrost landforms in a continuum including string bogs, frost hummocks, peat plateaus, and open-system pingos (Rapp and Rudberg, 1960; Salmi, 1970; Wramner, 1973; Jahn, 1976; van Everdingen, 1978; Harris, 1982; van Everdingen, 1982; Pollard and French, 1985; Åkerman and Malmström, 1986; Lagerbäck and Rodhe, 1986; Pollard, 1988, 1991; Zoltai, 1993).

Although the literature chronicles palsas attaining 12 m in overall height and areal dimensions of 500 m² or more, palsas more commonly rise to maximum heights of approximately 3 m above the host bog water table with longitudinal axes less than 10 m in length (Washburn, 1983; Gurney, 2001). The general scientific consensus attributes the elevation gained by palsas to the formation of segregation ice and consequential vaulting of underlying mineral-laden silt/clay sediments that occurs when the permafrost core makes contact

with an underlying sediment substrate (Zoltai and Tarnocai, 1971; Åhman, 1976; Åkerman and Malmström, 1986).

During the 1950s, field studies identified a morphological variant of the archetypical peat-covered palsa: the so-called mineral-cored or minerogenic palsa (Lundqvist, 1953). Svensson (1964), Wramner (1965), and Forsgren (1968) among others also reported alternate palsa forms comprised of predominantly mineral cores. More recently, Åhman (1977) and Seppälä (1980) documented the stratigraphy of mineral-cored palsas while Lagarec (1982) referred to similar landforms as mineral cryogenic mounds. Mineral-cored palsas typically possess a thinner surface peat layer or no peat cover at all and higher concentrations of ice-embedded mineral fines than do traditional peat palsas (Seppälä, 1980).

Several attempts have been made to classify palsas solely based on morphologic characteristics observed during limited field surveys. Apart from the previously mentioned work of Pissart (2003), other proponents have advanced a morphologically based classification scheme for palsas (Salmi, 1972; Åhman, 1977; Allard *et al.*, 1986; Nelson *et al.*, 1992; Eisner *et al.*, 2003). By not appreciating the equifinality of geomorphologic processes, the morphocentric approach risks misinterpretation of field observations when investigators fail to realize that different earth surface processes may manifest in apparently similar landform expressions (Chorley and Kennedy, 1971). By not focusing on palsa geomorphologic processes, these studies lacked a genetic basis to warrant any claim to distinguish these so-called mineral-cored palsas from peat-covered palsas, which too contain mineral-embedded permafrost cores.

To make matters worse, such investigations typically have occurred during clement summer field seasons thereby ignoring key geomorphologic

events, introducing recurrent observational bias, and amplifying the potential for erroneous conclusions. To illustrate this point, Outcalt *et al.* (1986) and Nelson *et al.* (1992) advocated to categorize as palsas certain apparently similar anthropogenic landforms studied in Alaska during brief summer field seasons. From these accounts, it is readily apparent that the landforms discussed by Outcalt *et al.* and Nelson *et al.* resulted from distinctly different earth surface processes than those observed in palsas. Unfortunately, support for this morphocentric view gained high-profile acceptance in the scientific community (Washburn, 1983). In actuality, the landforms described by Nelson *et al.* and Outcalt *et al.* are most probably frost mounds or frost blisters similar to those observed elsewhere by periglacial geomorphologists who correctly identified them as frost blisters (Salvigsen, 1977; van Everdingen, 1978, 1982; Pollard and French, 1983, 1984; Åkerman and Malmström, 1986; Pollard, 1988, 1991; Pollard and van Everdingen, 1992).

The continuing myopic focus with form over process in palsa studies lead to premature proposals first by Harris (1993) and later others (Pissart, 2000, 2002; Delisle *et al.*, 2003) for the adoption of the term “lithalsa” to differentiate these landforms on a morphologic basis from typical peat-covered palsas. Such proposals are arbitrary without the support of long-term studies of the underlying geomorphologic processes central to landform development. Antithetical to the advancement of our understanding of genetic periglacial processes, the morphocentric approach has: (a) inappropriately deflected attention away from a correctly balanced form-and-process systems approach to the study of palsas, (b) inadvertently introduced subjectivity into the classification of palsas as distinct landforms, and (c) ultimately belied the critical

underlying geomorphologic processes that affect palsa emergence, existence, and decline.

1.32 Constituent Earth Materials

The classic palsa exhibits an upper peat layer ranging in thickness from less than 1 m to over 7 m of fibrous, mesic, and/or aquatic peat, corresponding to the thickness of peat in the host bog (Brown, 1973). Given its unique temporally dependent properties and behavior in subarctic bog environments, peat has long been identified as a key palsa material, which helps to modulate thermal fluxes through embryonic palsas and, with the passage of time and loss of fabric integrity, serves to hinder further palsa aggradation ultimately leading to palsa decline. As Chapter 4 of this thesis demonstrates, peat's subtly eccentric qualities when interacting with other key palsa materials play a much more pronounced role in palsa genesis, development, decline, and recurrence than heretofore appreciated.

Active layer thicknesses in palsas generally vary between 0.5–1 m depending on location (Brown, 1968). The presence of aggradation ice in the active layer and segregation ice lenses at depth within archetypical peat-covered and variant mineral-cored palsas is a defining trait. Aggradation ice results from the seasonal freezing of meteoric precipitation (*i.e.*, snowmelt and rainfall) that accumulates within the active layer of palsas and regelation at the base of the active layer. This suprapermafrost ice becomes deposited in annually layers as much as 40 cm thick (Allard and Rousseau, 1999).

Harris (1989) suggests that suprapermafrost ice aggrading from snowmelt and rainfall migrating under the influence of thermal gradients and gravity

contributes more to the overall growth of palsas and other ice mounds than subsurface ice growth. Field studies by Seppälä (1982) indicate that segregation ice involving the migration of groundwater under the influence of thermal gradients (*i.e.*, cryosuction) exerts a primary control over palsa growth, particularly when primary and secondary heaving of underlying sediments occurs. Based on the current consensus, aggradation ice and segregation ice both exert significant influence over the course of palsa development.

Below the active layer, scientists have reported laminar segregation ice lenses from 1–2 cm to as much as 10–15 cm thick within peat-covered palsas (Zoltai and Tarnocai, 1971; Seppälä, 1976; Åhman, 1977). Investigators have observed palsas underlain by up to 8 m of segregation ice and 2 m or more of ice-impregnated mineral sediment substrate consisting of silt, sand, and/or till (White *et al.*, 1969; Brown and Kupsch, 1974). Oriented perpendicular to the advancing freezing front, segregation ice crystals interlace to form horizontal ice lenses interconnected with roughly 5–10 mm thick ice lamellae (Forsgren, 1968; Salmi, 1970). As palsas develop, stresses and strains within the landforms result in ice lens fractures, intrusion of groundwater, and *in situ* freezing of ice veins along fracture surfaces (Åkerman, 1982).

Mineral-cored palsas have shown evidence of a reticulate system of intrusive ice lens/vein complexes containing varying ice and mineral content within their structure that varies with depth (Zoltai and Tarnocai, 1975; Åhman, 1976; Delisle *et al.*, 2003). Reports of ice lens stratigraphy in peat palsas compared to mineral-cored palsas have documented that impure inclusions occur within both forms, although mineral-cored palsas may consist almost exclusively of

mineral silt and sediment with less evident ice lamellae in contrast to what is often observed in classic peat-covered palsas (Washburn, 1983).

The nature and spatial geometry of permafrost in palsas is one of the least investigated of palsa features. Based on this available information, investigators presumed that permafrost extended directly beneath those areas where surface probing indicated its presence (Špolanskaya and Evseyev, 1973). As more field investigations ensued, a clearer view of how ice aggrades in peatlands, bogs, and fens became known (Salmi, 1970; Jahn, 1976). Near-surface permafrost in palsa fields closely mirrors local ground surface contours (Zoltai and Tarnocai, 1975; Seppälä, 1980). Moving deeper below the ground surface, the permafrost boundary surface has been interpolated by most investigators as spherical or ovoid in shape; however, judging from the limited subsurface explorations depicted in these studies, few have confirmed the actual extent of permafrost at depth (Lagerbäck and Rodhe, 1986).

Where palsa-constituent permafrost meets the adjoining seasonally frozen bog layer, which is submerged for a time before completely melting at the periphery of palsas, investigators have reported permafrost boundaries that curve away from the palsa at some angle (P'yavchenko, 1955; Jahn, 1976; Blyakharchuk and Sulerzhitsky, 1999). Other investigators have reported ice lenses varying in shape from biconvex to downwardly concave ice masses having “mushroom-shaped” morphologies with bases comprised of pure ice strata, ice-rich silt/clay sediments, and/or glacial till (Svensson, 1970; Zoltai and Tarnocai, 1971; Sollid and Sørbel, 1974). Once making contact with the

underlying substrate, palsa-constituent permafrost is often shown to fuse with basal permafrost present within the mineral sediment layer (Zoltai and Tarnocai, 1971).

The composition of the mineral sediments beneath palsas reflects not only the native geologic formations from which they eroded but also the poorly drained and reductive bog environments under which they were deposited. Typically the fine-textured and sometimes mottled sediments include silts, clays, and silt/clay intercalations displaying a grey, bluish, or greenish cast indicative of the ferrous, dolomitic, or siliceous rock formations from which these sedimentary beds originated. The elevated interstitial porosity and low effective porosity characteristic of these underlying clay- and silt-bearing sediments afford optimal conditions for primary and secondary ice heaving which contributes significantly to palsa upheaval during aggradation (Taber, 1929; Beskow, 1935; Tsyтовich, 1963; Solov'ev, 1973).

1.33 Environmental Factors Influencing Distribution

Palsas have been reported widely dispersed throughout the Arctic and Subarctic primarily within the discontinuous permafrost zone and, to a lesser degree, in the southern continuous permafrost zone. Extensive field assays in the discontinuous permafrost zone have documented palsas across northern regions of Eurasia in Japan (Takahashi and Sone, 1988), Russia (Baranov, 1959; Špolanskaya and Evseyev, 1973; Makeev and Keržentsev, 1974; Jahn, 1976), Finland (Seppälä, 1972; Luoto and Seppälä, 2002, 2003), Sweden (Forsgren, 1968; Åkerman and Malmström, 1986; Lagerbäck and Rodhe, 1986; Zuidhoff and Kolstrup, 2000), Norway (Sollid and Sørbel, 1974; Åhman, 1976; Matthews *et al.*, 1997), and Iceland (Thorarinsson, 1951; Friedman *et al.*, 1971). In North America,

palsa studies have been most extensive in Canada (Wenner, 1947; Allington, 1961; Brown, 1968; Zoltai, 1971; Brown, 1975; Zoltai and Tarnocai, 1975; Payette *et al.*, 1976; Cummings and Pollard, 1989, 1990; Doolittle *et al.*, 1992) and, to a lesser degree, the United States (Brown and Péwé, 1973; Péwé, 1975; Washburn, 1979; Collins *et al.*, 1984). An inextricable link between peat (or organic soil) covered palsas and their host bogs or fens emerges from the literature showing that palsas generally congregate in palsa fields comprised of many individual landforms occasionally exhibiting the entire geomorphologic sequence (Svensson, 1986).

Recognized as a necessary precursor to the advent of environmental conditions suitable for palsas, the Pleistocene glaciation eroded geologic formations, disrupted ecosystems, redistributed earth materials, deranged drainage systems, affected regional climate, and helped create circumstances amenable for permafrost aggradation. Glaciation, local geology, ecology, and climate —particularly spatial and temporal variations in snow cover— exercise an overarching influence on palsa occurrence within Northern landscapes (Fries and Bergström, 1910; Zoltai and Tarnocai, 1971; Brown, 1973; Seppälä, 1990, 1994). Pleistocene glaciation exerted pronounced effects on Subarctic landscapes in general and the paludification of the Schefferville area in particular.

Present within glaciated areas with positive water balances, palsas may be found in ombrotrophic bog or minerotrophic fen environments where low hydraulic gradients, impermeable substrates, topographic convergence, and local climate perpetuate the build-up of significant peat-bearing overburden deposits (Hustich, 1957). Precipitation maintains water and nutrient throughputs in ombrotrophic bogs while groundwater migrates through minerotrophic fens,

respectively, to sustain local paludal ecosystems and to create environments conducive to palsa development (Price and Waddington, 2000).

Despite its obvious importance, very little attention has been focused on how the hydrogeology of bog or fen environments affects palsa development. The influence that local hydrogeology may exert to modulate the effects of other environmental factors has been largely overlooked by periglacial scientists with the exception of brief references in the literature which note its potential value in helping to explain the thermodynamics occurring in peatland environments (Romanov, 1968; Moore, 1987; Thorhallsdottir, 1994).

As essential to palsa occurrence as the linkage to bog and fen systems are the microclimatic factors that effectively control palsa genesis, existence, decline, and recurrence. Lundqvist (1961) first established that palsas in Sweden occur at locations where ambient air temperatures for 200 days a year remain below 0 °C and precipitation between April and November is less than 300 mm. Other Scandinavian investigators suggest that a -1 °C mean annual ambient air temperature is a more typical criterion for palsa development (Sollid and Sørbel, 1974; Åhman, 1977; Seppälä, 1986). In North America, palsa occurrence has been established to closely correlate with the 0 °C mean annual air isotherm and precipitation (Brown, 1963, 1968). Seasonal changes in the magnitude and timing of snowfall, snowmelt, rainfall, and evapotranspiration have long been viewed as critical to overall palsa development (Fries and Bergström, 1910; White *et al.*, 1969; Zoltai and Tarnocai, 1971).

Building on significant research identifying snow accumulation as a permafrost-limiting factor (Granberg, 1973; Nicholson, 1976), Seppälä has pioneered the investigation of palsa geomorphology by systematically

establishing how changing snow cover conditions over palsa fields have a pronounced effect not only on palsa occurrence but also on the entire palsa geomorphologic sequence (Seppälä, 1972, 1982, 1986, 2003). Seppälä has also hypothesized that wind turbulence induced by the development of a single palsa may cause unevenness in the nearby snowpack surface and spawn an entire palsa field (Seppälä, 1986). Further investigations of the palsa developmental sequence have identified wind abrasion as a contributing factor to palsa degradation (Seppälä, 2003).

Palsa fields tend to occur in areas where minimal local snowpack thicknesses exist, thereby maximizing localized seasonal frost penetration (Seppälä, 1982). Snowpack thickness is initially controlled by local topography, which affects near-surface wind flow patterns and helps propagate conditions optimal to palsa genesis and development beyond the leeward snow deposition zone and within areas subject to more pronounced wind scour (Granberg, 2004). As palsas advance through their developmental sequences, incremental micro-scale changes in snowpack accumulations through time at first serve to enhance heat loss and consequential frost penetration at individual palsa sites as they aggrade. Later as palsa degradation ensues, increasing snowpack accumulations gradually impede heat loss thereby limiting frost penetration and contributing to a progression of processes that ultimately lead to palsa decline (Seppälä, 1994).

1.34 Palsas as Indices of Global Climatic Change

Past investigations have reported palsas existing within the southern continuous permafrost zone of Siberia (Gorbunov, 1969), Svalbard (Salvigsen, 1977), and the Canadian Arctic archipelago (Brown, 1973; Blake, 1974). However, the coincident occurrence of palsas with the distal limit of the discontinuous permafrost zone in

the Northern Hemisphere initially stimulated academic interest in this periglacial landform as an indicator of the southern limit of permafrost (Brown, 1973). Since this region is where ground temperatures at the depth of zero annual amplitude remain very close to the 0°C isotherm, palsas have long been viewed as readily apparent indices of global climatic change.

As physical expressions of permafrost occurrence, palsas have been monitored to gain insight into short- and long-term fluctuations in global climate. Canadian researchers have reported that permafrost at its southernmost margin exists mainly in peatlands at temperatures very near the melting point; inferring from these observations that permafrost in these locations may be transient, aggrading and degrading in response to fluctuating climatic or earth surface conditions (Gold *et al.*, 1972). Entering mid-1990s climatic data and site-specific palsa-constituent data into a mathematical model, other investigators predicted that palsa aggradation could indeed occur under then existing environmental conditions (An and Allard, 1995).

In Sweden, researchers have monitored palsas to assess episodic permafrost expansion during a warming trend that occurred in the late 1980s (Kullman, 1989; Nihlén, 2000). Russian scientists have attempted to correlate the Holocene pollen stratigraphic record at a palsa site in western Siberia to historic climatic events (Blyakharchuk and Sulerzhitsky, 1999). Other investigations in Norway have concluded that palsas are sensitive to climatic change as well as anthropogenic impacts (Sollid and Sørbel, 1998). Regional thermal amelioration observed in Sweden has been linked to a 1–1.5 °C rise in mean annual air temperature rise believed to have resulted in an approximate 50% decline in the

areal expansion of palsas and a general trend toward palsa degradation (Zuidhoff and Kolstrup, 2000; Zuidhoff, 2002).

Although it has become popular to view palsas as indices of global climatic change, it is important to note that palsa fields often contain individual landforms at varying stages of development and therefore must be held suspect as unqualified climatic indicators (Svensson, 1986). The inference of a direct linkage between palsa aggradation or degradation and climatic fluctuations may be overly simplistic since palsas naturally respond to a complex array of seasonally variable environmental factors such as water table fluctuations, affecting more transient earth material behavioral characteristics (Svensson, 1970; Friedman *et al.*, 1971; Nihlén, 2000; Coultish and Lewkowicz, 2003).

From this perspective, palsas likely respond more to cumulative shifts in a set of key environmental factors above or below critical threshold levels than to isolated fluctuations in any single variable. Under this scenario, palsas in close proximity may aggrade and degrade in response to the same climatic conditions (Kershaw, 2003). Especially in the absence of long-term year-round assessments, an emphasis on the importance of climatic parameters to the exclusion of other environmental and earth material influences risks arrival at misleading conclusions. Long-term thermal assessments are essential to a comprehensive evaluation of how regional climate affects palsa aggradation and degradation trends. Near-term local microclimatic variables coupled with site-specific earth material behavioral characteristics and earth surface processes probably mask the true effects of longer-duration climatic changes.

1.4 Process-Focused Investigations

Building upon the experimental findings and theoretical precepts established by Taber (1930), Beskow (1935), and Carslaw and Jaeger (1947; 1947), the advent of process-focused investigations in palsa geomorphology began in the 1950s as a natural outgrowth of earlier descriptive landform assessments. Inspired by the quantitative systems approach to geomorphology advocated by Strahler (1954) and others, the academic shift toward process-oriented field investigations strove to quantify the temporally and spatially dependent geomorphologic parameters elemental to evolving palsa landform systems.

Pursuing synergistic lines of scientific inquiry, Russian scientists pioneered experimental field studies measuring thermal, physical, and chemical variability in permafrost environments (Baženova, 1953; Kudryavtsev, 1959; Švetsov, 1959). Early Scandinavian process studies applied this general systems knowledge and shifted attention toward investigations of year-round heat flow through palsas. These field investigations were marked by the first use outside Russia of intrusive techniques to acquire subaerial and subsurface temperature data at remote palsa field locations (Lindqvist and Mattsson, 1965). In particular, early investigators explored how seasonal variations in environmental factors interacted with one another to affect temporally and spatially dependent changes during palsa development.

1.41 Processes Contributing to Palsa Aggradation

The transition of palsas through emergence, aggradation, and decline is driven by heat flow. Heat flow is affected greatly by the transient changes in palsa materials, not the least of which is the temporal and spatial variability of snow

cover within bog and fen environments. This subsection discusses those aggradational processes that have been systematically evaluated through quantitative field experiments.

In a landmark investigation in northern Norway, Lindqvist and Mattsson (1965) installed eight temperature-sensing thermistor assemblies at various locations and depths within a 3.6-m high palsa. Ranging in depths from 0.1–4.0 m, individual thermistors measured temperature variations within the palsa on a weekly basis from October 1964 through September 1965. Lindqvist and Mattsson documented significant geomorphologic findings on how heat flow and earth materials behave in palsas.

Based on analyses of temperature variations within the shallow palsa horizons, investigation findings concluded that the active layer was an effective thermal barrier due to the insulating qualities of peat and the pronounced heat consumption capacity (*i.e.*, specific heat capacity) afforded by melting ice as the active layer advanced to its maximum depth. Given the elevated heat capacity of ice and ephemeral nature of warm season temperatures in subarctic and arctic settings, the advancement of the seasonal thaw boundary within the active layer has been shown to progress at an ever-declining rate approximating the square root of time (Jahn and Walker, 1983).

Other researchers reported isothermal temperatures near 0 °C at depths below 2 m and temperatures ranging between -0.4 °C to -1.2 °C at depths below 4 m within palsas (Lindqvist and Mattsson, 1965; Delisle and Allard, 2003). Dissipating as the active layer refroze during the late fall/early winter, release of latent heat was identified as a significant factor affecting the overall annual

thermal regime of palsas. Investigation results also found a strong correlation between shallow snow accumulations and elevated heat loss across the entire palsa.

The first process-focused study conducted in Canada involved the systematic assessment of ground and air temperature measurements at the Mer Bleue peat bog in southern Ontario (Williams, 1968). This study is particularly notable in that Williams analyzed year-round meteorological and subsurface temperature data in light of temporal changes in the bog-constituent earth materials to help identify key factors influencing the thermal characteristics of paludal ecosystems.

Comparing a lowland vegetated bog with adjacent exposed sand ridges, Williams found that near-surface heat exchange, soil thermal properties, and snow depth and density were predominant controls on subsurface temperature variations between the two locations. Prolonged saturated bog conditions were shown to efficiently dissipate heat primarily through advection and evaporation within the active layer thereby remaining cooler than the adjacent permeable sand ridges, which absorbed increasing heat loads through radiation and convection as exposed mineral soil became dry.

Williams also acknowledged how the higher latent heat of fusion contributed to the preservation of subsurface frost within saturated peat-covered areas due to the slower rate of observed active layer thaw under identical heat exchange conditions. Cold air drainage into the bog accounted for monthly and annual ground surface temperatures several degrees cooler than abutting ridge locations. These findings were corroborated later by Svensson (1970; 1986), and Špolanskaya and Evseyev (1973) who cited similar microclimatic controls on

palsa landform development. A multi-year study of diurnal fluctuations in the thermal regime at various fen sites near Schefferville, Québec also emphasized the combined influences of snow cover, peat-related thermal properties, and microclimatic factors in helping control temperature regimes within peatland environments (Moore, 1987).

Year-round thermal studies at three field sites in northern Sweden assessed how variations in the apparent thermal diffusivities of palsa materials affected heat transfer behavior in two peat-covered palsas and a mineral-cored palsa (Westin and Zuidhoff, 2001; Zuidhoff, 2003). Investigation findings demonstrated that peat-covered palsas experienced less pronounced heat fluxes throughout the year compared to the sparsely-vegetated mineral-cored palsa. Differences in the persistence of snow cover and apparent thermal diffusivities of the exposed earth materials covering the landforms (*i.e.*, peat versus sparsely vegetated surficial layers) explained the continued persistence of peat-covered palsas and degradation of mineral-cored palsas in the study area.

These findings confirm the results of the pioneering year-round field investigations of palsas conducted in Finland (Seppälä, 1976, 1980, 1982, 1990, 1994, 2003). Seppälä undertook in 1990 the first systematic study to determine the relationship between snow depth, snow density, and frost penetration as it pertains to palsa emergence and aggradation (Seppälä, 1990). Investigation findings confirmed earlier intuitive indications identifying snow depth as a key factor limiting palsa development.

Seppälä further established during this work that the physical and thermal characteristics of the snowpack are also important determinants of heat flow within palsa fields. Resulting from wind-driven consolidation and

deflation, spatial variability in snow density within the palsa field reached maximum values of 0.42 over palsas, twice the densities observed in other portions of the bog. Investigation findings also identified the presence of high-density snow thicknesses less than 30 cm during the mid-winter thermal minima as an optimal condition for ice lens growth leading to palsa inception.

Seppälä's research suggested that thicker low-density snow accumulations along the palsa perimeter deterred ice lens growth there. Deflation of the snowpack at critical times during the frost season was therefore shown to help control the growth of segregation ice in palsa fields. From 1976–1979, experimental study of palsa aggradational processes dramatically demonstrated how deliberate removal, and later addition, of snow cover during the winter resulted in palsa inception and decline within a 5-m² test plot (Seppälä, 1982, 2003). An assessment conducted in central Sweden at the southernmost permafrost limit confirmed Seppälä's conclusions about the importance of seasonally thinning snow cover as a controlling factor in palsa aggradation (Nihlén, 2000).

Mathematical modeling conducted by Canadian researchers using data collected from northern Québec remains the sole quantitative investigation of the ice segregation process in palsas (An and Allard, 1995). This modeling study found that ice segregation occurring over a 60-year period could produce a 3-m high palsa under prevailing conditions existing during the 1990s. After this growth phase, ice was predicted to segregate along the basal ice interface at a declining rate due to the limiting effect of heat flux attenuation at depth within aggrading palsas.

More recent studies at a site in northwestern Québec investigated the underlying geomorphologic processes controlling palsa development (Delisle and Allard, 2003). Study findings document the isothermal nature of the palsa permafrost core. Ice protrusions and groundwater intrusions near the adjacent water body were believed to result from preferential groundwater flow and convective heat transfer under a local hydraulic gradient at the base of the permafrost zone. Although sub-atmospheric pressures at the 10.55 m level were attributed to cryosuction, the study concluded that ice segregation was not a significant ice-forming process.

1.42 Processes Contributing to Palsa Degradation

Few quantitative assessments of palsa degradational processes have been published largely due to the difficulty in measuring quantifiable changes in the geomorphologic processes themselves. Of those quantitative studies that have appeared in the literature, the process-focused research of Seppälä and Zuidhoff is most prominent (Seppälä, 1976, 1982; Zuidhoff and Kolstrup, 2000; Luoto and Seppälä, 2002; Zuidhoff, 2002; Luoto and Seppälä, 2003; Seppälä, 2003; Zuidhoff, 2003).

Degradational processes affecting palsas can appear at the outset of palsa emergence as in the case of the development of micro-fissures within surficial peat due to winter-induced desiccation (Salmi, 1970; Sollid and Sørbel, 1974; Seppälä, 1982). As palsa development progresses, thermokarst erosion along surficial fissures increases as the fissures widen resulting in heightened heat flow during summer months and diminished heat loss during winter months due to increased snow deposition within the fissures (Luoto and Seppälä, 2003; Wetzel *et al.*, 2003).

Studying palsas in western Finnish Lapland, Seppälä observed that wind-driven snow and ice crystals abraded the surficial peat layer of palsas (Seppälä, 2003). Ablation of surficial peat through continued winter wind scour has been inferred to become an increasingly important growth control as palsas gained elevation throughout their development.

Thermokarst erosion has long been recognized as an important degradational process leading to palsa decline (Kachurin, 1959; Martynov, 1959; Lindqvist and Mattsson, 1965; Åhman, 1976). This process is pronounced within surficial fissures that transect palsas as well as along palsa peripheries where it leads to calving or block erosion (Salmi, 1972; Seppälä, 1976, 1982, 1986). As erosion continues, circular thermokarst ponds have been reported to develop where palsas previously existed (Svensson, 1969; Sollid and Sørbel, 1974; Luoto and Seppälä, 2003). By mapping and statistically analyzing existing and former palsa sites in northern Finland, Luoto and Seppälä (2003) have reported an increased incidence of thermokarst occurrence believed to be in response to environmental conditions unfavorable to palsa development.

Given the comparative absence of process-focused investigations, the advancement of our understanding of palsas as landform systems has been delayed by the lack of long-term year-round geomorphologic process research. It is crucial that future research redirect its focus on how geomorphologic form and process operate within landform systems to create and destroy palsas over time.

1.5 Conceptual Models of Palsa Development

Three primary conceptual models have been presented in the literature to explain how palsas emerge as they do within bog and fen environments. These

conceptual models can be variously labeled as the “buoyancy” hypothesis, the “ecocline” hypothesis, and the “snowpack” hypothesis. Although they differ as to which incipient geomorphologic processes are considered significant to palsa nascency, all three conceptual models generally agree on young- and mature-phase geomorphologic processes affecting continued palsa development and eventual decline through time. Since the mature-phase geomorphologic processes have already been presented in prior sections, this discussion will focus on the young-phase processes identified by conceptual model proponents.

1.51 The “Buoyancy” Model

The “buoyancy” conceptual model has been offered by a number of investigators to explain palsa emergence and development (Kershaw and Gill, 1979; Allard *et al.*, 1986; Nelson *et al.*, 1992). Proposing a “floating” ice lens as the incipient precursor to full-fledged palsa development, Nelson *et al.* (1992) have viewed the formation of pore ice in the shallow horizon of highly porous peat beds as the initial condition from which palsas form. Following development of the low-density pore ice core, opportunistic enrichment of the growing ice mass is predominantly afforded by continued ice segregation through cryosuction (Taber, 1929, 1930). Although not stated outright, Nelson *et al.* also implied that gas bubbles apparent in segregation ice cores of nascent palsas could help further lower bulk ice density and thereby enhance overall buoyancy.

Other researchers investigating palsa formations in the Yukon Territory have elaborated on the “buoyancy” conceptual model by measuring electrical resistivity at various depths within segregation ice cores collected from palsas “floating” in a 5-m deep bog (Harris and Nyrose, 1992). Field observations noted that the buoyant palsa permafrost cores: (1) consisted of interstitial ice resulting

from *in situ* freezing of fen surface water, (2) separated from underlying unfrozen peat and fen water strata during summer months, (3) indicated the same moisture transfer processes occur in both peat-covered peat and mineral-cored palsas, and (4) were overlain by a relatively dry peat layer supporting hydrophobic *Cladina*, *Ericaceae*, and *Betula* species. The authors ascribed significance to the presence of a 2-m thick peat layer reaching a height of 40 cm above the bog water table as a critical initial condition permitting the commencement of palsa formation at this site.

1.52 The “Ecocline” Model

Following up on the similar but independently published hypotheses of Lundqvist (1961) and Sjörs (1961), Canadian botanists first proposed the “ecocline” conceptual model as an outgrowth of their research on plant community evolution in northern Ontario (Railton and Sparling, 1973). These researchers systematically assessed how changing plant ecology influenced permafrost occurrence in palsas by correlating the effects of plant succession with temporal changes in palsa surface albedo as palsas passed through the developmental sequence. Investigation findings established that: (1) a linkage exists between moss, lichen, and bare peat covers as palsas aggrade and degrade; (2) plant succession directly controls the surface albedo, the insulating peat layer’s thermal characteristics, and heat flux amplitudes through palsas over time; and (3) palsas develop continuously under current environmental conditions and are not relic landforms. Rönkkö and Seppälä (2003) refuted these conclusions based on studies in northern Finland.

Research following a similar line of inquiry inferred that the distribution of wooded palsas and a mineral-cored palsa closely correlated with subarctic

mid-taiga and forest-tundra ecological communities, respectively (Payette *et al.*, 1976). The presence of a less than 20-cm thick moss-peat layer was determined to cause palsa inception by ameliorating summer heat flow at the distal limit of permafrost in southern Norway (Matthews *et al.*, 1997). Following up on his important earlier research, Zoltai (1993) has also linked palsa genesis, development, and decline to plant succession and forest fire incidence in northwestern Alberta.

1.53 The “Snowpack” Model

As discussed previously, the connection between temporal and spatial snowpack variability and palsa occurrence has long been recognized (Fries and Bergström, 1910). Local topography, wind direction, and winter wind scour have been shown to create variations in snowpack thickness in bog and fen environments. No periglacial scientist has dedicated more effort to exploring the intricacies of the linkage between snow cover and palsa genesis than Seppälä (1982; 1986; 1990; 1994).

In paludal settings where snow deposition is minimized and/or snowpack deflation is maximized, heat flow through near-surface peat strata facilitates ice growth during optimal winter conditions. Once exposed above the bog water table, the insulating effect of peat is improved through continued drying thus enabling ice lenses to persist under suitable microclimatic conditions.

Established nascent palsas have been suspected to progressively disrupt near-surface wind flow patterns and snow deposition, thereby helping to change the spatial distribution of snow cover that further engenders the development of entire palsa fields. Serving to limit lateral palsa aggradation later in the palsa developmental sequence, thicker accumulations of snow cover along palsa

peripheries are seen as yet another reflection of the pronounced role this temporally variable exogenic earth material imposes on palsa development. As palsas degrade, snow's insulating qualities contribute to palsa decline by helping limit winter heat loss, which ultimately results in accelerated thermokarst erosion and eventual palsa decline.

1.6 Data Gap Analysis of Published Research

Based on the foregoing review of existing palsa research, the study of palsa geomorphology should be redirected toward more detailed quantitative investigations of what is happening within and around palsas to affect their continued development. To achieve this objective, renewed efforts toward the year-round study of the exogenic and endogenic earth processes are required. As with all science, productive advances in periglacial geomorphology result more through carefully selecting the focus of key scientific research than by choosing investigatory methods, by improving the accuracy of measurements and predictions, and most certainly by avoiding inconsequential nomenclatural debate. This review of currently published palsa literature has identified several significant data gaps in our collective understanding of palsas as follows:

- Excluding passing references to the presence of air and/or gas in palsa-constituent permafrost, no research has been published that recognizes peatland gases as key agents in palsa geomorphology. Chapters 3 and 4 discuss the vital role that peatland gases are believed to play in palsa development.
- Existing periglacial research has not investigated how the hydrogeology of palsa bog and fen systems affects control over the course of palsa genesis and

development. When viewed in a hydrogeologic context, palsas develop in bogs and fens, which are unique in that they are aerobic water-bearing strata overlaying anaerobic water-bearing strata separated by a semi-confining peat layer. Chapters 3 and 4 discuss how this coupled aerobic/anaerobic surface water system may affect palsa geomorphology.

- Of the three currently published conceptual models of the palsa developmental sequence, none fully explain how endogenous processes initiate ice growth—as the necessary precursor to palsa emergence—in one location versus another. Chapter 4 will present a more detailed account of the endogenous processes influencing ice nucleation in palsa systems.
- The existing literature on palsas has not fully recognized the role equifinality plays in geomorphologic process-response systems. This prevailing condition underscores the need for long-term year-round study of permafrost landforms to avoid misinterpreting unrelated landforms as palsas due to a preoccupation with morphology and futile nomenclatural debate at the expense of a more complete understanding of key underlying geomorphologic processes. Chapters 3 and 4 show how geomorphologic form and process interact as palsas proceed through the developmental sequence.
- Existing research has not adequately delved into the complexities of palsa geomorphologic systems. This thesis attempts to assess the dynamic nature of geomorphologic processes, earth material behaviors, and the resulting feedback/response systems that are central to palsa emergence, development, decline, and recurrence. In this regard, Chapter 5 offers suggestions for future research.

1.7 Research Basis, Approach, and Goals

This thesis presents the scientific findings of original research, which was conducted between June 1976 and January 1978, and focused on a multi-faceted investigation of palsa geomorphology. This thesis concentrates on how palsas develop by investigating the classical elements of geomorphology —earth materials, earth processes, and time— at an upland bog representative of palsa bogs in the vicinity of Schefferville, Québec. The research approach developed for this thesis draws upon many related fields of pure and applied science including geography, physics, geology, engineering, soil science, botany, geochemistry, and hydrogeology. The goal of this study is to investigate the central elements of palsa geomorphology from a process-focused systematic perspective.

Toward this overarching objective, the research presented in Chapter 3 assessed: (1) the character and behavior of palsa materials (*i.e.*, peat, water, ice, methane, and air), (2) the underlying physical and biogeochemical processes affecting heat transfer within palsas, (3) how earth materials and processes within palsas interact, and (4) how these earth materials and processes change over time to cumulatively affect the evolution of palsa geomorphologic systems near Schefferville, Québec. Based on these original research findings and pertinent pre-existing research, Chapter 4 formulates a predictive conceptual model that helps explain why and how palsas develop, and helps predict where and when palsas are likely to emerge, develop, decline, and recur in the uplands surrounding Schefferville, Québec.

1.8 Initial Geomorphologic Hypotheses of Palsa Development

To fulfill the research goals outlined above, the research methods implemented during execution of this thesis test three hypotheses. Conceived with the intent of advancing the science of periglacial geomorphology beyond the bounds of prior investigations, the hypotheses that drive this research include:

- Hypothesis No. 1 – Palsa heat budget estimates are indices of whether palsas are aggrading or degrading in the vicinity of Schefferville, Québec;
- Hypothesis No. 2 – Near-surface thermal patterns in palsas vary as palsas progress through the developmental sequence based on the transient behavioral characteristics of palsa materials; and
- Hypothesis No. 3 – The submerged peat layer in bogs affects thermodynamic and hydrogeologic flow thereby facilitating permafrost aggradation and preserving permafrost mass in palsas.

The above noted hypotheses form the bases for the research premise and methodology presented in Chapter 2, and the research results and conclusions discussed in Chapters 3 and 4. Chapter 5 presents research findings, which test each of the above noted hypotheses in consideration of the adequacy of supporting data, and offers ideas for future scientific investigations.

Chapter 2:

Boundary Ridge Study Site and Research Methodology

2.1 Regional Background and Physical Setting

Directly abutting the Québec-Newfoundland provincial border roughly 12 kilometers west-northwest of Schefferville, Québec, the Boundary Ridge study site (the “site”) is a ± 0.8 -ha palsa bog where three palsas at varying developmental phases occur within a perched basin (see Figure 2.1). Situated near the transition between sporadic to widespread discontinuous permafrost zones in northern Québec, the site’s geographical coordinates are 55° 3’ 12”N, 67° 15’ 18”W. Resting at the foot of Boundary Ridge’s talus-covered southwestern slope, the site lies at an elevation of 800 m ASL with local topography gradually sloping southwesterly toward the Howells River valley.

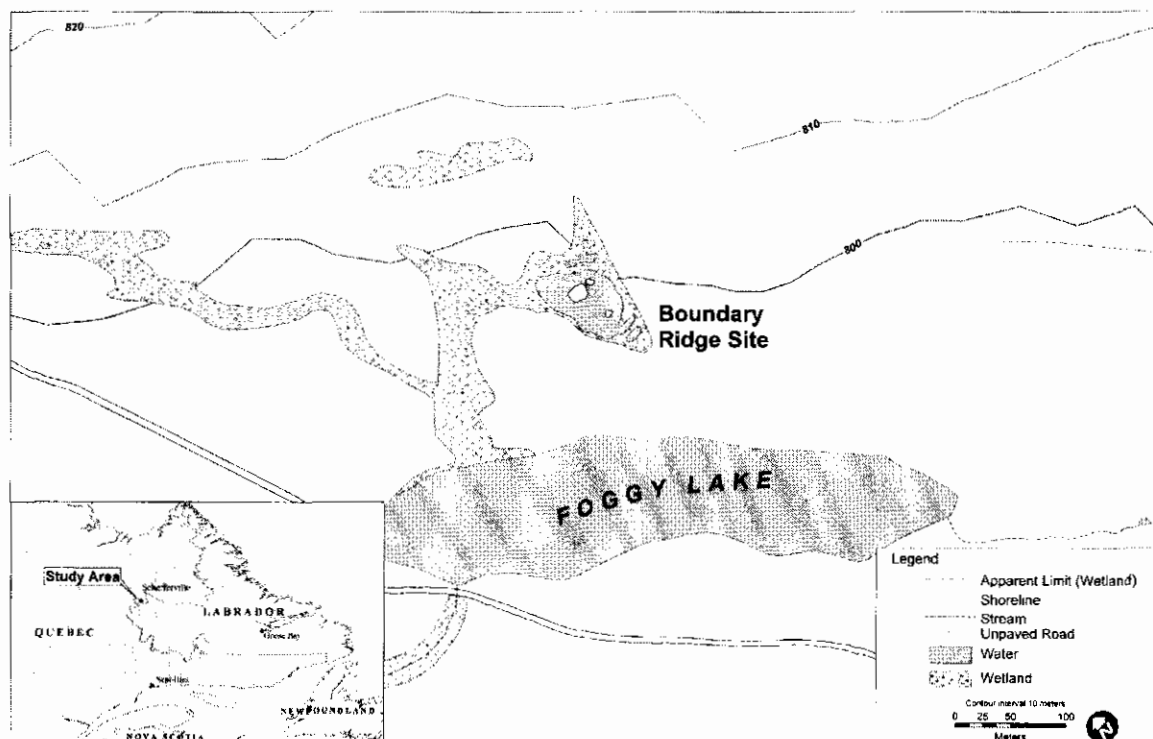


Figure 2.1. Boundary Ridge Site Map. (Contours derived from Shuttle Radar Topography Mission data provided by USGS) [Drafted by M. Przybyla]

2.2 Regional Geology and Site Hydrogeology

Traversing the Labrador-Ungava Peninsula along a northwest-southeast axis, the Labrador geosyncline consists of a 700-mile long belt of Precambrian metamorphosed sedimentary deposits left during Proterozoic period from 2500 to 570 million years ago (Zajac, 1974; Krishnan, 1976). The geologic record of the Schefferville region reflects several Precambrian unconformities indicating extended periods of erosion. One such period created the Sub-Huronian surface that was subsequently folded downward to form the Labrador Trough. After receiving Proterozoic deposits, the resulting beds within the Labrador Trough were further deformed, uplifted, and again subjected to peneplanation before the onset of the Paleozoic era. The Labrador-Ungava Peninsula experienced major uplift and deformation during the late Cenozoic era producing sub-parallel fault systems within the extensively folded northwest-southeasterly trending ridge-valley complexes characteristic of the Schefferville region.

Inferred from the lack of glacial deposition near Schefferville, Québec, the ice dispersal zone of the Labrador-Ungava lobe deranged the regional drainage network as the Pleistocene glaciation advanced and left a widespread wetland dominated landscape after the ice shield receded ± 6000 years BP. Relic meltwater channels are the principal geologic artifacts evident near Schefferville, Québec. Following Pleistocene glaciation, the central Labrador-Ungava Peninsula is believed to have experienced more widespread periglacial activity than at present.

The remnants of past geologic deformation, uplift, and erosion are evident at and in the vicinity of the site. A contact fault between the Lower

Slate and Denault Dolomite formations underlies the Boundary Ridge palsa bog and bisects the site along a north-northwest/south-southeasterly strike (see Figure 2.2, Bedrock Geology Map). Two additional roughly parallel contact faults exist between the Fleming Chert Breccia and Denault Dolomite formations, lying roughly 300 m hydrologically upgradient at the crest of

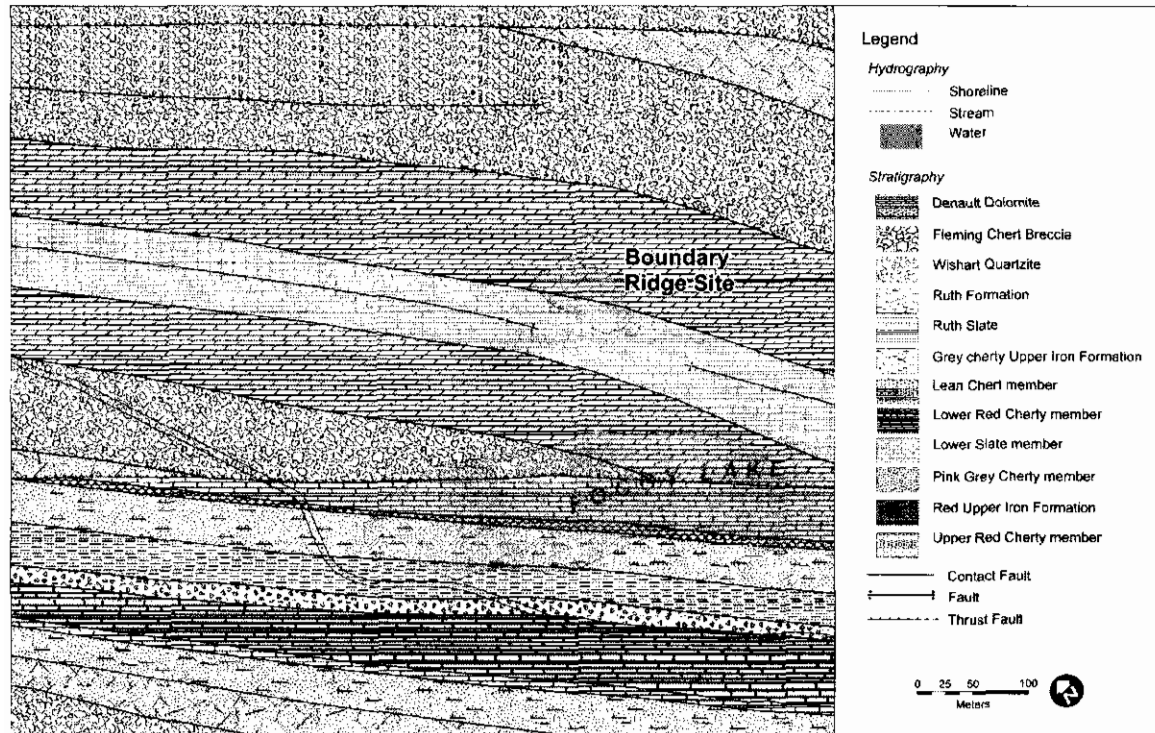


Figure 2.2. Bedrock Geology Map. (Reeves, 1972; Neimant-Verdriet and Krishnamurty, 1973). [Drafted by M. Przybyla]

Boundary Ridge and downgradient of the site halfway to Foggy Lake. A divergent fault along the limestone facie skirts the western margin of the palsa bog (Reeves, 1972; Neimant-Verdriet and Krishnamurty, 1973).

The Boundary Ridge bog is characterized by hydrogeologic system flow occurring both above and below the semi-confining *Sphagnum*/sedge peat layer and the seasonal frost layer during different times of the year. Rainfall and snow/ice meltwater contribute oxygenated water through the

upper aerobic bog while anoxic mineral-laden groundwater likely flows through the lower semi-confined bog as a result of an underlying contact fault between the Lower Slate member (Ruth Formation) and the Denault Dolomite.

Discharging to Foggy Lake, the inferred southerly surface water/ groundwater flow direction across the site is affected by the seasonal frost, semi-confining peat layer, permafrost, and bedrock controls of the northwest-southeasterly trending raised valley within which the perched Boundary Ridge palsa bog is located. The dominant *Sphagnum* moss community surrounding the palsa bog acidifies surface water and groundwater migrating through the site. The resulting wetland ecosystem has evolved into a predominantly acidophilic plant community.

2.3 Site Vegetation

Lying between Foggy Lake to the southwest and Boundary Ridge to the northeast in Labrador, the Boundary Ridge site rests at the base of Boundary Ridge's southerly facing slope. Five palsas reside in the bog at varying points along the developmental sequence, flanked by a string bog to the northeast and ephemeral frost hummocks to the east. Both the string bog and hummocks are located within a *Sphagnum* moss community that surrounds the palsa bog (see Figure 2.3, Vegetation Map). Dwarf birch-willow-spruce complexes lie beyond the *Sphagnum* moss beds north and east of the site while a lichen-dwarf birch-spruce complex lies to the west. High- and low-density sedge communities including some reed plants exist within the bog itself, nearly encircling all five palsas. Weathered fibrous peat covers the majority of the exposed palsa surfaces with lichen and *Sphagnum* moss existing along the palsa peripheries.

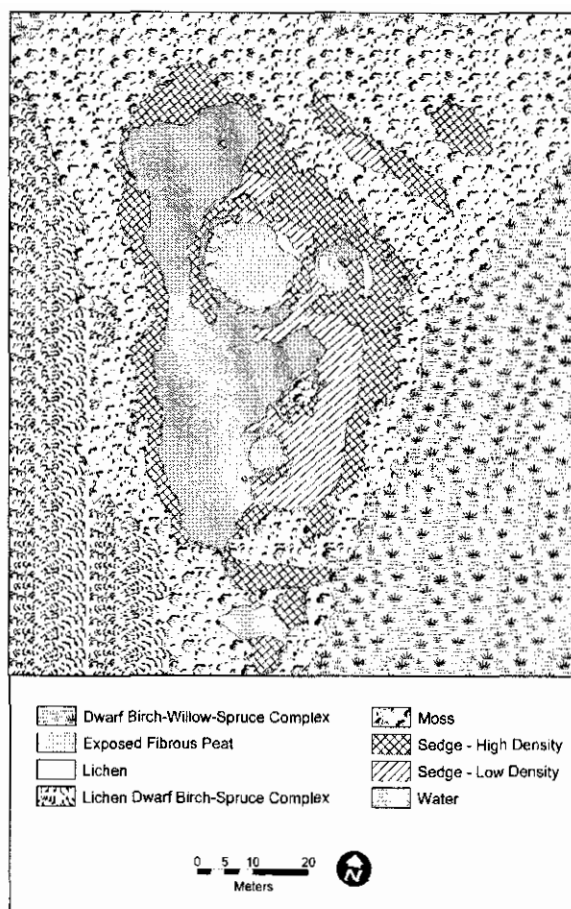


Figure 2.3. Vegetation Map. (from color infrared aerial photography). [Drafted by M. Przybyla]

The sedge, reed, and moss communities at the site have contributed to the deposition of sequential layers of vegetative debris creating an interlocking mat reaching a thickness of up to 1.25 m of fibrous, mesic, and saturated peat beneath existing vegetation and open water. In the northern portion of the bog, the peat layer thins to roughly 0.5 m and the overlying water correspondingly deepens in a thermokarst depression where one or more palsas were present at one time. The base of the peat layer across the bog floats up to

approximately 0.75 m above the silt/clay substrate and weathered bedrock, which underlie the entire palsa bog. This characteristic of bogs in the Schefferville, Québec region is quite evident since the peat mats undulate under the weight of pedestrian traffic.

Trapped in numerous pockets beneath the tightly-woven floating peat mat across the site, peatland gas has been generated as the site's sedges, reeds, and *Sphagnum* mosses together with insect carcasses and other biological detritus undergo methanogenic decomposition before becoming peat deposits. The resulting peatland gas accumulates in pockets that have been observed in bogs throughout the Schefferville, Québec area. By

measuring the duration of off-gas emissions after penetrating submerged peat mats with a 1.5-cm diameter hollow metal pipe, volumetric estimates of peatland gas accumulations at the site were estimated to range between a few cm^3 to $\pm 0.8 \text{ m}^3$ at various locations.

2.4 Boundary Ridge Site as a Representative Palsa Bog

Trends in key climatological parameters were compared to determine the degree to which the September 1976–August 1977 term of study is representative of the 1955–1980 time period. Given that this thesis assesses annualized heat flux within the Boundary Ridge palsas, no attempt is made to evaluate or present detailed short-duration climatic data.

Table 2.1 compares September 1976–August 1977 and 1955–1980 climatic parameters. The monthly temperature maxima for the short- and long-term datasets both occurred in July, while the monthly minima were observed in January. The mean monthly temperatures for both datasets closely agree. The monthly rainfall maxima for the short- and long-term datasets occurred in August 1977 and July 1975, respectively, while monthly rainfall minima were reported in November and October, respectively. The difference between the monthly mean rainfall values for the two periods is insignificant. Monthly snowfall maxima for the short- and long-term datasets show a significant difference, although the maximum snowfall events for both periods occurred in April 1976 and April 1975, respectively. Monthly snowfall minima are identical for both time periods, while monthly mean snowfall values for the 1976–1977 and 1955–1980 periods generally correspond.

Table 2.1: Comparative Summary of Key Climatic Data, Schefferville, Québec

Parameter	1955-1980 ¹	1976-1977 ¹
Temperature (°C)		
Monthly maxima	14.4	13.9
Monthly minima	-30.1	-24.5
Monthly mean	-4.9	-4.8
Rainfall (mm)		
Monthly maxima	177.8	168.2
Monthly minima	1.8	0.1
Monthly mean	33.9	33.4
Snowfall (mm) ²		
Monthly maxima	143.5	102.9
Monthly minima	0.1	0.1
Monthly mean	31.5	40.6

Notes: ¹ Data compiled by McGill University personnel (Barr and Wright, 1981).

² Snowfall data are listed as water equivalents.

The observed trends in these key data generally agree with the climatological data trends evident in the more extensive 1948–1990 meteorological database (Environment Canada, 1990). Based on the historic climatic data compiled for the Schefferville, Québec (A) Meteorological Station, the September 1976–August 1977 term of study at the Boundary Ridge site is representative of long-term climatic conditions existing in the Schefferville, Québec area.

During the initial thesis planning phase, an inventory of palsa bogs surrounding Schefferville, Québec was conducted to determine the optimal research site location. Site selection criteria included palsa bogs that: (a) contained palsas in different stages of landform development, (b) displayed an archetypical morphology, (c) remained largely undisturbed, (d) located in a typical upland setting, and (e) were accessible year-round by truck, snowmobile, or skis. This qualitative assessment concluded that the palsa field at the Boundary Ridge site best satisfied the selection criteria and was a suitably representative palsa research location.

2.5 Methodology

The goals of this thesis are to conduct original research investigating the dynamic nature of earth surface processes and earth materials affecting palsa landform systems in the vicinity of Schefferville, Québec and to formulate a conceptual model providing new insights into the palsa geomorphologic sequence within the broader context of existing periglacial research on this subject. To achieve these overarching objectives, field techniques and analytical methods were employed to implement a holistic study of the various physical and chemical factors playing central roles in palsa geomorphology. This section provides a summary of the methodology selected for this research, which will be discussed in greater detail in the following chapters.

2.51 Determination of Palsa Stratigraphy

Subsurface explorations of palsa stratigraphy were completed from June–November 1976 immediately before the installation of five thermistor cable assemblies at the Boundary Ridge site. Using a 3.18-cm diameter carbide-tipped stainless steel hand auger, each borehole was manually advanced to maximum depths of 2.6 m below ground surface (bgs). Auger refusal occurred at all five locations at depths where highly consolidated frozen silt- and clay-containing sediments existed.

Three of the five borehole locations were situated on two palsas; two boreholes being advanced within a $\pm 171\text{-m}^2$ palsa (one near its center; the other at its southern margin) characteristic of the mature developmental phase located in the north-central portion of the bog (Palsa A) and another borehole

at a $\pm 32\text{-m}^2$ palsa representative of a young developmental phase located in the southern portion of the Boundary Ridge bog (Palsa B) as shown on Figure 2.1. A third $\pm 25\text{-m}^2$ palsa situated in the eastern portion of the bog (Palsa C) was not cored since it was: (1) previously disturbed by foot traffic, (2) covered by a wooden plank providing entry and egress to Palsa A, and (3) not suitable for this research.

Raised ± 0.9 m above the surrounding bog, Palsa A displayed a stratigraphic profile, which included weathered fibrous peat within an active layer extending from $\pm 0\text{--}0.5$ m bgs, peat intercalations decreasing with depth within peatland gas-containing permafrost from $\pm 0.5\text{--}1.05$ m bgs, and peatland gas-containing ice from $\pm 1.05\text{--}2.6$ m bgs until refusal. At the depth of refusal, frozen bluish-green to grey silt/clay sediments indicative of the site's native ferrous and dolomitic bedrock formations were encountered.

Palsa B rose ± 0.6 m above the surrounding bog. Its stratigraphic profile included less weathered fibrous peat within an active layer present from $0\text{--}0.55$ m bgs, peat intercalations decreasing abruptly with depth within peatland gas-containing permafrost from $\pm 0.55\text{--}0.75$ m bgs, and peatland gas-containing ice from $\pm 0.75\text{--}1.6$ m bgs. Similarly at the 2.4 depth of refusal, frozen bluish-green to grey silt/clay sediments were encountered.

Two additional boreholes were advanced before installing thermistor cable assemblies in the ephemeral frost hummocky terrain along the eastern bog margin (ref. Cable 4) and in the bog itself (ref. Cable 5). The stratigraphy observed during the Cable 4 installation included moss-covered mesic peat from $\pm 0\text{--}0.15$ m bgs, saturated peat from $\pm 0.15\text{--}1.95$ m bgs before encountering refusal at the silt/clay interface. Serving as both the background

data point and a backup temperature gauge, Cable 5 was anchored into the bog sediments and partially submerged in the bog from 0–1.5 m leaving 0.5 m (and one thermistor) exposed above the bog surface to collect ambient air and near-surface snow temperature measurements.

Samples were collected continuously from auger flights as boreholes were advanced at each thermistor cable location. Palsa-constituent samples were placed in 25-cc stainless steel containers before being preserved on ice in an insulated cooler during transport to McGill Subarctic Research Laboratory. Undisturbed peat samples were also collected at the site for laboratory examination of key physical characteristics including bulk density, thermal conductivity, and volumetric specific heat.

2.52 Physical Properties of Palsa Materials

The physical characteristics of palsa materials were compiled by testing site-specific samples and using published data sources. Volumetric fractions of solid (peat), aqueous (water), and gaseous (peatland gas and air) phases were determined by gravimetric methods. Thermal conductivity (λ), specific heat (ρc_p), latent heat (L_f), thermal diffusivity (α), and thermal inertia ($\sqrt{\lambda \cdot \rho c_p}$) data were also obtained.

λ is a measure of the ability of media to conduct heat. Measured in watts per meter per degree Kelvin ($\text{W m}^{-1} \text{K}^{-1}$), λ describes a material's ability to conduct heat due to molecular motion (Carslaw and Jaeger, 1947). ρc_p is the ratio of the heat transferred by the unit mass of a medium to a corresponding temperature change, expressed in joules per kilogram per degree Kelvin ($\text{J kg}^{-1} \text{K}^{-1}$). L_f is the unit quantity of heat required for an isothermal change in state of a unit mass of

matter measured in kJ kg^{-1} . Having units of $\text{m}^2 \text{s}^{-1}$, α is a measure of how quickly earth materials change temperature under non-steady state conditions. $\sqrt{\lambda \cdot \rho c_p}$ governs how earth materials adjust to the periodic temperature changes acting upon them within the context of a multi-layered thermodynamic system. $\sqrt{\lambda \cdot \rho c_p}$ determines how rapidly earth materials transfer energy from one layer to the next in response to temperature change.

Site-specific density (ρ) and λ were measured in the laboratory on undisturbed peat samples. Table 2.2 summarizes the mean values obtained from these laboratory measurements. All other parameters were calculated or compiled from available published sources (Bolz and Tuve, 1973; Cutnell and Johnson, 1995). ϕ_w , ϕ_p , and ϕ_g are the representative volumetric fractions of palsa materials (*i.e.*, water, peat, and gas) expressed as percentages in Table 2.3.

Table 2.2: Palsa Material Properties

Parameter	ρ (kg m^{-3})	λ ($\text{W m}^{-1} \text{ } ^\circ\text{K}^{-1}$)	c_p ($\text{J kg}^{-1} \text{ } ^\circ\text{K}^{-1}$)	L_f (kJ kg^{-1})	α ($\times 10^{-7} \text{ m}^2 \text{ s}^{-1}$)	$\sqrt{\lambda \cdot \rho c_p}$ ($\text{kJ m}^{-2} \text{ s}^{-0.5}$)
Peat	105.92	0.066	1550	—	4.02	104.1
Water ¹	999.70	0.587	4193	—	1.40	1568.6
Ice	917.00	2.177	1958	334	12.1	1977.1
Methane ^{2,3}	0.68	0.033	2223	58	218.31	22.3
Snow	300.00	0.160	2090	0.058	2.55	316.7
Air	1.29	0.025	1005	—	192.83	5.7

Notes: ¹ Values published or calculated for 10 °C.

² Values published or calculated for 0 °C.

³ Primary constituent of peatland gas.

Table 2.3: Volumetric Fractions of Palsa Materials ^{1,2,3}

Depth (m)	— Cable 1 —			— Cable 2 —			— Cable 3 —			— Cable 4 —			— Cable 5 —		
	ϕ_p	ϕ_w	ϕ_s	ϕ_p	ϕ_w	ϕ_s	ϕ_p	ϕ_w	ϕ_s	ϕ_p	ϕ_w	ϕ_s	ϕ_p	ϕ_w	ϕ_s
-0.50	—	—	—	—	—	—	—	—	—	—	—	—	—	—	100
0.00	—	—	—	—	—	—	—	—	—	—	—	—	—	100	—
0.05	14	50	36	14	50	36	13	50	37	—	—	—	—	—	—
0.10	14	50	36	14	50	36	13	50	37	—	—	—	—	—	—
0.20	14	76	10	14	76	10	13	75	12	—	—	—	—	100	—
0.35	14	76	10	14	76	10	13	75	12	14	74	12	—	—	—
0.50	14	79	7	14	76	10	15	80	5	—	—	—	—	—	—
0.65	11	79	10	14	79	7	9	91	—	14	83	3	—	—	—
0.80	13	84	3	11	87	2	—	100	—	—	—	—	—	100	—
1.00	5	95	—	5	95	—	—	100	—	14	86	—	—	—	—
1.20	—	100	—	—	100	—	—	100	—	—	—	—	—	100	—
1.40	—	100	—	—	100	—	—	100	—	—	—	—	—	—	—
1.70	—	100	—	—	100	—	—	100	—	14	86	—	—	—	—
2.00	—	100	—	—	100	—	—	100	—	—	—	—	—	—	—
2.30	—	100	—	—	100	—	—	—	—	—	—	—	—	—	—
2.60	—	—	—	—	—	—	—	—	—	—	—	—	—	—	—

Notes: ¹ Depth increments are standardized to facilitate ϕ value comparisons between thermistor cable locations.

² ϕ values are expressed as percentages (%) of total wet weight.

³ ϕ values for a given depth increment are listed in the row for the upper limit of that depth increment.

The aggregate effective thermal conductivity (λ_{eff}) of the site's unfrozen active-layer peat was determined for four active-layer samples in the laboratory. Using an established heat probe method (De Vries and Peck, 1958) and the average λ_{eff} value, palsa material data were entered into Equation 2.1 developed by Gold and Lachenbruch (1973):

$$\lambda_{eff}^n = \lambda_w^{\phi_w} \cdot \lambda_p^{\phi_p} \cdot \lambda_s^{\phi_s} \quad (2.1)$$

where λ_{eff} is the weighted geometric mean of effective thermal conductivity for the aggregate medium ($0.343 \text{ W m}^{-1} \text{ °K}^{-1}$), and λ_w , λ_p , and λ_s are listed in Table 2.2. Manipulating Equation 2.1, the site-specific thermal conductivity value for peat (λ_p) was derived following the mathematical progression in Equation 2.2:

$$\lambda_p^{\phi_p} = \frac{\lambda_{eff}}{\lambda_w^{\phi_w} \cdot \lambda_g^{\phi_g}} \therefore \lambda_p = \left[\frac{\lambda_{eff}}{\lambda_w^{\phi_w} \cdot \lambda_g^{\phi_g}} \right]^{\frac{1}{\phi_p}} \quad (2.2)$$

Replacing the λ_{eff} term with its measured experimental value, inputting the published λ_w and λ_g values, and entering the measured ϕ values for each palsa material into Equation 2.2, the resulting calculation of λ_p in the unfrozen state is $0.066 \text{ W m}^{-1} \text{ } ^\circ\text{K}^{-1}$. The derived λ_p value agrees with available published values for peat (Bolz and Tuve, 1973). Using Equation 2.1, λ_{eff} was calculated for n selected palsa depth increments to obtain representative aggregate values for each palsa stratum at each monitoring location.

Given the extended periods of sub-zero temperatures at the site, λ values for aggregate palsa materials in the frozen state were also estimated. Taking into account the volumetric expansion of water upon freezing, Equation 2.3 was modified to estimate aggregate frozen-state λ_{eff} values as follows:

$$\lambda_{eff}^n = \left[\lambda_i^{(1+\Delta\phi_i)\phi_w} \right] \left[\lambda_p^{\left(1-\frac{\Delta\phi_i}{n-1}\right)\phi_p} \right] \left[\lambda_g^{\left(1-\frac{\Delta\phi_i}{n-1}\right)\phi_g} \right] \quad (2.3)$$

where λ_i is the thermal conductivity of ice, $\Delta\phi_i$, is the volumetric expansion coefficient of ice (0.088), and other variables are as previously described. The resulting representative aggregate λ_{eff} values for selected palsa depth increments were then entered into the instantaneous heat flux density formulae as an initial step in calculating annual heat flux budgets for each monitoring location.

2.53 Preliminary Assessment of Peatland Gas Distribution

After observing gas pockets in peatlands throughout the Schefferville, Québec area, a preliminary survey of entrapped gas pockets within and beneath the submerged peat layer at the Boundary Ridge site was conducted. Peatland gas presence (and volumetric estimates) was confirmed by: (a) measuring the duration of ignited off-gas emissions across the site after penetrating submerged peat mats with a 1.5-cm diameter hollow metal pipe, and (b) observing gas emissions from boreholes (also confirmed by ignition) drilled along Palsa B's periphery.

Archaeal methanogens populating peatlands metabolize the peat substrate thereby generating methane (CH_4), CO_2 , and in certain sulfide-rich aquifers H_2S . Although the scope of this preliminary gas assessment did not include confirmatory laboratory analysis, CH_4 is considered to be a prevalent peatland gas constituent (Beswick *et al.*, 1998; Beckwith *et al.*, 2003, 2003). Peatland gases may also contain CO_2 , H_2S , and/or other volatile and semi-volatile constituents — the most significant of which is CH_4 . Melloh and Crill (1996) and Friberg *et al.* (1997) also have reported variations in peatland gas emissions associated with the seasonal thawing of snow and ice cover in bogs.

Despite its preliminary nature, this assessment of peatland gas pockets at the site was recognized as an overlooked and potentially critical element to better understand the palsa developmental process. Chapters 3 and 4 discuss in more detail how peatland gas may affect thermodynamic and hydrogeologic flux within palsa fields.

2.54 Temperature Measurements

The thermistor cable assemblies used to measure near-surface temperatures at the site were constructed of 2.9-cm diameter wooden broomsticks, amphenol multiplex connectors, multiple paired-wire telephone cable, Fenwal Model GB32P2 glass probe thermistors, solder, shrink-fit tubing, silicon sealant, and electrical tape following a methodology developed by Fritton et al. (1974).

The Fenwal Model GB32P2 glass probe thermistors had been tested and confirmed to be stable by A.S. Judge and A.M. Jessop of the Earth Physics Branch of Energy, Mines and Resources Canada (Jessop, 1972; Judge and Jessop, 1978). Each thermistor was individually calibrated in an ice bath to determine its resistance at 0 °C and appropriate calibration curve (Judge, 1972). The thermistor cable assemblies used at the Boundary Ridge site attempted to improve on an original Russian design (V.A. Obruchev Institute of Permafrost Studies, 1961) by: (1) eliminating potentially conductive construction materials, (2) maintaining tight tolerances between the borehole annuli and broomstick diameters for the thermistor cable assemblies, (3) positioning thermistors to maximize contact with subsurface strata, and (4) using rapid-response thermistors.

The locations of the five thermistor cables are shown on Figure 2.4 (Equipment Installation Plan). To assess the progress of thermal stabilization following the installation process, the thermistor cables were regularly gauged during the initial summer months using a Wheatstone bridge. Resistance readings measured by the Wheatstone bridge were then converted to temperature values based on the initial thermistor calibration curve and

standardized conversion formulas (Judge, 1972). From September 1976 through August 1977, temperature data were collected on an approximately weekly schedule during summer months and on a less frequent basis during winter months, which varied as weather permitted. Thermal data also included ambient air (or near-surface snow during winter) and bog water temperature measurements over the same period.

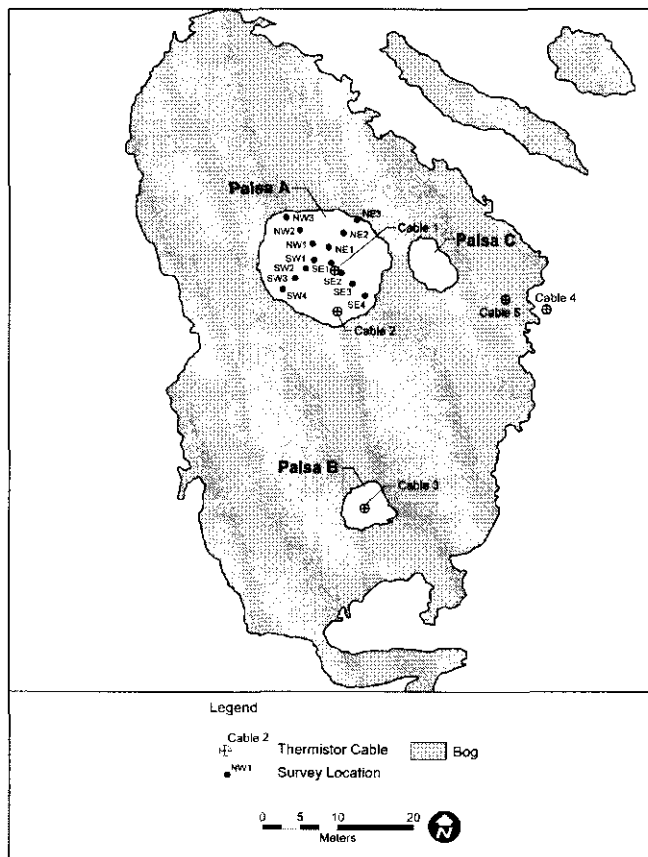


Figure 2.4. Equipment Installation Plan. [Drafted by M. Przybyla]

Thermal profiles were created to graphically depict transient heat flux for each monitoring location and observation date. These graphs were then analyzed to identify temporal and spatial changes in heat flow patterns within the two subject palsas and at the background bog/fen monitoring locations. Time- and depth-correlated temperature data collected were compiled into a

database. Heat flux estimates for each depth interval were then calculated by entering incremental depth-specific volumetric fraction and thermal conductivity values for palsa materials using an established method (Nicholson, 1976). Integrating the heat flux calculations continuously throughout the palsa strata over the 12 months of available temperature data

generated annualized heat budgets for the two palsas. Chapter 3 details the theoretical and practical aspects of the heat budget analyses and discusses the significant investigation findings resulting from the original research conducted at the Boundary Ridge site.

2.6 Methodological Constraints

The annualized Q_H estimates were assessed as to the practical limitations of the data collection process, sample size, underlying theoretical assumptions, and site-specific variables. The Boundary Ridge dataset includes temperature measurements that were recorded on a roughly weekly schedule from April to October and on a less frequent basis from November to March. Given the discontinuous nature of the temperature observations, the resulting annualized heat flux estimates do not account for short-term heat variations and, therefore, are only useful for assessing Q_H for periods of a month or more.

Based on Fourier's heat conduction law, instantaneous Q_H estimates for each depth interval at Cables 1–5 were calculated using Equation 2.4 and integrated through time following the method developed by Nicholson (1976):

$$Q_H = \int_{i=1}^n \frac{\partial T_i}{\partial z_i} \cdot \lambda_{eff_i} \quad (2.4)$$

where $\frac{\partial T_i}{\partial z_i}$ is the thermal gradient and λ_{eff_i} is the effective thermal conductivity

(in the frozen and unfrozen states) for each depth interval. To evaluate the potential error propagation in Equation 2.4, descriptive statistics were derived from the Boundary Ridge experimental data set as shown in Table 2.4.

Table 2.4: Descriptive Statistics for Cables 1–3 Q_H Parameters

Cable No.	Parameter	n ¹	\bar{x} ²	Min/Max	σ ³	S_e ⁴	S_x ⁵
1	Temperature differential (∂T)	440	0.01	-9.82/5.33	1.35	0.065	0.01
	Depth differential (∂z)	440	0.21	0.05/.60	0.14	0.007	0.005
	Thermal conductivity (λ_m)	440	1.28	0.14/2.18	0.75	0.036	0.01
	Instantaneous heat flux (Q_i)	401	0.23	-49.97/34.02	5.90	0.294	0.2
2	Temperature differential (∂T)	471	0.01	-3.53/7.36	1.15	0.053	0.01
	Depth differential (∂z)	471	0.21	0.05/0.80	0.12	0.005	0.005
	Thermal conductivity (λ_m)	471	1.46	0.14/2.18	0.75	0.035	0.01
	Instantaneous heat flux (Q_i)	433	0.15	-16.61/12.06	3.99	0.192	0.1
3	Temperature differential (∂T)	510	0.12	-3.42/9.05	1.31	0.058	0.01
	Depth differential (∂z)	510	0.18	0.05/0.40	0.10	0.004	0.005
	Thermal conductivity (λ_m)	510	1.30	0.14/2.18	0.84	0.037	0.01
	Instantaneous heat flux (Q_i)	471	0.45	-62.75/33.26	5.42	0.250	0.04

Notes: ¹ Sample size.
² Sample mean.
³ Standard deviation.

⁴ Standard error.
⁵ Parametric uncertainty.

The incremental errors in the heat flux variables ∂T_i , ∂z_i , and λ_i contribute to the cumulative uncertainty, S_Q , in the instantaneous heat flux (Q_i) calculation. Equation 2.5 describes this error propagation as:

$$S_Q = \bar{Q}_i \sqrt{\left(\frac{S_T}{\partial T}\right)^2 + \left(\frac{S_z}{\partial z}\right)^2 + \left(\frac{S_\lambda}{\lambda}\right)^2} \quad (2.5)$$

where S_T , S_z , and S_λ are the incremental uncertainties associated with the measurement of temperature, depth, and thermal conductivity, respectively. The cumulative uncertainties, S_Q , in the Q_H calculations are $\pm 0.2 \text{ MJ m}^{-2}$ for Cable 1, $\pm 0.1 \text{ MJ m}^{-2}$ for Cable 2, and $\pm 0.04 \text{ MJ m}^{-2}$ for Cable 3.

The Q_H calculation is predicated on the assumptions that steady-state heat flow occurs solely by conductive transfer, through homogeneous media, along a singularly linear pathway, and in a direction perpendicular to an

advancing freezing plane. In actuality, site conditions indicated that forces acting upon the palsas have produced fissures in the active-layer peat, which cause deviations in local heat flow patterns. Similarly, permafrost-zone deformation introduced nonconductive heat transfer along orthogonal vectors primarily through advective and/or dispersive flow.

Subsurface hydraulic flow patterns near the palsas also favor potential departures from Fourier's idealized steady-state premise. Given the relative thermal isolation of the bog's lower water-bearing zone, the potential for lateral, nonlinear, and non-steady state heat flow appears to be most pronounced along the Palsa A periphery (ref. Cable 2) and background locations (ref. Cables 4 and 5). As a result, near-surface transient heat flow conditions at these locations are expected to introduce error, although such errors are likely minimized by isothermal conditions in the bog's lower water-bearing zone.

Additional potential sources of error stemmed from observational error — instrument- and operator-induced measurement bias being primary sources. Efforts to mitigate such errors included establishing standard operating procedures (*e.g.*, routine instrument calibration, replication of temperature readings and laboratory procedures), and data verification/validation. This year-long study generated valid order-of-magnitude Q_H estimates of actual heat flux since heat transfer was predominantly conductive over sufficiently long measurement time intervals. The Q_H data therefore are valid for the purpose of providing an initial assessment of palsa thermodynamic status.

2.7 Research Introduction

Chapters 3 and 4 include two manuscripts detailing the research goals, approach, results, and conclusions obtained during the completion of this thesis program. Manuscript No. 1 presents original research on palsa thermodynamic behavior and the underlying processes affecting palsa development. Building on Chapter 3, Manuscript No. 2 (Chapter 4) introduces a new dynamic conceptual model of palsa development spanning from antecedent ice nucleation —the precursor to embryonic palsas— to palsa decline and recurrence. As with the other chapters, references noted in the manuscript texts are included in the combined list of references at the end of this thesis.

Chapter 3:
Seasonal Thermodynamic and Dynamic Geomorphologic Processes Operating
upon Palsas at Boundary Ridge near Schefferville, Québec

Context in Thesis

From the review of published research presented in Chapter 1, it is apparent that exogenic and endogenic processes affecting palsa development have received insufficient attention. This manuscript presents original research on seasonal thermodynamics and dynamic geomorphologic processes observed at the Boundary Ridge site. It summarizes the findings of a 12-month monitoring and analysis program on palsa geomorphology in the Schefferville, Québec area from September 1976–August 1977. These findings test Hypotheses Nos. 1–3 proposed in Chapter 1 and form the basis for the new dynamic conceptual model of palsa development presented in Chapter 4.

Abstract

A 12-month study of palsa dynamics investigated thermodynamic and geomorphologic processes affecting palsa development near Schefferville, Québec. Site observational and heat flux data collected at the Boundary Ridge site from September 1976–August 1977 show how geomorphologic processes change over time by assessing palsas at varying developmental stages. This study provides a quantitative assessment of seasonal heat flux patterns and underlying geomorphologic processes observed at palsas in varying phases of development.

3.1 Introduction

From the review of published research on palsas, it is apparent that exogenic and endogenic processes acting upon palsas have received insufficient attention over the years. This paper presents the findings of a 12-month study of palsa geomorphology near Schefferville, Québec from September 1976–August 1977. This research quantitatively assesses year-round heat flux within two palsas representative of young and mature developmental phases, and compares results to heat flux patterns observed at two background wetland locations.

The quantitative analytical techniques used herein derive annualized heat flux estimates from spatially and temporally integrated heat flow data to gain a deeper understanding of the underlying physical and biogeochemical processes controlling palsa development. The overarching goal of this research was to investigate palsa geomorphology through a systematic analysis of seasonally changing thermodynamic patterns. This research assessed: (1) the character and behavior of palsa materials (*i.e.*, peat, water, ice, peatland gas [*i.e.*, methane], and air), (2) the underlying physical and chemical processes affecting heat transfer within palsas, (3) how earth materials and processes within palsas interact, and (4) how these earth materials and processes change over time to cumulatively affect the evolution of palsa geomorphologic systems near Schefferville, Québec.

3.2 Physical Setting

The Boundary Ridge study site (the “site”) is a ± 0.8 -ha palsa bog within a perched basin abutting the Québec-Newfoundland provincial border roughly 12 kilometers west-northwest of Schefferville, Québec (see Figure 3.1). Situated near the transition between sporadic to widespread discontinuous permafrost

zones in northern Québec, the site's geographical coordinates are 55° 3' 12"N, 67° 15' 18"W. Resting at the foot of Boundary Ridge's talus-covered southwestern slope, the site lies at an elevation of 800 m ASL with local topography gradually sloping southwesterly toward the Howells River valley.

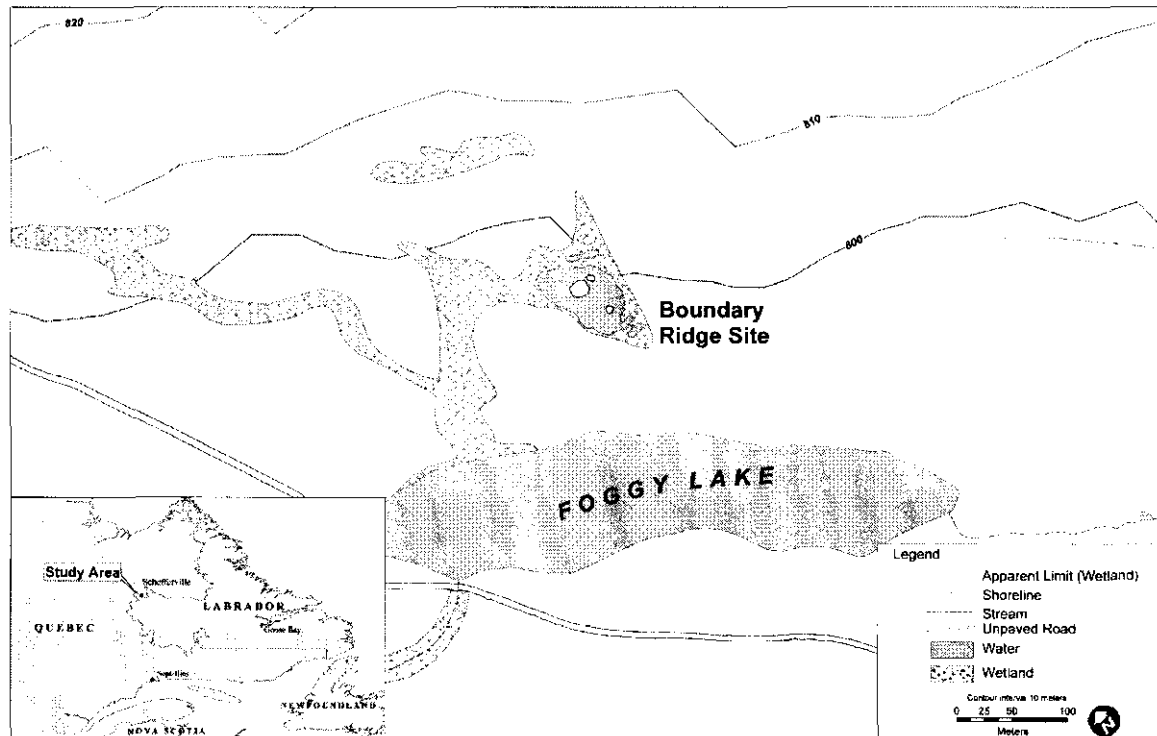


Figure 3.1. Boundary Ridge Site Map. (Contours derived from Shuttle Radar Topography Mission data provided by USGS) [Drafted by M. Przybyla]

Using conventional terminology (Seppälä, 1986), three palsas occur at the site including a $\pm 171\text{-m}^2$ and $\pm 0.9\text{-m}$ high mature palsa located in the north-central portion of the wetland (Palsa A), a $\pm 32\text{-m}^2$ and $\pm 0.6\text{-m}$ high young palsa located in the southern portion of the wetland (Palsa B), and a $\pm 25\text{-m}^2$ and $\pm 0.4\text{-m}$ high mature palsa situated in the eastern portion of the wetland (Palsa C), which was previously disturbed by foot traffic and not suitable for research. Three thermokarst depressions within the bog mark the locations of what are believed to have been former palsas.

The Boundary Ridge bog is characterized by hydrogeologic system flow occurring both above and below the semi-confining *Sphagnum*/sedge peat layer and the seasonal frost layer during different times of the year. Rainfall and snow/ice meltwater contribute oxygenated water through the upper aerobic bog while anoxic groundwater flows through the lower semi-confined bog. Discharging to Foggy Lake, the inferred southerly surface water and groundwater flow direction across the site is affected by the seasonal frost, semi-confining peat layer, permafrost, and bedrock controls of the northwest-southeasterly trending raised valley within which the perched Boundary Ridge palsa bog is located. The dominant *Sphagnum* moss/sedge community surrounding the palsa bog acidifies surface water and groundwater migrating through the site.

3.3 Methodology

The research program included survey, palsa/bog stratigraphic, aboveground and subsurface thermal, and physical palsa material data collection. This year-round study of seasonal thermodynamic patterns used heat flux estimates to assess palsa aggradation/degradation and compared variations in heat flow patterns with survey data to determine changes in the permafrost mass balance of palsas.

3.31 Site Surveys

Closed-loop instrument surveys of the Boundary Ridge site were performed at regular intervals. Fixed to a benchmark on a Denault Dolomite outcrop north of the site, leveling surveys determined the elevations along palsa transects. Survey data included topographic, water table, and seasonal snow/ice elevations. Given their closed-loop nature, survey data were accurate to ± 0.03 cm.

3.32 Subsurface Explorations and Sampling

Palsa stratigraphy was investigated immediately before installing five thermistor cable assemblies at the site. Using a 3.18-cm diameter carbide-tipped hand auger, soil borings were manually advanced to refusal at 2.6 m below ground surface (bgs). Auger refusal occurred at all five locations where highly consolidated frozen silt and clay marked the underlying sediment interface. Three of the five boreholes were situated at two palsas; two within Palsa A (one near its center; the other at its southern margin) and another within Palsa B (see Figure 3.2, Equipment Installation Plan). Two additional boreholes were advanced; one along the eastern bog margin and the other in the bog itself.

Raised ± 0.9 m above the bog, Palsa A's stratigraphy included weathered fibrous peat within an active layer extending from 0– ± 0.5 m bgs, peat intercalations decreasing with depth in permafrost from ± 0.5 –1.05 m bgs, and permafrost with mineral intercalations increasing with depth from ± 1.05 –2.6 m bgs until refusal. At the depth of refusal, frozen bluish-green to grey silt/clay sediments indicative of the site's native ferrous and dolomitic bedrock formations were encountered. All permafrost samples emitted odors attributed to peat decay.

Palsa B rose ± 0.6 m above the bog. Its stratigraphy included less weathered active-layer fibrous peat from 0– ± 0.55 m bgs, peat intercalations decreasing abruptly with depth within permafrost from ± 0.55 –0.75 m bgs, ice from ± 0.75 –1.6 m bgs, and unfrozen saturated sediments from ± 1.6 –2.4 m bgs. Permafrost samples emitted gaseous odors indicative of peat decay and bluish-green to grey silt/clay sediments were encountered at refusal.

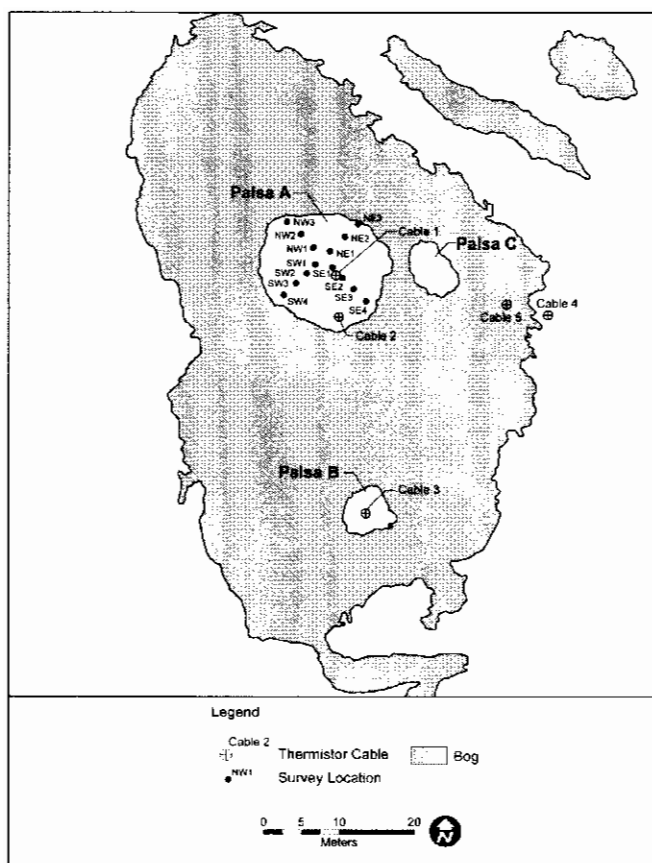


Figure 3.2. Equipment Installation Plan. [Drafted by M. Przybyla]

Two more boreholes were drilled just before installing thermistor cables at the bog margin (Cable 4) and in the bog itself (Cable 5). Cable 4 stratigraphy included moss-covered mesic peat from 0–±0.15 m bgs and saturated peat from ±0.15–1.95 m bgs before refusal at the silt/clay interface. As a background data point, Cable 5 was anchored into bog sediments and partially submerged in the bog from 0–1.5 m leaving 0.5 m (and one thermistor) exposed above the bog.

Samples were collected continuously from auger flights as boreholes were advanced at each thermistor cable location. Palsa samples were placed in 25-cc stainless steel containers before being preserved on ice in an insulated cooler during transport to McGill Subarctic Research Station.

Volumetric fractions of solid (peat), aqueous (water), and gaseous (peatland gas and air) phases were determined by gravimetric methods. Undisturbed peat samples were also collected at the site for laboratory examination of key physical characteristics including bulk density, thermal conductivity, and volumetric specific heat. Table 3.1 summarizes the mean thermal property values for palsa materials obtained from these laboratory

measurements. All other parameters were calculated or compiled from available published sources (Bolz and Tuve, 1973; Cutnell and Johnson, 1995).

Table 3.1: Thermal Properties of Palsa Materials

Parameter	ρ (kg m ⁻³)	λ (W m ⁻¹ °K ⁻¹)	c_p (J kg ⁻¹ °K ⁻¹)	L_f (kJ kg ⁻¹)	α (x10 ⁻⁷ m ² s ⁻¹)	$\sqrt{\lambda \cdot \rho c_p}$ (kJ m ⁻² s ^{-0.5})
Peat	105.92	0.066	1550	—	4.02	104.1
Water ¹	999.70	0.587	4193	—	1.40	1568.6
Ice	917.00	2.177	1958	334	12.1	1977.1
Methane ^{2,3}	0.68	0.033	2223	58	218.31	22.3
Snow	300.00	0.160	2090	0.058	2.55	316.7
Air	1.29	0.025	1005	—	192.83	5.7

Notes: ¹ Density.
² Thermal conductivity.
³ Specific heat capacity at constant pressure.
⁴ Latent heat of fusion.
⁵ Thermal diffusivity.

⁶ Thermal inertia.
⁷ Values published or calculated for 10 °C.
⁸ Values published or calculated for 0 °C.
⁹ Primary constituent of peatland gas.

3.33 Temperature Measurements

Five thermistor cables were installed at the Boundary Ridge site to measure *in situ* temperatures (ref. Figure 3.2; Cables 1–5). The Fenwal Model GB32P2 glass probe thermistors were confirmed to be stable by A.S. Judge and A.M. Jessop of the Earth Physics Branch of Energy, Mines and Resources Canada (Jessop, 1972; Judge and Jessop, 1978). Each thermistor was individually calibrated in an ice bath to determine its resistance at 0 °C and appropriate calibration curve (Judge, 1972).

All temperature measurements were obtained with a Wheatstone bridge, which sequentially gauged in-line electrical resistance through each thermistor circuit. Avoiding unnecessary measurement bias, the Wheatstone bridge helped eliminate instrument-induced bias since it used a lower electrical impulse to gauge in-line resistance than digital instruments. Thermistor resistance readings were then converted to temperature values based on thermistor calibration data and standardized conversion formulas (Judge, 1972). From September 1976 to

August 1977, temperature data were collected approximately weekly during summer months and less frequently, as weather permitted, during winter months. Data were plotted to assess heat flow patterns at the palsa and background monitoring locations.

3.34 Annual Heat Flux Budgets

Time- and depth-correlated temperature data for Cables 1–5 collected from September 1976–August 1977 were compiled to determine variations in heat flux (Q_H). Based on Fourier's heat conduction law, instantaneous Q_H estimates for each depth interval at Cables 1–5 were calculated using Equation 3.1 (Nicholson, 1976):

$$Q_H = \int_{i=1}^n \frac{\partial T_i}{\partial z_i} \cdot \lambda_{eff,i} \quad (3.1)$$

where $\frac{\partial T_i}{\partial z_i}$ is the thermal gradient and $\lambda_{eff,i}$ is the effective thermal conductivity

(in the frozen and unfrozen states) for each depth interval at the Cable 1–5 monitoring locations. The differences in instantaneous Q_H for adjacent depth increments were integrated continuously over successive time periods to obtain net period Q_H , expressed in millions of joules per square meter (MJ m^{-2}). Monthly net Q_H were derived by sequentially totaling the net period Q_H differentials. Integrating the monthly net Q_H totals continuously over the year-long term of study for each Cable 1–5 location generated order-of-magnitude estimates of annual heat flux.

As was typically the case, the data collection dates were not synchronized with the first or last days of monthly periods, which had no effect on the overall

annual Q_H estimates since the data were integrated continuously over the year. The inclusion of net period Q_H estimates, which straddled successive months, within the month that the majority of the intervening days occurred similarly minimized temporal bias of monthly net Q_H estimates.

This year-long study generated order-of-magnitude Q_H estimates of actual heat flux since heat transfer was predominantly conductive over sufficiently long measurement time intervals. The Q_H data therefore are valid for the purpose of providing an initial assessment of palsa thermodynamic status.

3.35 Heat Flux Budget Error Estimation

Table 3.2 summarizes the descriptive statistics derived from the Boundary Ridge experimental data set and used to evaluate the potential error propagation in Equation 3.1. The incremental errors in the heat flux variables ∂T_i , ∂z_i , and λ_i

Table 3.2: Descriptive Statistics for Cables 1–3 Q_H Parameters

Cable No.	Parameter	n ¹	\bar{x} ²	Min/Max	σ ³	S_e ⁴	S_x ⁵
1	Temperature differential (∂T)	440	0.01	-9.82/5.33	1.35	0.065	0.01
	Depth differential (∂z)	440	0.21	0.05/.60	0.14	0.007	0.005
	Thermal conductivity (λ_s)	440	1.28	0.14/2.18	0.75	0.036	0.01
	Instantaneous heat flux (Q_i)	401	0.23	-49.97/34.02	5.90	0.294	0.2
2	Temperature differential (∂T)	471	0.01	-3.53/7.36	1.15	0.053	0.01
	Depth differential (∂z)	471	0.21	0.05/0.80	0.12	0.005	0.005
	Thermal conductivity (λ_s)	471	1.46	0.14/2.18	0.75	0.035	0.01
	Instantaneous heat flux (Q_i)	433	0.15	-16.61/12.06	3.99	0.192	0.1
3	Temperature differential (∂T)	510	0.12	-3.42/9.05	1.31	0.058	0.01
	Depth differential (∂z)	510	0.18	0.05/0.40	0.10	0.004	0.005
	Thermal conductivity (λ_s)	510	1.30	0.14/2.18	0.84	0.037	0.01
	Instantaneous heat flux (Q_i)	471	0.45	-62.75/33.26	5.42	0.250	0.04

Notes: ¹ Sample size.

² Sample mean.

³ Standard deviation.

⁴ Standard error.

⁵ Parametric uncertainty.

contribute to the cumulative uncertainty, S_Q , in the instantaneous heat flux (Q_i) calculation. Equation 3.2 describes this error propagation as:

$$S_Q = \bar{Q}_i \sqrt{\left(\frac{S_T}{\partial T}\right)^2 + \left(\frac{S_z}{\partial z}\right)^2 + \left(\frac{S_\lambda}{\lambda}\right)^2} \quad (3.2)$$

where S_T , S_z , and S_λ are the incremental uncertainties associated with the measurement of temperature, depth, and thermal conductivity, respectively. The cumulative uncertainties, S_Q , in the Q_{ii} calculations are $\pm 0.2 \text{ MJ m}^{-2}$ for Cable 1, $\pm 0.1 \text{ MJ m}^{-2}$ for Cable 2, and $\pm 0.04 \text{ MJ m}^{-2}$ for Cable 3.

3.4 Results and Discussion

The thermodynamic and geomorphologic processes operating on permafrost-induced landforms can be best understood by investigating heat transfer through: (a) seasonal variations in near-surface temperature patterns, (b) spatial and temporal variability of unidirectional steady-state heat flow, (c) spatial and temporal variations in lateral temperature changes and heat flux, (d) long-term geothermal influences acting on the base of the permafrost zone, and (e) long-term variability of near-surface temperatures and heat flow in response to climatic change (Gold and Lachenbruch, 1973). This research investigated palsa processes by examining the first three heat transfer behaviors and foregoing study of the latter two, which were beyond the existing scope of study.

3.41 Spatial and Temporal Variations in Temperature

Temperature plots for selected depths at each of the five thermal monitoring locations illustrate marked differences between the young and mature palsa phases, and site background conditions (see Figures 3.3 – 3.7). The lower effective

thermal conductivity (λ_{eff}) and effective thermal diffusivity (α_{eff}) of Palsa A active-layer peat helped preserve surficial conditions favorable to ice growth from the onset of the winter frost season into May 1977 (see Figure 3.3b). The more efficient insulating qualities of Palsa A peat coupled with evaporative cooling within the lower active layer also contributed to diminished active-layer heat gain during the summer thaw season compared to Palsa B (cf. late August 1977 data in Figures 3.3b and 3.5b).

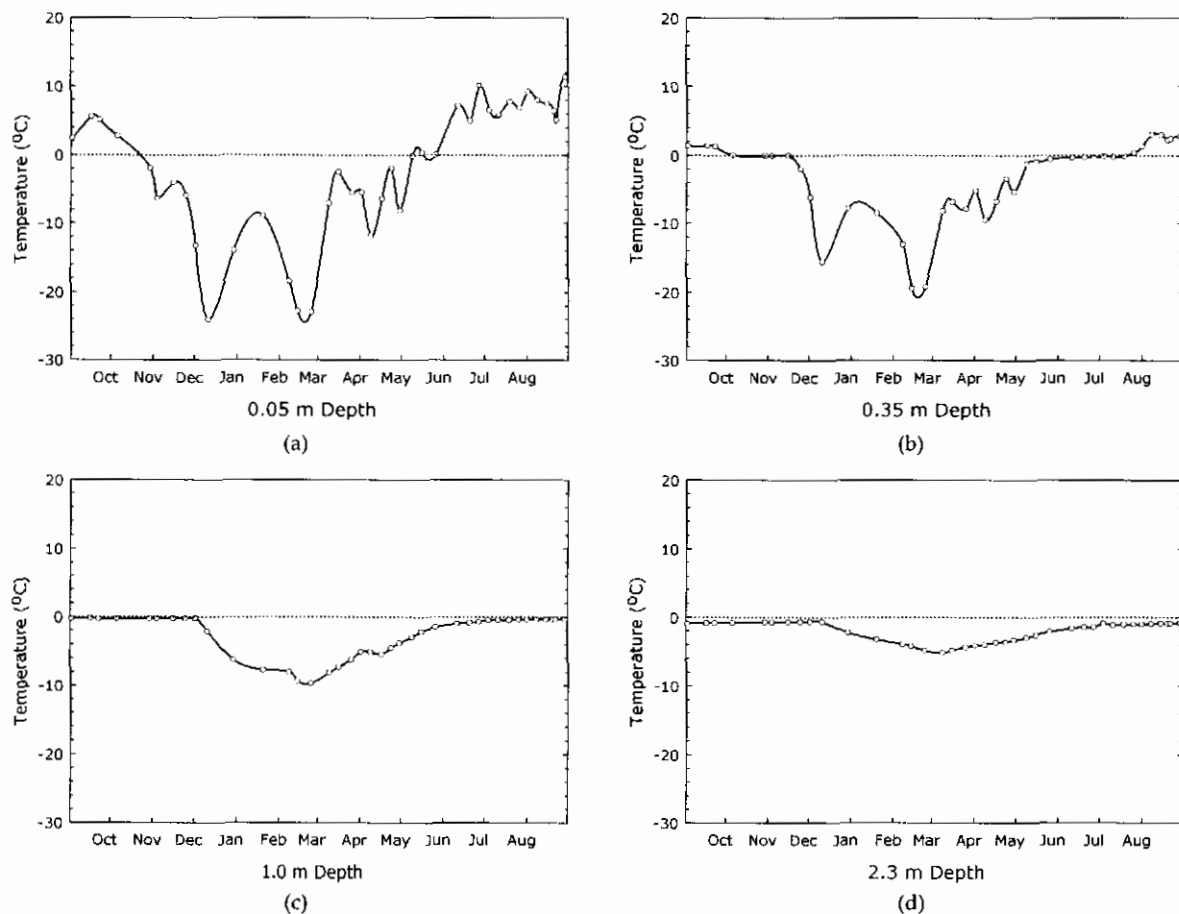


Figure 3.3. Annual temperature variations near the center of Palsa A (Cable 1) in the: (a) upper active layer, (b) lower active layer, (c) upper permafrost, and (d) lower permafrost. Note the “zero curtain” effect illustrated by (b), (c), and (d).

The “zero-curtain” effect at Palsa A extended from early October to early December, and again from June through August, as a result of latent heat transfer

coinciding with advancing and receding frost fronts within the lower active layer and underlying permafrost zone (see Figure 3.3b, c, and d). Interrupted only by the winter cold wave, permafrost maintained isothermal equilibrium throughout much of the year (see Figure 3.3c and d). The prolonged isothermal condition exhibited by Palsa B (ref Figure 3.5c and d) mirrored that observed at Palsa A.

The nearly 2½ months that passed between the mid-December 1976 penetration of the winter cold wave within Palsa A's lower permafrost zone and the occurrence of the early March 1977 thermal minima confirmed that phase lags increased as palsas developed and helped preserve overall permafrost mass throughout the year (see Figure 3.3d). As shown by Cable 1 data from the 2.3 m depth interval, site conditions suitable for ice growth existed for a 7-month period from mid-December 1976 to mid-June 1977 at Palsa A. Mature palsa development appears to be controlled primarily by permafrost growth at the base of the active layer and secondarily by ice growth within permafrost.

Annual temperature variations within the active layer at Cable 2 indicated thermal attenuation and phase lag patterns similar to those observed near Palsa A's center (cf. Figures 3.3 and 3.4). The reduced amplitude of minimum temperatures occurring in December 1976 and February 1977 is likely caused by thicker snowcover and less efficient vertical heat transfer near Palsa A's periphery than at its center, as previously established (Seppälä, 1990, 1994). Despite proximity to the permafrost/water interface along the Palsa A periphery, these observations suggest that Palsa A's permafrost core retained ice mass at the 1.0-m depth — an effect that apparently diminished with depth (see Figures 3.3d and 3.4d). Temperatures conducive to ice growth persisted for almost one month longer near the center of Palsa A than at its southern periphery.

Year-round temperature patterns for the young-phase Palsa B (ref. Figure 3.5; Cable 3) were different than those at Palsa A. Resulting from the higher λ_{eff} , α_{eff} , and moisture retention capacity of active-layer peat, Palsa B thermal maxima and minima were greater than Palsa A, suggesting that peat's insulating

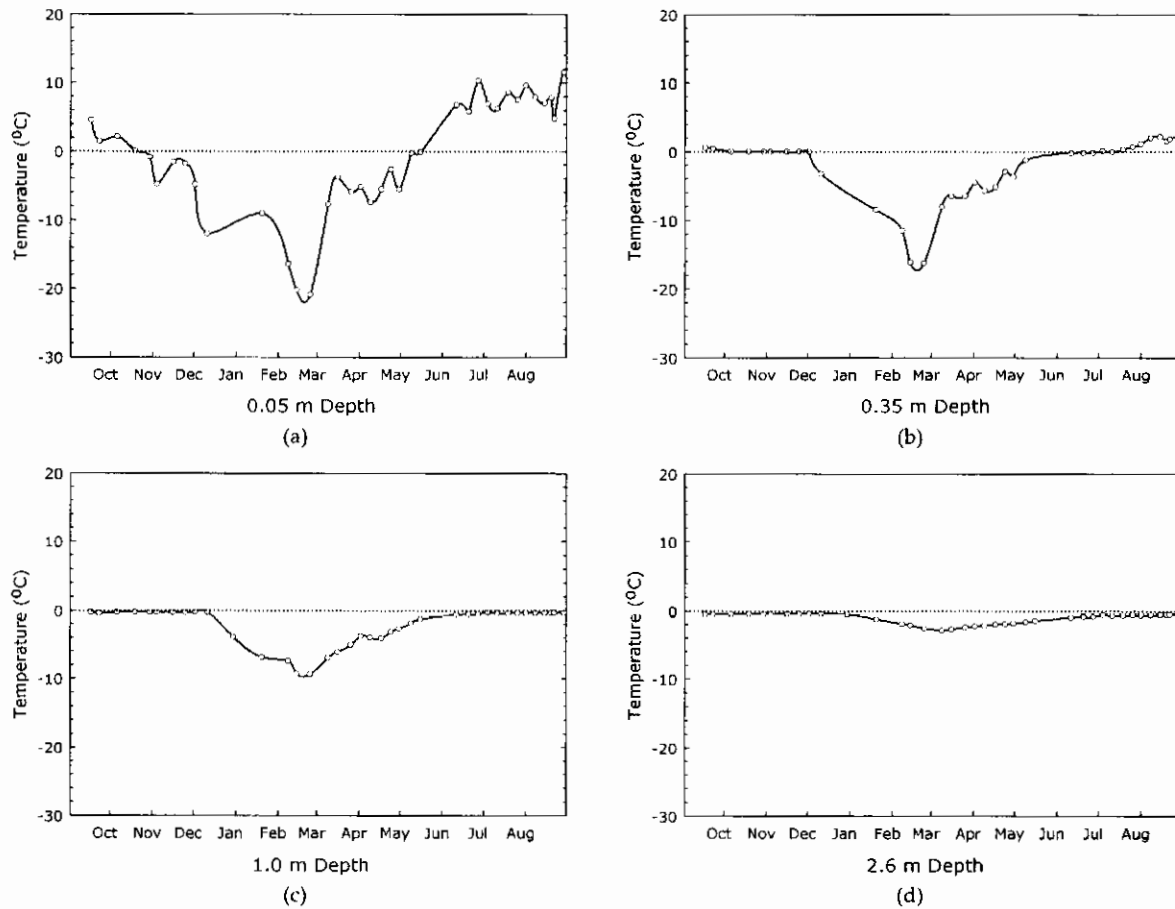


Figure 3.4. Annual temperature variations near the southern periphery of Palsa A (Cable 2) in the: (a) upper active layer, (b) lower active layer, (c) upper permafrost, and (d) lower permafrost. Note the higher temperature minima in the active layer shown by (a) and (b), but similar temperature patterns in the permafrost zone compared to Palsa A's central monitoring location (ref. Figure 3.3).

quality becomes increasingly less conductive over time. Supporting scientific findings document this hysteretic behavior of peat when subjected to repeated drying/rewetting cycles (Fuchsman, 1986; Egglesmann, 1988; Mooney, 2003).

Active-layer thermodynamics at Palsa B during the summer thaw season illustrate the so-called “heat-valve” effect, which is governed by $\sqrt{\lambda \cdot \rho c_p}$ of earth

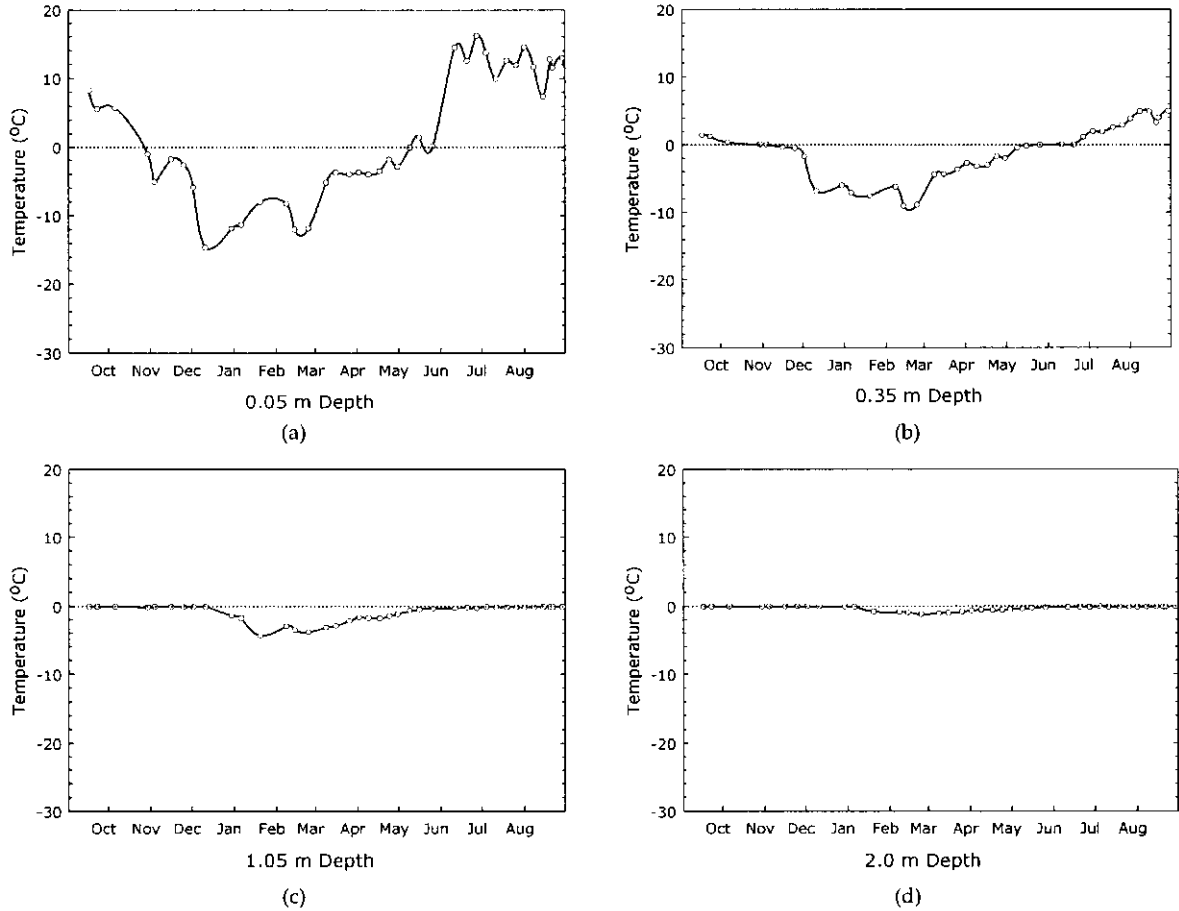


Figure 3.5. Annual temperature variations near the center of Palsa B (Table 3) in the: (a) upper active layer, (b) lower active layer, (c) upper permafrost, and (d) lower permafrost. Note the greater active layer thickness and the shift to higher temperature maxima and minima within the active layer and permafrost zone compared to Palsa A.

materials (see Table 3.1) (Gold and Lachenbruch, 1973). Holding other variables constant, $\sqrt{\lambda \cdot \rho c_p}$ is less sensitive to the freezing of saturated palsa materials than λ and thereby influences surficial thermodynamics in multi-layered palsa systems by favoring heat loss during the winter frost season to heat gain during the summer thaw season. This preferential thermodynamic process is as important to young palsas as it is to mature palsas.

Temperature data recorded at the background bog location revealed several important heat flow characteristics (see Figure 3.6). The amplitude and periodicity of temperature disturbances in the shallow-bog surface water above the semi-confining peat layer were significantly attenuated or absent below the submerged peat layer (cf. Figure 3.6a and c). The effects of summer heat gain diminished in amplitude and increased in phase lag with depth below the submerged upper portion of the semi-confining peat layer. By the time thermal disturbances reached the 1.25-m depth, temperatures were less than half and phase lag was more than 6 weeks later than existed above the peat layer.

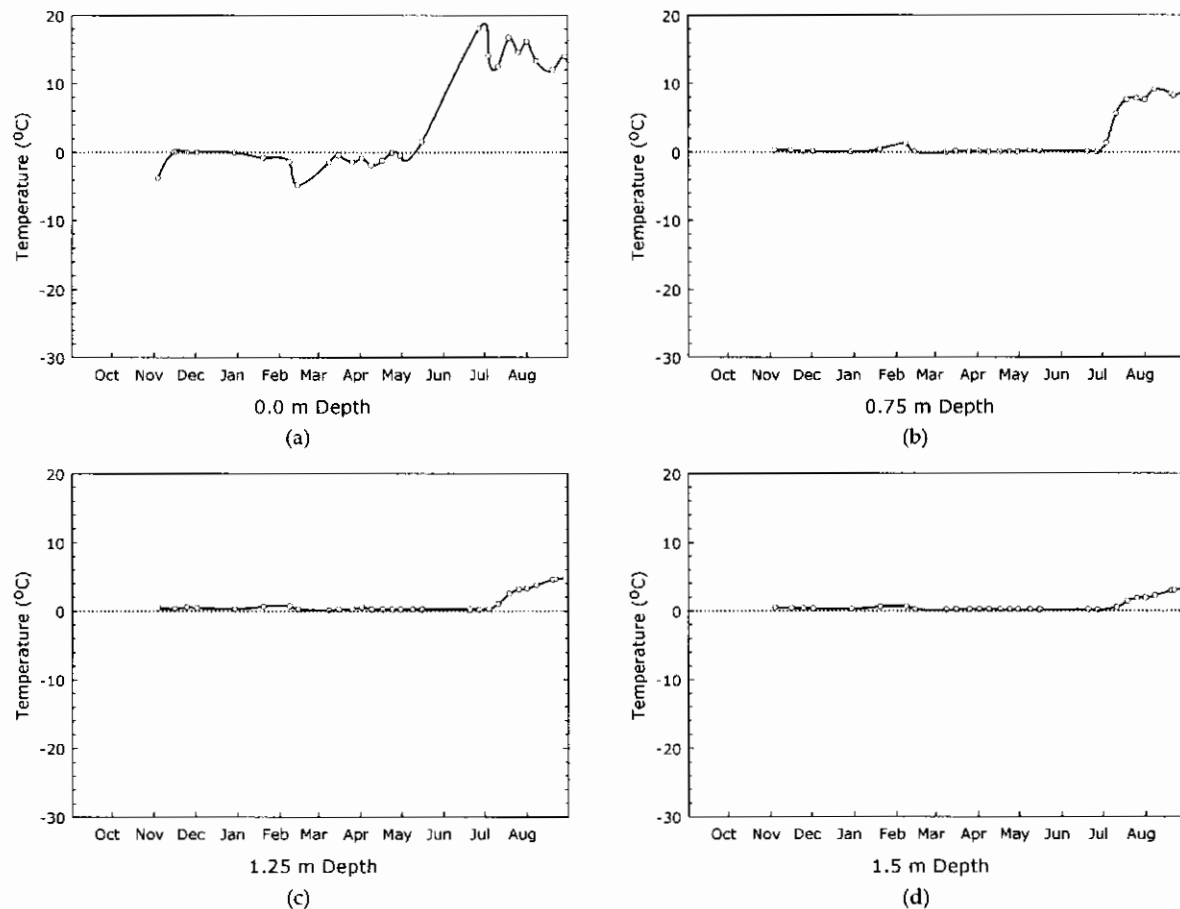


Figure 3.6. Annual temperature variations at the background bog monitoring location (Cable 5).

The semi-confining peat layer existing within the Boundary Ridge bog preserved isothermal conditions throughout much of the year, maintained temperatures within the semi-confined water-bearing zone near or below $\pm 4^{\circ}\text{C}$, and perpetuated a static water column beneath it. These conditions created a year-round environment favoring opportunistic ice growth where water temperature remained near 0°C for eight months of the year requiring minimal energy exchange to initiate and continue the freezing process as the seasonal frost front advanced. Given this context, the submerged semi-confining peat layer not only exhibited influence over hydrogeologic system flow through the bog, but also exerted appreciable control over thermodynamic transfer.

Comparing Figures 3.3, 3.4, and 3.6, the prolonged period during which ice segregated near the bog/sediment interface at the base of Palsa A appeared to be coincident with and perpetuated by the low lateral thermodynamic gradients resulting from isothermal conditions in the bog's lower water-bearing zone. Based on these data, the submerged semi-confining peat layer contributed significantly to site conditions favorable to palsa emergence and continued development.

3.42 Palsa A Heat Flux Dynamics

Reviewing Palsa A active-layer data in Tables 3.3 and 3.4, negative monthly heat flux within individual active-layer depth intervals during the summer season appear to be related to transient conditions such as evaporation, an effective heat dissipator. Total annual active-layer Q_H for Palsa A was $147.1 \pm 0.2 \text{ MJ m}^{-2}$ at the central monitoring location (0.1–0.5 m) and $104.5 \pm 0.1 \text{ MJ m}^{-2}$ at the peripheral monitoring location (0.1–0.65 m). Excluding other heat sinks and sources, the annual net Q_H at these locations would be sufficient to melt 0.44 m^3 and 0.31 m^3 of ice (or a 44-cm and a 31-cm thick ice layer per 1-m^2 area), respectively.

Table 3.3: Summary of Estimated Heat Flux for Palsa A Central Location

Depth (m)	1976				1977								Totals
	Sep	Oct	Nov	Dec	Jan	Feb	Mar	Apr	May	Jun	Jul	Aug	
0.10-0.20	-2.4	5.1	6.4	23.4	3.4	9.9	2.6	4.6	0.9	1.2	8.3	-1.3	62.1
0.20-0.35	0.8	-4.8	-8.2	41.5	-8.3	25.9	8.1	8.0	-2.2	5.7	-12.3	-14.6	39.6
0.35-0.50	1.5	1.6	-6.6	-19.6	-4.5	30.9	17.7	7.6	-4.3	-1.3	15.7	6.7	45.4
0.50-0.65	2.5	-4.2	-5.1	-50.0	2.8	-51.5	-13.7	-12.7	4.5	5.3	1.2	12.6	-108.4
0.65-0.80	-1.2	5.2	0.1	-1.2	1.3	-4.8	-0.8	-0.6	1.0	0.7	0.1	-0.5	-0.8
0.80-1.00	2.6	-1.2	-0.2	0.8	3.5	2.9	1.9	0.5	0.4	0.3	0.2	0.9	12.6
1.00-1.20	-2.9	-1.7	-0.6	-0.3	3.8	7.0	3.2	1.3	-1.3	-2.3	-2.0	-1.4	2.8
1.20-1.40	1.1	0.4	0.3	-2.2	2.8	2.3	2.3	0.9	3.0	0.3	0.2	-0.2	11.2
1.40-1.70	-0.2	-0.4	-0.3	-2.5	-1.0	19.7	1.6	1.1	-2.2	1.2	1.3	1.2	19.5
1.70-2.30	1.7	2.3	1.5	-3.2	-1.7	-32.2	-1.0	-2.5	1.3	-1.3	-1.6	-1.9	-38.6
Totals	3.5	2.3	-12.7	-13.3	2.1	10.1	21.9	8.2	1.1	9.8	11.1	1.5	45.6

Note: ¹ Heat flux density values are expressed as millions of joules per square meter (MJ m^{-2}).

Permafrost-zone heat flux at these two locations show expected negative heat flow patterns. Deviations toward positive monthly Q_H within individual permafrost-zone depth intervals during the winter season may be attributed to water intrusion along fractures and fissures in the palsa's permafrost core caused by thermal deformation. Total annual permafrost-zone Q_H for Palsa A was $-101.5 \pm 0.2 \text{ MJ m}^{-2}$ at the central location (0.5–2.3 m) and $-82.9 \pm 0.1 \text{ MJ m}^{-2}$ at the peripheral location (0.65–1.6 m). Excluding other heat sinks and sources, the annual

Table 3.4: Summary of Estimated Heat Flux for Palsa A Southern Periphery

Depth (m)	----- 1976 -----				----- 1977 -----								Totals
	Sep	Oct	Nov	Dec	Jan	Feb	Mar	Apr	May	Jun	Jul	Aug	
0.10-0.20	1.1	3.2	-1.7	-1.7	-1.3	-6.4	5.1	3.1	0.5	21.0	3.7	-2.7	23.8
0.20-0.35	0.0	0.0	-7.6	17.1	0.3	18.6	7.5	3.3	—	—	—	—	39.2
0.35-0.50	-0.2	-4.2	-6.6	-11.3	-11.5	-10.9	-4.1	-5.9	-1.5	4.0	11.5	2.8	-37.7
0.50-0.65	1.4	8.1	6.9	-6.8	4.6	7.7	5.8	10.5	4.2	—	—	36.9	79.3
0.65-0.80	-1.0	-6.0	-4.2	-5.6	-6.3	-13.0	1.2	-8.9	-2.0	-3.7	-1.6	-3.7	-54.6
0.80-1.00	-0.2	0.9	0.7	2.7	7.4	21.4	6.8	6.2	0.7	2.5	1.5	1.3	52.0
1.00-1.15	0.7	1.3	-0.5	-0.8	0.4	-6.4	-3.6	-2.9	-1.8	-1.7	-0.8	-0.7	-16.8
1.15-1.30	2.7	17.0	12.9	19.0	15.7	27.5	21.3	20.8	9.6	7.1	1.2	12.6	167.4
1.30-1.55	-4.0	-27.6	-19.7	-26.9	-16.7	-32.7	-25.1	-27.1	-11.8	—	—	-76.9	-268.4
1.55-1.80	1.0	9.7	7.3	9.2	4.7	4.8	5.1	8.0	4.0	3.7	-0.9	6.4	63.0
1.80-2.00	-0.1	0.1	-0.3	0.7	1.7	1.6	3.9	2.4	0.8	-0.4	0.6	0.3	11.3
2.00-2.40	0.2	0.7	0.5	-2.9	-6.5	-8.5	-5.0	-2.1	—	4.3	—	—	-19.3
2.40-2.60	0.0	0.0	0.1	-0.2	-7.5	-10.9	-6.6	-2.5	0.5	—	9.3	0.7	-17.2
Totals	1.7	3.3	-12.2	-7.3	-15.0	-7.2	12.3	5.0	3.2	36.8	24.3	-22.9	22.0

Notes: ¹ Heat flux density values are expressed as MJ m^{-2} .

² —, indicates that temperature data were not available and heat flux was not calculated.

permafrost-zone Q_H at these locations would be sufficient to freeze 0.30 m^3 and 0.25 m^3 of ice, respectively. Results show an annual net gain for Palsa A of $45.6 \pm 0.2 \text{ MJ m}^{-2}$ at the central location and $22.0 \pm 0.1 \text{ MJ m}^{-2}$ at the peripheral location, indicating a potential aggregate annual loss of permafrost totaling 0.14 m^3 and 0.06 m^3 of ice (or a 14-cm and a 6-cm thick ice layer per m^2), respectively.

Figures 3.7 and 3.8 illustrate heat flux behavior at the Palsa A monitoring locations by plotting Table 3.3 and Table 3.4 values. Heat flux within the active layer at both locations was nominal through November 1976 due to significant L_f transfer. Heat flux maxima were most pronounced in the active layer's upper levels in response to L_f radiated prior to ice growth at depth. Ice formation at other depth intervals reflected similar contemporaneous heat transfers from freezing palsa layers to adjacent overlying layers. The February 1977 minima reflected an observational bias for all monitoring locations caused by a relatively warm mid-winter event during which two temperature readings were taken. The distinct differences between heat flux patterns for the Palsa A central and peripheral locations appear to be caused by lateral and anisotropic heat transfer resulting from palsa material heterogeneity and boundary conditions existing in proximity to the water/permafrost interface along Palsa A's margin.

The 1.3–1.55 m heat flux curve (ref. Figure 3.8) at Palsa A's periphery may be related to peatland gas pockets observed within and beneath the adjacent submerged semi-confining peat layer. Although this discussion refers to CH_4 , it is understood that peatland gases may contain CO_2 , H_2S , and/or other volatile and semi-volatile constituents — the most significant being CH_4 (Beckwith *et al.*, 2003, 2003). By measuring the duration of off-gas emissions (confirmed by ignition) after penetrating submerged peat mats with a 1.5-cm diameter hollow

metal pipe, volumetric estimates of peatland gas accumulations across the site were made. Peatland gas pockets were most prevalent around Palsa A and B, in the northern portion of the Boundary Ridge bog, and in areas where *Carex* species grew. Peatland gas pockets within and beneath the submerged semi-confining peat layer observed at depths of ± 1.2 – 1.8 m below the Boundary Ridge bog water table are estimated to range between a few cm^3 to ± 0.8 m^3 . The λ and $\sqrt{\lambda \cdot \rho c_p}$ parameters for peatland gas (i.e., CH_4) are two to three orders of magnitude less than that of water thereby contributing to conditions favorable to permafrost preservation. The L_f gain in the overlying 1.15–1.3 m stratum also indicated that freezing occurred from June–July 1977 in the 1.3–1.55 m stratum.

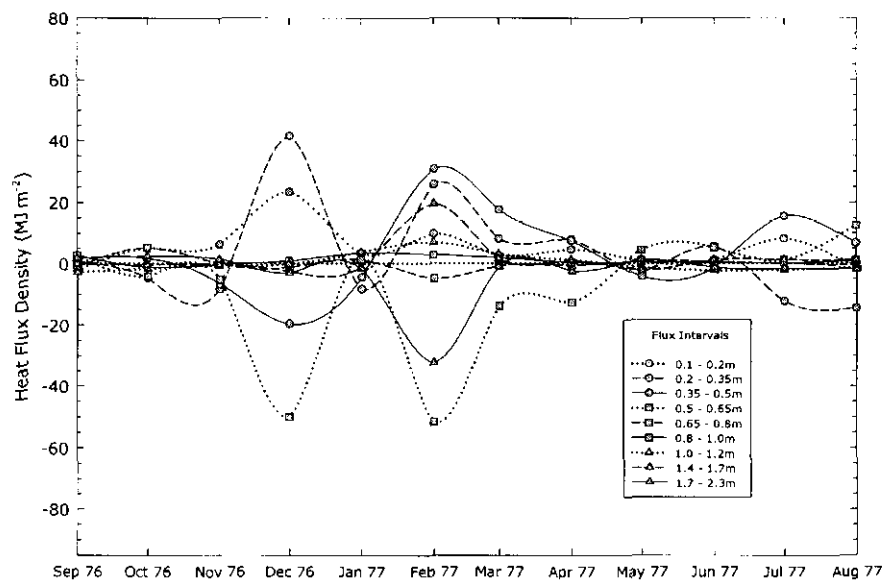


Figure 3.7. Monthly heat flux estimates for the Palsa A central monitoring location. The "zero curtain" effect is evident through November 1976 and again from May to July 1977 between which ice growth occurred from December 1976 to May 1977. Permafrost within Palsa A existed in an isothermal state for 7 months of the year.

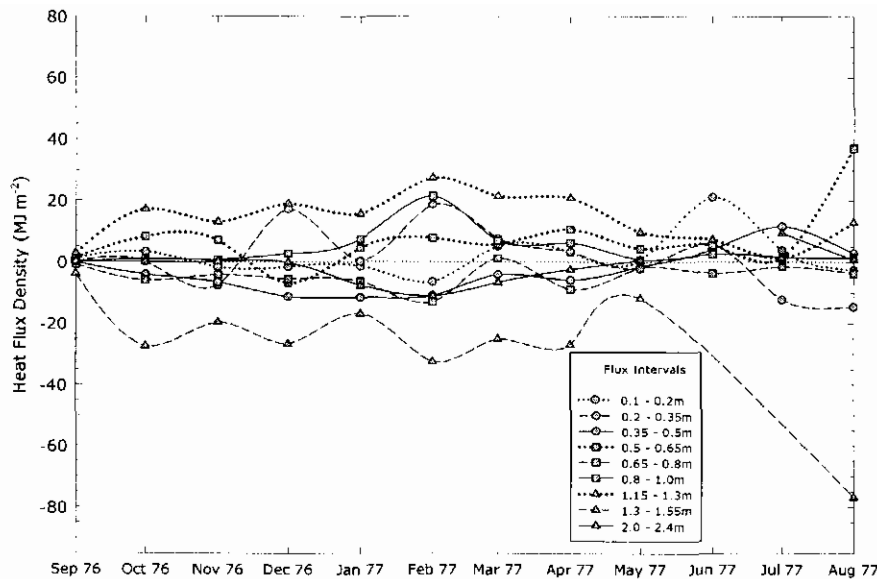


Figure 3.8. Monthly heat flux estimates for the Palsa A southern peripheral monitoring location. Lateral heat flux and other boundary conditions near the permafrost margin resulted in characteristically different heat flow patterns. Note the predominance of negative heat flow at the 1.3–1.55 m flux interval where peatland gas was present.

Figures 3.9 and 3.10 identify those depth intervals within Palsa A where heat gain and loss were prevalent. These graphs display descriptive statistics for the annual heat flux data presented in Tables 3.3 and 3.4. These statistics include the mean (dotted line), median (solid line within box), 75th percentile (upper box limit), 25th percentile (lower box limit), 95th percentile (upper whisker), and 5th percentile (lower whisker) values.

Figure 3.9 indicates Cable 1 active-layer heat gain (0.1–0.5 m), freezing in the upper permafrost zone (0.5–0.65 m), permafrost-zone isothermal conditions (0.65–1.7 m), and minimal freezing at the ice/sediment substrate interface (1.7–2.3 m). Figure 3.10 shows Cable 2 active-layer heat gain (0.1–0.35 m), active-layer heat loss (0.35–0.5 m), alternating permafrost-zone heat gain/loss (0.5–1.3 m), significant heat loss in the entrapped peatland gas layer (1.3–1.55 m), and more significant permafrost aggradation at the lower permafrost/bog interface

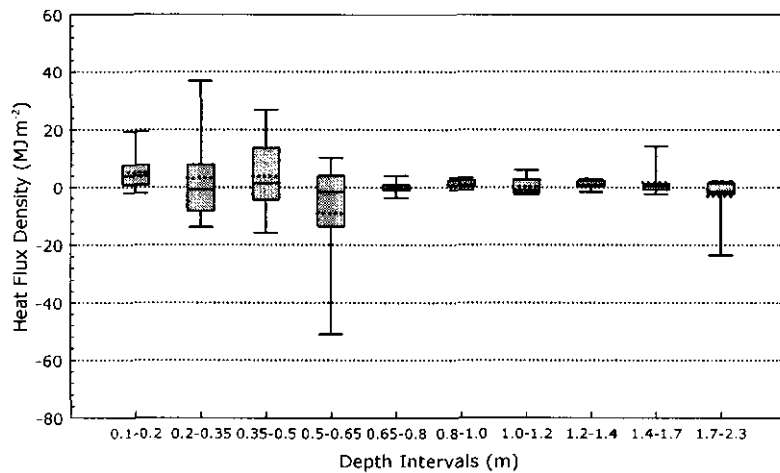


Figure 3.9. Heat flux statistics for the Palsa A central monitoring location. Conditions favorable to loss of permafrost mass existed in the active layer, below which gains in permafrost mass are evident at the upper and lower limits of the permafrost zone. Palsa A remains largely isothermal from 0.65–1.7 m.

(1.7–2.3 m) compared to Cable 1. Permafrost-zone heat gain is attributed to L_f transfer from adjacent underlying freezing strata. Despite its admitted bias toward heat loss due to the lack of June–July 1977 data, Q_H at the 1.3–1.55 m

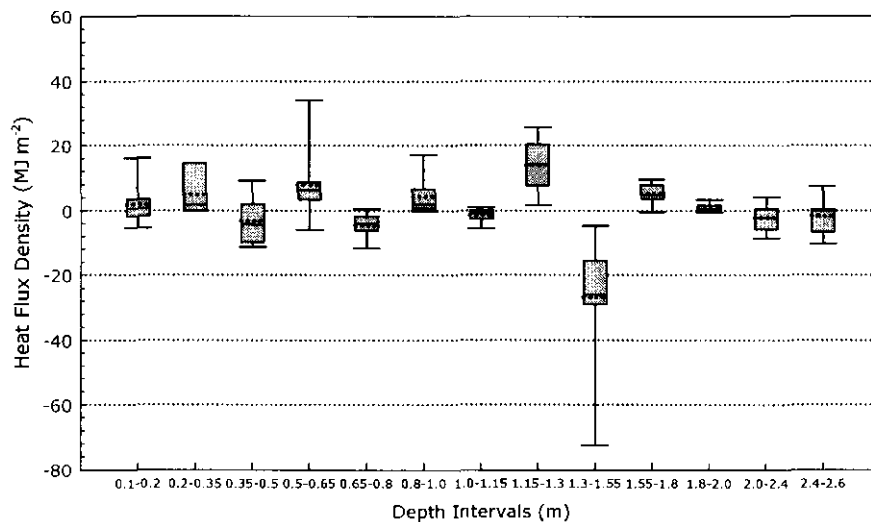


Figure 3.10. Heat flux statistics for the Palsa A southern peripheral monitoring location. With alternating intervals of heat gain and loss, most permafrost mass growth occurred within the active-layer base, 1.3–1.55 m interval, and underlying sediment interface.

depth interval was coincident with the submerged peat layer in the adjacent bog, indicating a correspondence with peatland gas pockets and suggesting the importance of peatland gas as a key palsa material. Under-estimation of the gaseous fraction within this stratum may have resulted in an over-estimation of Q_H .

3.43 Palsa B Heat Flux Dynamics

Table 3.5 summarizes Palsa B active-layer heat fluxes that are similar to those at Palsa A. Total annual active-layer (0.1–0.45 m) heat flux for Palsa B was $211.86 \pm 0.04 \text{ MJ m}^{-2}$. Deviations toward positive monthly heat fluxes within the permafrost zone during the winter season may be attributed to water intrusion along fractures and fissures, which developed in the permafrost zone as a result of thermal stress and deformation. Total annual permafrost-zone heat flux was $-86.09 \pm 0.04 \text{ MJ m}^{-2}$. Excluding other heat sinks and sources, annual net Q_H at Palsa B (0.1–1.6 m) was $125.77 \pm 0.04 \text{ MJ m}^{-2}$, sufficient to melt 0.38 m^3 of ice (or a 38-cm thick ice layer per 1-m^2 area).

Table 3.5: Summary of Estimated Heat Flux for Palsa B

Depth (m)	--- 1976 ---				----- 1977 -----								Totals
	Sep	Oct	Nov	Dec	Jan	Feb	Mar	Apr	May	Jun	Jul	Aug	
0.10-0.20	4.96	16.98	-5.74	-25.23	-8.95	-8.99	-1.73	-2.45	2.97	39.36	35.16	33.10	79.46
0.20-0.35	0.15	2.54	6.20	15.79	3.85	8.74	3.00	1.39	0.08	2.78	-1.55	-3.90	39.06
0.35-0.45	-1.66	-0.69	-13.18	77.31	23.75	27.46	5.04	3.37	-1.50	0.07	2.18	-28.79	93.34
0.45-0.60	2.08	1.41	1.16	-94.11	-19.98	-20.60	2.52	-1.80	0.72	7.54	5.62	34.05	-81.38
0.60-0.80	-0.03	0.69	-0.83	-11.37	0.46	5.45	-0.47	0.95	0.06	-3.00	0.16	0.35	-7.59
0.80-1.05	-0.14	-1.78	-0.83	0.21	2.93	0.63	3.37	3.00	1.31	1.96	0.73	2.00	13.40
1.05-1.30	0.00	2.14	0.83	0.74	-3.27	-2.95	-1.44	-1.40	-0.02	0.53	0.08	0.32	-4.42
1.30-1.60	0.33	0.11	0.47	-1.65	-2.85	-5.01	-1.05	0.43	0.91	0.22	0.91	1.09	-6.10
Totals	5.69	21.40	-11.92	-38.31	-4.06	4.73	9.24	3.49	4.53	49.46	43.29	38.22	125.77

Note: ¹ Heat flux density values are expressed as millions of joules per square meter (MJ m^{-2}).

Figure 3.11 illustrates heat flux behavior for selected depth intervals at the Palsa B monitoring location by plotting Table 3.5 values. Active-layer heat fluxes were nominal through November 1976 as a result of significant L_f transfer.

Q_H maxima and minima were most pronounced at the base of the active layer and at the upper permafrost boundary, respectively, in response to L_f radiated as the adjacent lower depth interval froze. The amplitudes of Palsa B Q_H maxima and minima were greater than those for Palsa A, reflecting the higher λ_{eff} and α_{eff}

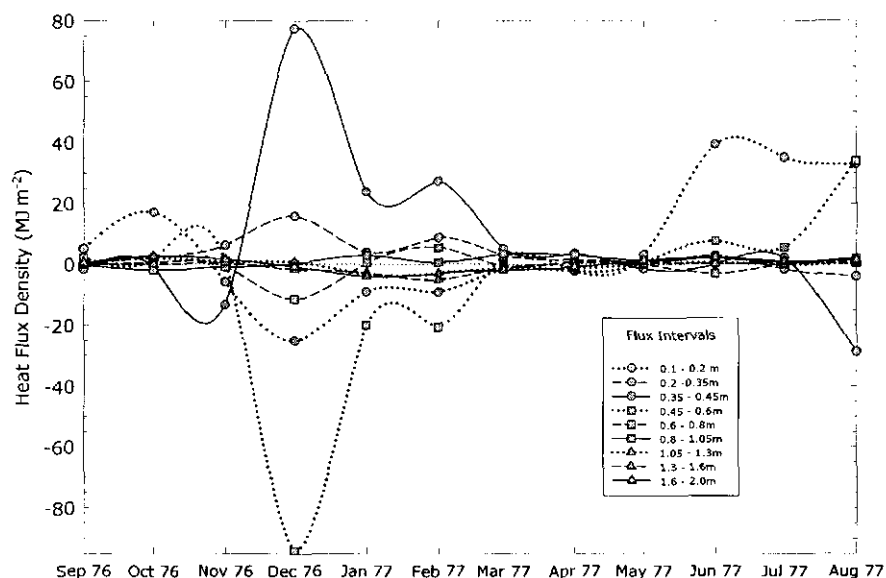


Figure 3.11. Monthly heat flux estimates for the Palsa B monitoring location. Note the "zero curtain" effect September to November 1976 and again from April to August 1977. Permafrost within Palsa B existed in an isothermal state for 8 months of the year.

of Palsa B's active-layer peat. Based on Q_{II} statistics, active-layer ice growth contributed more significantly to young-phase palsa development than permafrost-zone aggradation (see Figure 3.12).

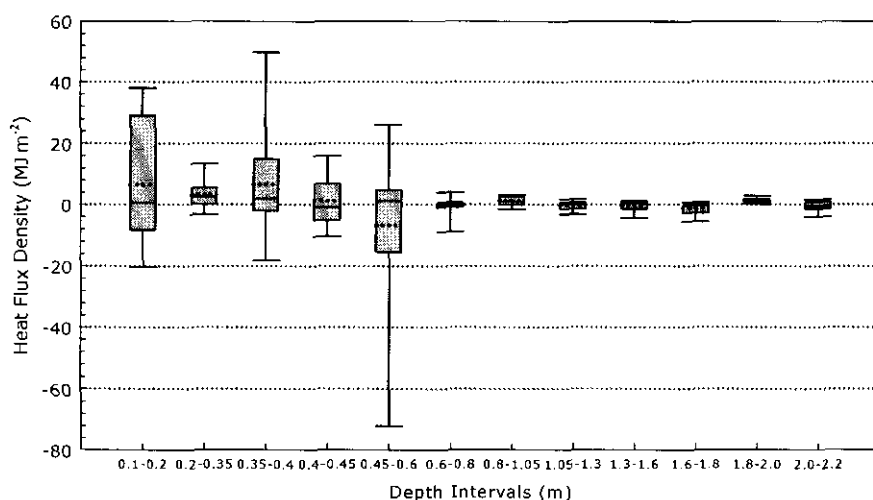


Figure 3.12. Heat flux statistics for Palsa B. As shown by the 0.45–0.6 m data, ice growth at the base of the active layer was greater than basal ice growth during the young phase of palsa development.

3.5 Survey Results

Representative closed-loop survey results presented in Figure 3.13 show a direct correlation with seasonal variations in Q_H measured at Palsa A. Survey elevation

changes coincide with observed Q_H maxima and minima since Palsa A had contacted the bog's underlying sediment substrate. Palsa A SE4 survey data indicated a net elevation gain, coinciding with anomalous permafrost aggradation at Palsa A's southern periphery. Uplift and deformation of a growing permafrost lens protrusion into the adjacent bog would account for this observation.

Palsa B showed less of a correlation with seasonal heat flux variations since it was not in contact with the underlying sediment substrate. As a result, Palsa B demonstrated a closer relationship to water table fluctuations occurring in the Boundary Ridge bog, particularly during the period from May 1977–January 1978. Although Palsa B displayed a buoyant tendency, the tensile resistance exerted by the surrounding submerged fibrous peat mat restricted the “free floating” effect.

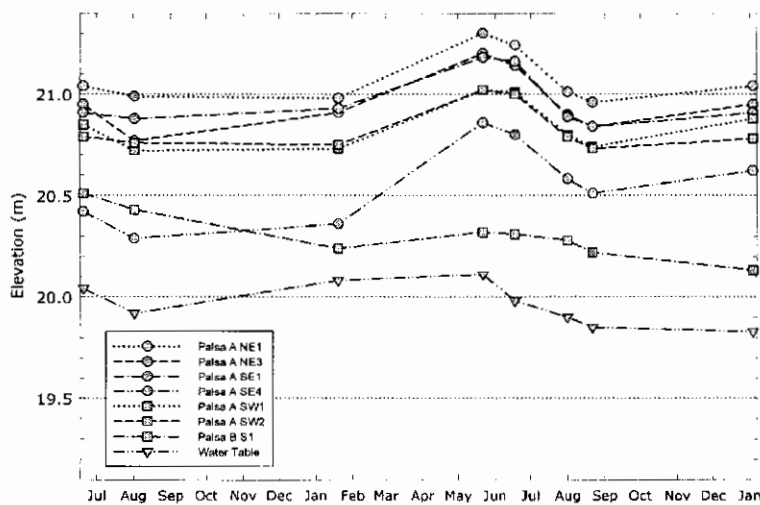


Figure 3.13. Representative survey results for Palsa A and Palsa B. Note the correlation of Palsa A ice growth and observed heat flux maxima. Palsa B shows a buoyant tendency, which varies with water table fluctuations, and less correlation with heat flux maxima.

3.6 Discussion and Conclusions

The conclusions of this study contribute to a deeper understanding of how palsa materials, processes, and bog environments influence palsa development. Active-layer ice growth was greater than permafrost-zone aggradation at Palsas A and B. Active-layer ice growth extended from November–March 1977, persisting through April 1977, at the Palsa A central monitoring location; while Palsa B active-layer ice growth extended from November 1976–March 1977. Permafrost-zone (basal) aggradation at Palsa A occurred from January–April 1977, exhibiting appreciable phase lag. Palsa B permafrost-zone (basal) aggradation occurred from December 1976–March 1977, showing less phase lag than Palsa A. Based on these findings, permafrost aggradation at the base of the active layer was prevalent during the young and mature palsa phases. Ice segregation (cryosuction) at depth was evident during the mature phase, but minimal during the young phase.

Although Palsa A experienced heat losses of lesser amplitude than Palsa B, these heat losses lasted longer resulting in more productive permafrost growth than observed at Palsa B. The higher λ_{eff} , α_{eff} , and apparent moisture retention capacity of Palsa B's active-layer peat contributed to increased net heat gain and consequently less freezing than Palsa A. The presence of peatland gas beneath Palsa B's permafrost lens also may have inhibited frost front advance at the base of the permafrost zone due to the less thermally conductive character of peatland gas pockets.

Q_H patterns observed at the Palsa A central and peripheral locations illustrated significant thermodynamic behavioral differences. Although the amplitude of sinusoidal Q_H patterns was greater at Palsa A's center than along its periphery, the duration of heat loss at the peripheral location was longer,

extending from October 1976–May 1977 at the base of the active layer. At the base of the permafrost zone, heat loss lasted from December 1976–May 1977 due to phase lag.

An anomalous heat loss pattern at the Cable 2 1.3–1.55 m depth interval indicated ice growth from October 1976 into late May 1977. Data suggest that significant permafrost aggradation occurred at this depth for at least eight months, indicating that lateral permafrost growth within and beneath the semi-confining peat layer is an important mature-phase palsa process. This conclusion confirms prior reports that permafrost in palsas assumes “mushroom-shaped” morphologies (Svensson, 1970; Zoltai and Tarnocai, 1971; Sollid and Sørbel, 1974). Excluding other heat sinks and sources, annual net Q_H was $45.6 \pm 0.2 \text{ MJ m}^{-2}$ at Palsa A’s center, $22.0 \pm 0.1 \text{ MJ m}^{-2}$ at Palsa A’s periphery, and $125.77 \pm 0.04 \text{ MJ m}^{-2}$ at Palsa B. The potential aggregate annual loss of permafrost totaled 0.14 m^3 , 0.06 m^3 , and 0.38 m^3 at the Palsa A (central), Palsa A (peripheral), and Palsa B monitoring locations, respectively. These data show a pattern of frozen mass loss and palsa degradation, which was most pronounced at Palsa B.

Survey elevation changes at Palsa A coincided with observed Q_H variations since this palsa had contacted the underlying sediment substrate. Palsa B survey data showed a weaker correlation with seasonal Q_H variations since it had not contacted the underlying sediment substrate. As a result, Palsa B demonstrated a closer relationship to water table fluctuations. Although Palsa B findings support the “buoyancy” conceptual model, the tensile resistance exerted by the surrounding submerged fibrous peat mat was shown to restrict the “free floating” effect (Kershaw and Gill, 1979; Allard *et al.*, 1986).

Interrupted only by the winter frost season, permafrost-zone isothermal conditions just below 0 °C existed within Palsa A and Palsa B for approximately seven and eight months of the year, respectively. L_f released as the frost front advanced, and absorbed as the frost front receded, helped preserve isothermal conditions within the Boundary Ridge palsas throughout most of the year. The $\sqrt{\lambda \cdot \rho c_p}$ of palsa materials—especially peat, air, and peatland gas—influenced palsa thermodynamics by favoring heat loss during the winter frost season to heat gain during the summer thaw season. This thermodynamic characteristic of palsas is important to both young-phase and mature-phase palsa development. The presence of insulating peatland gas beneath Palsa B's permafrost lens appears to have significantly affected Q_H and isothermal conditions at Palsa B by preserving permafrost-zone mass. These findings lend credence to the view that peatland gas is a key palsa material affecting palsa emergence and development.

The submerged semi-confining peat layer at the Boundary Ridge bog partitioned hydrogeologic system flow and attenuated surface heat transfer between the overlying unconfined water-bearing zone and the lower semi-confined water-bearing zone. Entrapped gas pockets impeded K_v and K_h by limiting the amount of interconnected pore space available for hydraulic flow. The peat layer created a static water column beneath it, which perpetuated isothermal conditions within the lower water-bearing zone near or below $\pm 4^\circ\text{C}$ throughout much of the year and isothermal aqueous temperatures near 0 °C for at least eight months of the year. Peatland gas pockets trapped within and beneath the peat layer help: (a) insulate permafrost lenses from heat gain, (b) uplift the permafrost mass, (c) improve permafrost's probability to endure, and (d) account for the circular form palsas typically assume. These conditions created a year-round environment favoring opportunistic frost front advance at

depth and requiring minimal energy exchange as frost fronts advanced. Based on these observations, the peat layer contributed significantly to creating site conditions conducive to palsa emergence and development.

The foregoing investigation findings provide new perspectives on how synergies between palsa materials, processes, and time affect thermodynamic flux in palsas and hydrogeologic flow within the wetlands that host them. This research demonstrates the value of year-round geomorphologic studies to deepen our understanding of periglacial phenomena.

Acknowledgements

We thank Richard Cossette who, along with many McGill Subarctic Research Station summer interns, provided exceptionally dedicated support during the field research program. We also acknowledge Hardy Granberg and Tim Moore for providing ongoing support, Garry Werren for conducting the plant assessments, and Michael Przybyla for drafting the site maps and plans. This research was funded by Iron Ore Company of Canada and Environment Canada grants, and various McGill University research assistantships, fellowships, and stipends.

Chapter 4:

A Conceptual Model of Dynamic Geomorphologic Processes Acting on Palsas at Boundary Ridge near Schefferville, Québec

Context in Thesis

This manuscript presents a conceptual model of palsa geomorphologic development based on data and observations at the Boundary Ridge site. It incorporates thermodynamic and hydrogeologic process findings discussed in Manuscript No. 1 into a new conceptual model of palsa development.

This manuscript introduces original research on palsa material behavior, peatland hydrogeology, and wetland biogeochemical fate and transport phenomena into a generalized dynamic process model that synthesizes key elements of the existing “buoyancy”, “ecocline”, and “snowpack” conceptual palsa development models (Fries and Bergström, 1910; Lundqvist, 1961; Sjörs, 1961; Zoltai, 1972; Railton and Sparling, 1973; Kershaw and Gill, 1979; Seppälä, 1982, 1986, 1994). The conceptual model presented here postulates: (a) what pre-existing site conditions are necessary for palsa development, (b) how palsas develop from the point of initial ice nucleation, and (c) where palsas are likely to occur in the future. Certain speculative elements of the proposed dynamic process model suggest opportunities for future research contributions that will advance our collective understanding of how earth material behavior, near-surface geomorphologic processes, and time conjoin to affect palsa development.

Abstract

A 12-month study of palsa dynamics investigated physical and biogeochemical processes affecting palsa development near Schefferville, Québec. Site observational and heat flux data collected at the Boundary Ridge site from September 1976 to August 1977 show how geomorphologic processes in palsas change over time by assessing palsas at varying developmental stages. This study provides new insights into how the changing character and behavior of palsa materials, antecedent ice nucleation, and peatland hydrogeology affect palsa genesis, development, and decline. By synthesizing thermodynamic and hydrogeologic data with ancillary research findings and key elements of existing palsa conceptual models, a new dynamic conceptual model of palsa development is presented that explains: (a) what pre-existing site conditions are necessary for palsa development, (b) how palsas develop from the point of initial ice nucleation, and (c) where palsas are likely to occur in the future.

4.1 Introduction

This paper presents the findings of a 12-month study of palsa dynamics near the Schefferville, Québec area of the Canadian subarctic. It focuses on unpublished site observations made at the Boundary Ridge site and heat flux data collected from September 1976 to August 1977 at two palsas in different stages of development. The overarching goal of this research was to investigate palsa geomorphologic processes through the systematic analysis of seasonally changing thermodynamic patterns. This research attempts to answer the following questions: (1) what are the character and behavior of materials (*i.e.*, peat, water, ice, and gases [particularly methane and air]) comprising palsas?, (2) what are the underlying physiochemical processes affecting heat

transfer within palsas?, (3) how do palsa materials affect dynamic processes?, and (4) how do the materials and processes evolve over time to influence palsa systems near Schefferville, Québec?

4.2 Physical Setting

The Boundary Ridge study site (the “site”) is a ± 0.8 -ha palsa bog within a perched basin abutting the Québec-Newfoundland provincial border roughly 12 kilometers west-northwest of Schefferville, Québec (see Figure 4.1). Situated near the transition between sporadic to widespread discontinuous permafrost zones in northern Québec, the site’s geographical coordinates are $55^{\circ} 3' 12''\text{N}$, $67^{\circ} 15' 18''\text{W}$. Resting at the foot of Boundary Ridge’s talus-covered southwestern slope, the site lies at an elevation of 800 m ASL with local topography gradually sloping southwesterly toward the Howells River valley.

Using conventional terminology (Seppälä, 1986), three palsas occur at the site including a $\pm 171\text{-m}^2$ and $\pm 0.9\text{-m}$ high mature palsa located in the north-central portion of the wetland (Palsa A), a $\pm 32\text{-m}^2$ and $\pm 0.6\text{-m}$ high young palsa located in the southern portion of the wetland (Palsa B), and a $\pm 25\text{-m}^2$ and $\pm 0.4\text{-m}$ high mature palsa situated in the eastern portion of the wetland (Palsa C), which was previously disturbed by foot traffic and not suitable for research. Three thermokarst depressions within the bog mark the locations of what are believed to have been former palsas.

The site is characterized by hydrogeologic system flow above and below the semi-confining peat layer and seasonal frost layer during different times of the year. Rainfall and snow/ice meltwater contribute oxygenated water to the

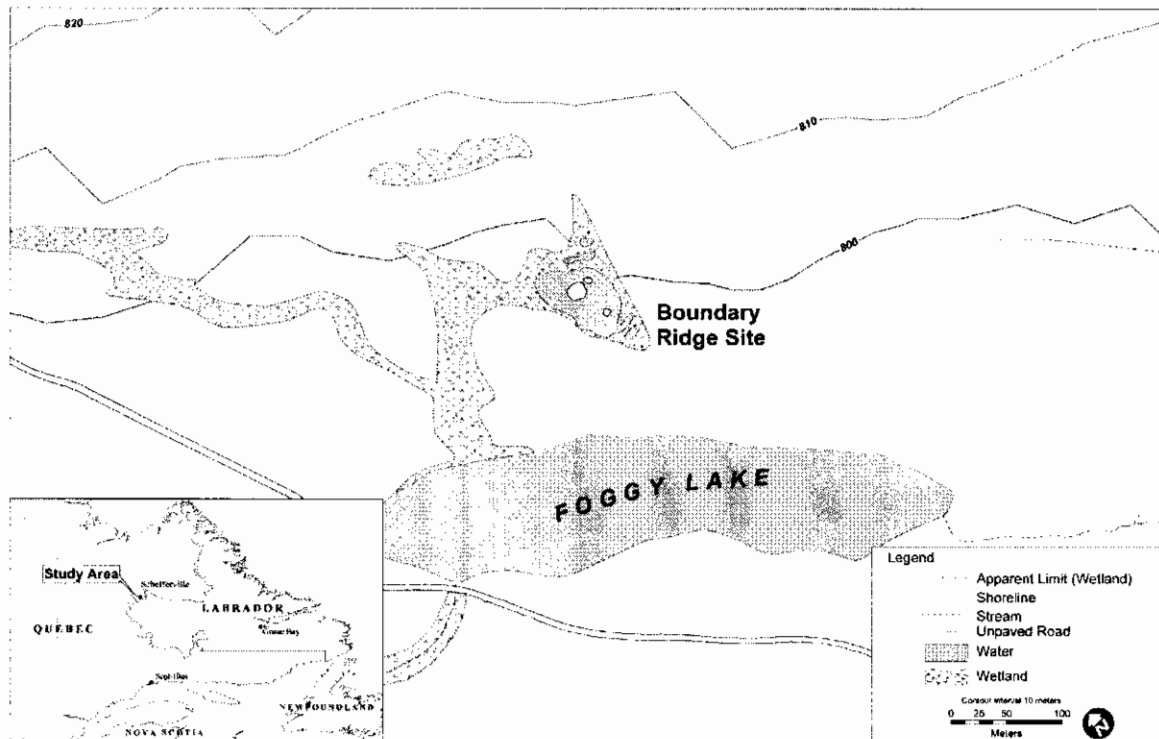


Figure 4.1. Boundary Ridge Site Map. (Contours derived from Shuttle Radar Topography Mission data provided by USGS) [Drafted by M. Przybyla]

upper aerobic water-bearing zone while anoxic mineral-laden groundwater likely flows through the lower semi-confined water-bearing zone as a result of an underlying contact fault between the Lower Slate member (Ruth Formation) and the Denault Dolomite (see Figure 4.2). Discharging to Foggy Lake, the inferred southerly surface water/groundwater flow direction is affected by the seasonal frost, semi-confining peat layer, permafrost, and bedrock controls of the northwest-southeasterly trending raised valley within which the perched Boundary Ridge palsa bog is located. The dominant *Sphagnum* moss/sedge community surrounding the palsa bog acidifies surface water and groundwater migrating through the site (see Figure 4.3).

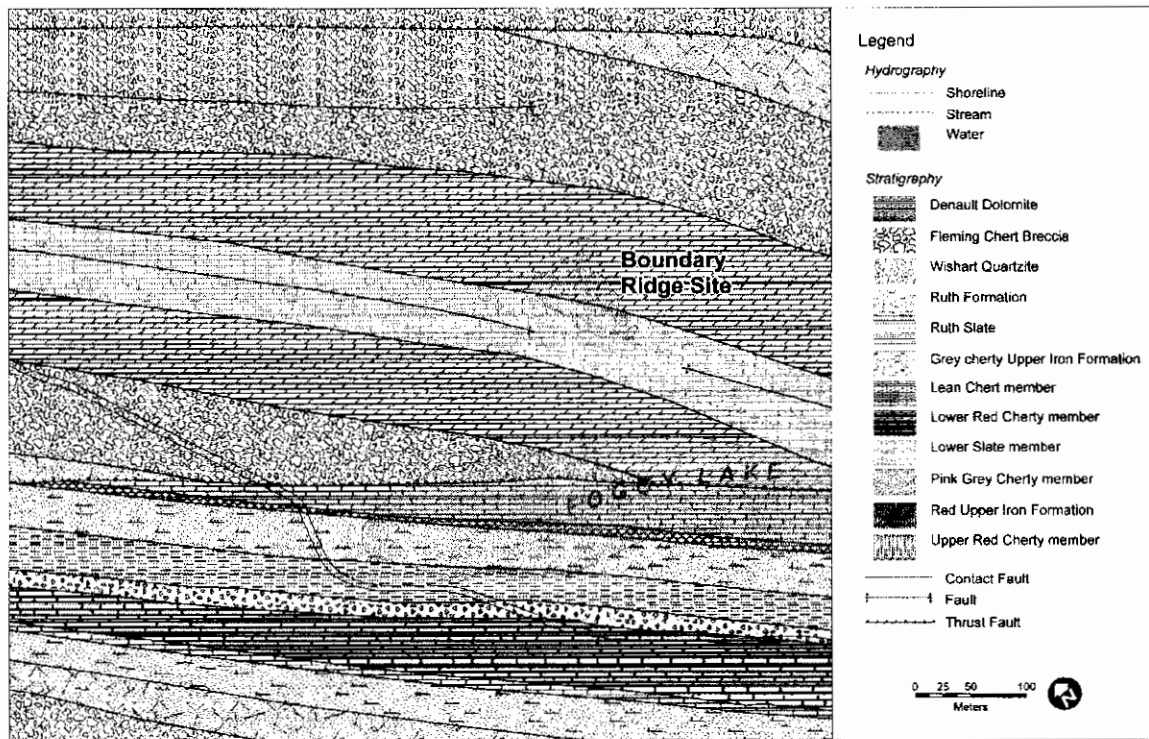


Figure 4.2: Bedrock Geology Map. (Reeves, 1972; Neimant-Verdriet and Krishnamurty, 1973)
[Drafted by M. Przybyla]

4.3 Palsa Material Behavior, Fate, and Transport

The evolving physical and biogeochemical properties of palsa materials strongly influence the geomorphologic processes operating upon palsas at the Boundary Ridge site. The single most important earth material determining the course of palsa development is peat. Peat exercises appreciable control over palsa development not only as a stratigraphic unit controlling thermodynamic and hydrogeologic processes in peatlands, but also through its unique physical and biogeochemical properties as a palsa-forming material, and source of decomposition byproducts including humic gels, other humic substances, and peatland gases, particularly methane (CH_4).

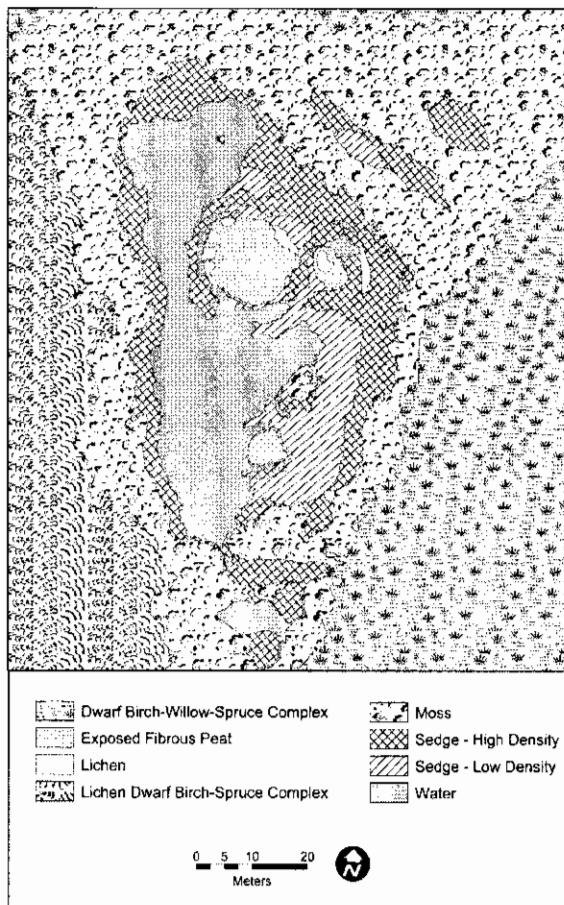


Figure 4.3. Vegetation Map. (from color infrared aerial photography). [Drafted by M. Przybyla]

4.31 Moisture Retention Hysteresis in Peat

Peat's ability to retain moisture far in excess of its dry bulk weight is well known (Fuchsman, 1986). The manner in which peat responds to environmental change over time is less well known, particularly concerning its hydrophobic behavior.

The moisture retention characteristics of peat demonstrate a pronounced hysteresis that is well documented by agricultural, wetland, and plant scientists (Egglesmann, 1988). This notable characteristic behavior of peat as a

key palsa material has been completely ignored in the palsa literature.

Water retention hysteresis in peat results from physical and biogeochemical changes that occur within peat deposits. When subjected to recurrent drying and rewetting cycles, peat loses its ability to retain moisture by up to $\pm 80\%$ over time (Fuchsman, 1986). This hysteretic behavior is attributed to both matrix compression as water evacuates interstitial voids within peat deposits and structural collapse of the peat fabric (*i.e.*, shrinkage) as it dries resulting in a diminished water retention capacity (Price and Schlotzhauer, 1999; Price and Waddington, 2000).

Recent studies show that water retention hysteresis in peat is driven by the biogeochemical behavior of humic gels as the humic substances comprising peat deposits undergo environmental change. Using low-field nuclear magnetic resonance relaxometry, scientists have investigated the kinetics of peat wetting processes at the microscopic scale (Langford *et al.*, 2002; Schaumann *et al.*, 2002). In conventional non-humic porous media, capillary forces tend to drive matrix rewetting from the smallest to the largest interstitial voids. Humic porous media rewet in accordance with increasing levels of activation energy, imbibing macropores first, then mesopores, and finally micropores.

When peat deposits are displaced from hydrodynamic equilibrium during the drying process, the time required to restore equilibrium includes the time needed for imbibition plus the time necessary for the collapsed rigid peat fabric to once again relax to accommodate the infusion of interstitial water (Lu and Pignatello, 2002; Mooney, 2003). As peat deposits dry, the gels contained within them also collapse thereby resulting in very slow aqueous uptake extending for up to tens of days before finally reaching micropores. Rewetting of dried humic gels requires activation energies well above 40 kJ mol^{-1} to affect the necessary “chemical” reconfiguration allowing water reinfusion (Langford *et al.*, 2002).

Since peat deposits experience substantial shrinkage of the peat fabric with drying, the cumulative effect of these physical and biogeochemical changes greatly improves both the degree and persistence of insulation afforded by exposed peat deposits. Direct observations at the Boundary Ridge site indicate that the desiccation of exposed peat deposits occurs predominantly under extended severe winter conditions and secondarily during shorter dry summer periods, consistent with earlier findings (Salmi, 1970; Seppälä, 1982).

4.32 Peatland Gas as a Key Palsa Material

The role that peatland gas plays as a key earth material in palsa development has also been largely ignored, although CH₄ production within boreal peatlands has been identified as a significant atmospheric carbon emission source (Beswick *et al.*, 1998; Moore *et al.*, 1998; Nykänen *et al.*, 2003). *Archaeal* methanogens populate the submerged semi-confining peat layer and metabolize the peat substrate thereby generating CH₄, CO₂, and in certain sulfide-rich aquifers H₂S. Peatland gases may contain CO₂, H₂S, and/or other volatile and semi-volatile constituents — the most significant of which is CH₄.

Trapped beneath the submerged semi-confining peat layer across the Boundary Ridge site, peatland gas is generated as the site's sedges, reeds, *Sphagnum* moss, insect carcasses, and other biological detritus undergo methanogenic decomposition during the peat-forming process. Investigators have reported high dissolved CH₄ concentrations and CH₄ gas at depths of ±0.7–3 m below the water table within and beneath semi-confining peat layers resulting from decomposing older peat substrate and younger plant biomass (Romanowicz *et al.*, 1993; Chanton *et al.*, 1995; Blodau and Moore, 2003).

Peatland gas accumulates in wetlands throughout the Schefferville, Québec area. By measuring the duration of off-gas emissions (confirmed by ignition) after penetrating submerged peat mats with a 1.5-cm diameter hollow metal pipe, volumetric estimates of peatland gas accumulations across the site were made. Peatland gas pockets were most prevalent near the Palsa A and B perimeters, in the northern portion of the Boundary Ridge bog, and generally in areas where *Carex* species grew. Gas pockets within and beneath the Boundary

Ridge bog's submerged peat layer observed at depths of ± 1.2 – 1.8 m below the water table were estimated to range between a few cm^3 to ± 0.8 m^3 .

Peatland gas results from the metabolism of available carbon-bearing substrate by native *Archaeal* methanogens under optimal year-round saturated conditions (Siegel *et al.*, 2001; Blodau and Moore, 2003). Researchers report that a “bubble confining layer” exists within submerged semi-confining peat layers where methanogenesis creates localized zones of over-pressurized CH_4 gas capable of ejecting a bolus of pore water 2 m above ground (Romanowicz *et al.*, 1995). Gas bubbles entrapped within peat have been shown to reduce hydraulic conductivity in both the vertical (K_v) and horizontal (K_h) directions (Baird and Waldron, 2003; Kellner *et al.*, 2004). Melloh and Crill (1996) and Friborg *et al.* (1997) also have reported significant seasonal variations in peatland gas emissions associated with the thawing of snow and ice cover in bogs, and the episodic release of peatland gas that accumulated over the preceding winter season.

The presence of peatland gas at the Boundary Ridge site is critical to palsa emergence and development. Among palsa materials, peatland gas is second only to air as an effective insulator (see Table 4.1, λ and $\sqrt{\lambda \cdot \rho c_p}$ values). The highly effective insulating qualities of peatland gas, particularly CH_4 , help

Table 4.1: Palsa Material Properties

Parameter	ρ (kg m^{-3})	λ ($\text{W m}^{-1} \text{ }^\circ\text{K}^{-1}$)	c_p ($\text{J kg}^{-1} \text{ }^\circ\text{K}^{-1}$)	L_f (kJ kg^{-1})	α ($\times 10^{-7} \text{ m}^2 \text{ s}^{-1}$)	$\sqrt{\lambda \cdot \rho c_p}$ ($\text{kJ m}^{-2} \text{ s}^{-1/2}$)
Peat	105.92	0.066	1550	—	4.02	104.1
Water ¹	999.70	0.587	4193	—	1.40	1568.6
Ice	917.00	2.177	1958	334	12.1	1977.1
Methane ²	0.68	0.033	2223	58	218.31	22.3
Snow	300.00	0.160	2090	0.058	2.55	316.7
Air	1.29	0.025	1005	—	192.83	5.7

Notes: ¹ Values published or calculated for 10°C .

² Values published or calculated for 0°C .

preserve frozen mass during warmer months by limiting direct aqueous contact and providing a thermal buffer against thaw along the lower surfaces of nascent peat-/sediment-containing ice lenses. Since growing ice lenses often possess downwardly concave profiles, they also trap small amounts of peatland gas over time thereby increasing the likelihood for permafrost aggradation.

4.33 Interaction of Peat and Peatland Gas in Palsa Development

Peatland gas accumulation within and beneath the semi-confining peat layer helps maintain an “open” structure within the tightly-woven peat mat. Gas-filled void spaces within the peat fabric provide favorable sites where opportunistic ice nucleation and continued freezing of materials within the submerged peat layer can occur when local environmental conditions permit.

Peat facilitates the lateral transport of aqueous fluids and gases while impeding vertical migration (*i.e.*, $K_h > K_v$) within the submerged semi-confining peat layer as a result of its anisotropic character (Beckwith *et al.*, 2003, 2003). Peatland gas bubbles themselves impede lateral groundwater migration by reducing the amount of interconnected pore space available for liquid flow (Baird and Waldron, 2003; Kellner *et al.*, 2004). The anisotropic and heterogeneous nature of the submerged semi-confining peat layer and the mobility of peatland gas pockets are believed to induce optimal conditions within the Boundary Ridge wetland for palsa emergence and development through opportunistic ice nucleation, continued ice lens growth, and permafrost mass preservation.

4.4 Process-Focused Conceptual Model of Palsa Development

Since environmental conditions within wetlands change over time scales of 10s, 100s, and 1000s of years, palsa emergence and development is the end-product of the complex interaction of an array of dynamic geomorphologic processes responding to temporal and spatial variations in key palsa materials and site-specific conditions. The dynamic conceptual model of palsa development presented here synthesizes key elements of the existing “buoyancy”, “ecocline”, and “snowpack” conceptual palsa models to conceive a new process model of palsa development. The conceptual model uses Seppälä’s terminology (1986) to identify phases of palsa development —embryonic, young, mature, and collapsing— for convenience alone, recognizing that these terms are not optimal from a process perspective. In reality, palsa development at any given time may exhibit one or more of these phase characteristics within all or any portion of the landform depending on site-specific conditions.

4.41 Embryonic Phase

Peat deposition within wetland environments is a necessary precursor to palsa emergence. As other investigators have postulated (Harris and Nyrose, 1992), an undisturbed accumulation of peat extending at least 1.5 m in thickness is sufficient to support palsa emergence near the distal limit of permafrost occurrence, considering that peat loses nearly half its thickness upon exposure to the atmosphere. Continual deposition of decaying biomass produces a tightly-woven peat fabric of biological detritus exhibiting anisotropic and heterogeneous structural characteristics and hydraulic/pneumatic behavior (*i.e.*, dual porosity) that facilitates lateral flow while inhibiting vertical flow (Ours *et al.*, 1997).

Continued peat deposition and decay eventually results in the creation of a submerged peat layer that may be in direct contact with or suspended above the underlying wetland substrate and contain entrained mineral sediment. Once established, the semi-confining peat layer partitions hydrologic flow through the wetland into an overlying aerobic water-bearing unit and an underlying anoxic water-bearing unit (Reeve *et al.*, 2000). *Archaeal* methanogens populate the semi-confining peat layer and metabolize the peat substrate thereby generating CH₄ and other gases. Ongoing methanogenesis generates significant amounts of gaseous CH₄, preferentially distributed in the ±0.7–3 m depth interval within and beneath the submerged peat layer where *Archaeal* methanogens reside (Romanowicz *et al.*, 1995; Siegel *et al.*, 2001; Blodau and Moore, 2003; Nykänen *et al.*, 2003).

Additional investigative findings suggest that elevated trace metal (Fe, Ni, and Co) and base cation (Ca, Na, and Li) concentrations may stimulate increased CH₄ production by endemic methanogens (Basiliko and Yavitt, 2001). Both of these conditions are believed to exist at the Boundary Ridge site. Figure 4.3 shows where *Carex* species grow near palsas. Iron-bearing Fleming Chert Breccia and Lower Slate (Ruth Formation), and calcium-bearing Denault Dolomite formations also occur within the site's catchment area (see Figure 4.2).

Due to the highly anisotropic and heterogenic nature of the semi-confining peat layer, peatland gas accumulations migrate laterally within the wetlands forming gas pockets of varying volume. Within these areas of accumulation, many gas/water interfaces exist where antecedent ice nucleation—the precursor of palsa emergence—randomly occurs. Triggered by seasonally advancing frost fronts, wetland conditions suitable for ice nucleation are optimized by the presence of a static water column maintained at year-round

temperatures approaching or less than 4°C, which perpetuate isothermal aqueous temperatures near 0°C for at least eight months of the year beneath the semi-confining peat layer (see Figure 4.4c and d).

Requiring minimal energy transfer, opportunistic ice nucleation, continued peat layer freezing, and ice lens coalescence within the submerged peat layer gradually produces a sufficient frozen mass to persist through successive warm seasons. Peatland gas pockets trapped beneath the downwardly concave permafrost lens help: (a) insulate it from heat gain, (b) uplift the permafrost mass, (c) improve its probability to endure, and

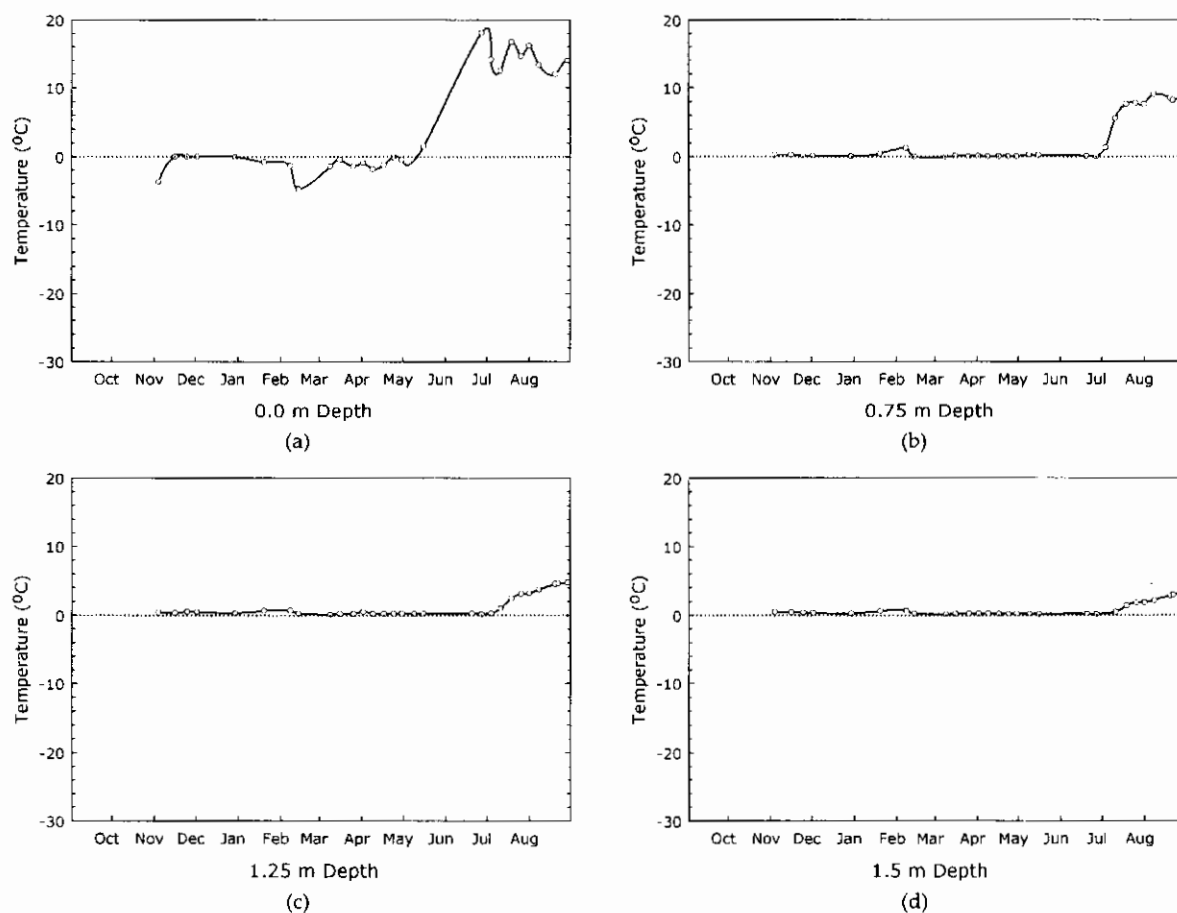


Figure 4.4. Annual temperature variations at the background bog monitoring location (Cable 5).

(d) account for the circular form palsas typically assume. Seigel *et al.* (2001) and Christensen *et al.* (2004) have observed peatland gas entrapment by seasonal ice released during annual thaw cycles.

Gaining and losing elevation with seasonal water table fluctuations, embryonic (and also young) palsas are suspended within the wetland's semi-confining peat layer (ref. Figure 4.5, Palsa B S1 data, and Figure 4.6, Equipment Installation Plan). Growing permafrost lenses begin to affect changes in the surrounding wetland. Uplift of the frozen peat layer above the water table with continued permafrost lens growth and peatland gas accumulation exposes the overlying peat to subaerial desiccation (more pronounced during the winter than summer months) and freezing (Salmi, 1972; Sollid and Sørbel, 1974; Seppälä, 1982). Evidence of winter desiccation and frost cracking was observed in April–June 1977 at the Boundary Ridge site where an embryonic palsa —10 m southwest of Palsa A— displayed extensive surficial micro-fissures in the exposed dried peat layer resulting from the prior winter's extreme weather conditions.

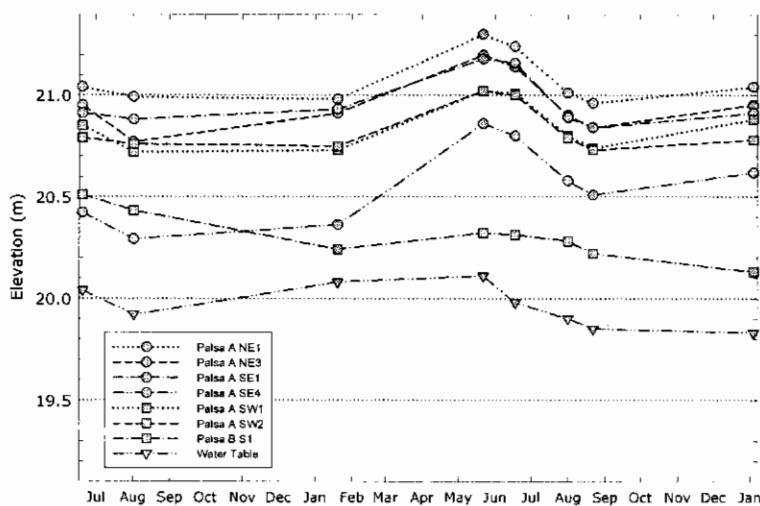


Figure 4.5. Representative survey results for Palsa A and Palsa B. Note the correlation of Palsa A permafrost growth and observed heat flux maxima. Palsa B shows a buoyant tendency, which varies with wetland water table fluctuations, and shows less of a correlation with heat flux maxima.

Mirroring the seasonal growth patterns of more developed palsas (see Figure 4.5), embryonic palsas exhibit a pulsating cyclic behavior whereby they protrude above the wetland surface from January through May and recede below the wetland surface during the remainder of the year. The embryonic phase of palsa development gradually transitions into the young phase as snow cover decreases during successive winter seasons, the palsa remains exposed above the water table throughout the year, and year-round heat transfer becomes optimized to aggrade permafrost mass.

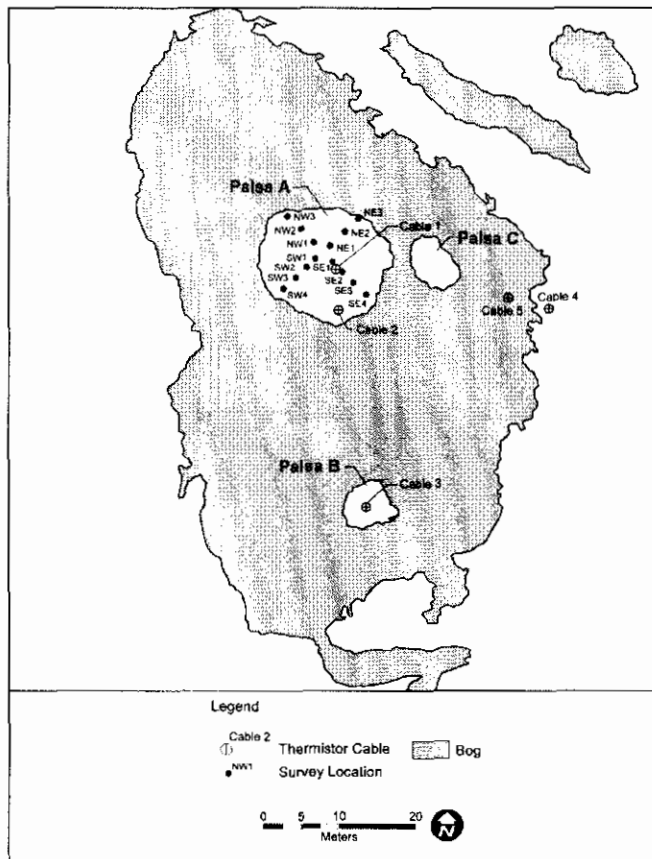


Figure 4.6. Equipment Installation Plan. [Drafted by M. Przybyla]

4.42 Young Phase

Peat responds to yearly atmospheric drying/rewetting cycles by gradually losing its ability to retain water in response to physical and biogeochemical changes within its fabric. This material transformation in peat's behavior improves its capacity as a highly effective insulator and drives landform progression into the young phase of palsa development. Young palsas accumulate permafrost mass

along the now continually exposed upper air/water interface at the base of the active layer and preserve permafrost mass (while incorporating frozen

peat/sediment) along the submerged lower peatland gas/water interface. As continued active layer expansion affects changes in the thermal properties of palsa materials, thermodynamic processes gradually limit heat gain through the active layer due to the “heat valve” effect (Gold and Lachenbruch, 1973).

The period of most productive ice aggradation begins with persistent palsa exposure above the water table when palsa materials, hydrogeologic processes, and thermodynamic flux: (a) maximize winter-season heat loss while minimizing winter-season heat efflux phase lags, and (b) minimize summer-season heat gain while maximizing summer-season heat influx phase lags. Decreased snow cover, increased active-layer depth, and proximity of the permafrost mass to the surface help maximize heat loss during this phase. Figure 4.7 depicts the spatial and temporal heat flux variations indicative of the young phase of palsa development.

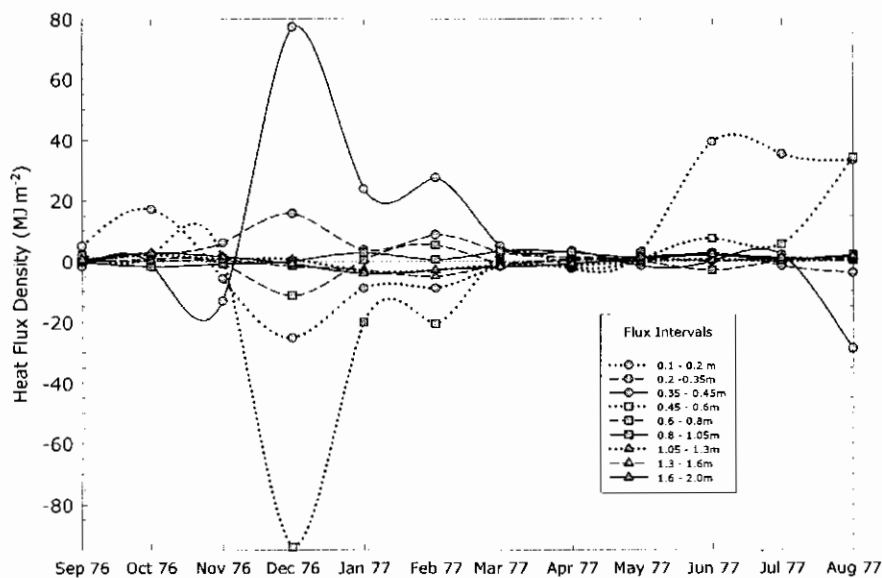


Figure 4.7. Monthly heat flux estimates for the Palsa B monitoring location. Note the “zero curtain” effect September to November 1976 and again from April to August 1977. Permafrost within Palsa B existed in an isothermal state for 8 months of the year.

Palsas achieve optimal conditions for ice aggradation when elevated heat loss through the central portion of the permafrost zone occurs, the suspended

permafrost core and underlying wetland substrate make contact, and cryosuction within the underlying sediment substrate ensues. Lateral peat-layer ice lenses also grow along the palsa perimeter as peatland gas is displaced outward from the palsa's central permafrost zone to collect beneath permafrost lens protrusions forming the "mushroom-cap" morphology at the palsa periphery reported by others (Svensson, 1970; Zoltai and Tarnocai, 1971; Sollid and Sørbel, 1974).

Peatland gas migration toward the palsa periphery beneath downwardly concave permafrost lens protrusions during this dynamic process creates additional regions for opportunistic permafrost aggradation while the central permafrost core gradually attains a condition of isothermal equilibrium. Gas pockets trapped in the adjacent peat layer also coalesce as lateral ice lens growth imparts a characteristically circular shape to palsas. This process results in differential uplift and permafrost deformation consistent with prior research findings (Åhman, 1976; Allard and Rousseau, 1999). Based on survey data collected at the Boundary Ridge site, contemporaneous differential uplift and subsidence, responding to thermodynamic flux within palsas, cause internal deformation and complex cryotic fabrics (cf. Figure 4.5, Palsa A NE1 and Palsa A SE4 data).

4.43 Mature/Collapse Phase

Continued palsa growth results in: (a) diminished snow cover over elevated portions of palsas, (b) increased snow cover along the palsa periphery, (c) increased exposure to abrasive winter processes, and (d) increasing loss of peat fabric integrity, which mark the advent of thermokarst processes characteristic of the mature/collapse phase (Seppälä, 1982, 2003). Continued

palsa aggradation also results in ever increasing heat gain across an enlarging exposed surface area as palsas grow in height and circumference. Increased distance between the central and peripheral permafrost core diminishes the preservative influence (*i.e.*, thermal inertia) of the central permafrost core, resulting in eventual palsa collapse.

Although these events gradually contribute to palsa decline within certain portions of the palsa, permafrost continues to aggrade in other portions of the palsa, particularly in peripheral zones where optimal conditions for opportunistic peat-layer ice growth remain. Figures 4.8 and 4.9 illustrate marked spatial and temporal variations in near-surface heat transfer within palsas as simultaneously aggrading and degrading portions of palsas respond dynamically to the endogenic geomorphologic processes and exogenic environmental factors acting upon them. This dynamic process helps explain why circular palsa ramparts remain after the central permafrost core undergoes thermokarst erosion and subsidence (Seppälä, 1986). The disparity between heat flux patterns occurring within the permafrost core of palsas reflects the dynamic differences in near-surface earth processes, evolving material behavioral characteristics, and thermal/mass fluxes during this phase.

The mature/collapse phase of palsa development continues as increased surficial weathering, thermokarst erosion, and block calving contribute to palsa degradation and net loss of permafrost mass (Seppälä, 1986; Zuidhoff, 2002; Seppälä, 2003). Eventually all that remains is a circular depression too deep for sedge and reed species to grow where a fully formed palsa once existed.

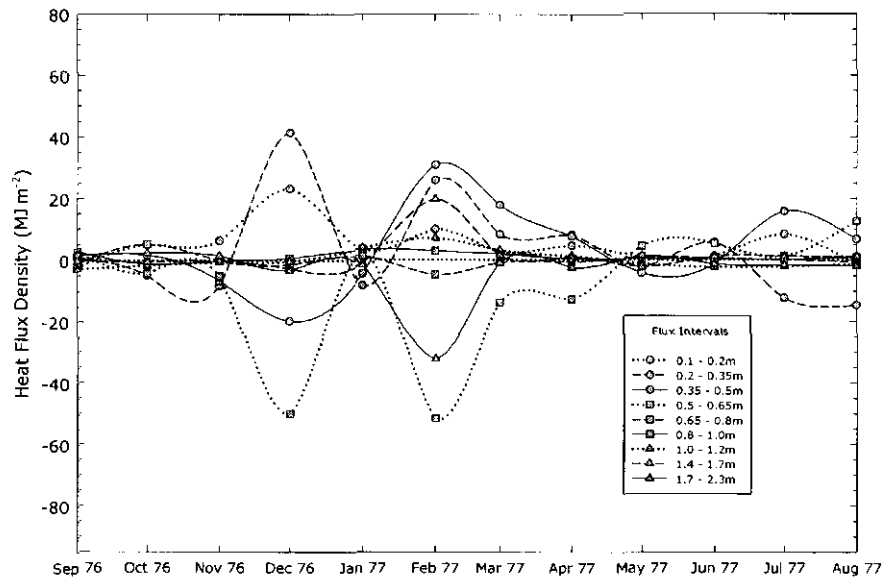


Figure 4.8. Monthly heat flux estimates for the Palsa A central monitoring location. The “zero curtain” effect is evident through November 1976 and again from May to July 1977 between which ice growth occurred from December 1976 to May 1977. Permafrost within Palsa A existed in an isothermal state for 7 months of the year.

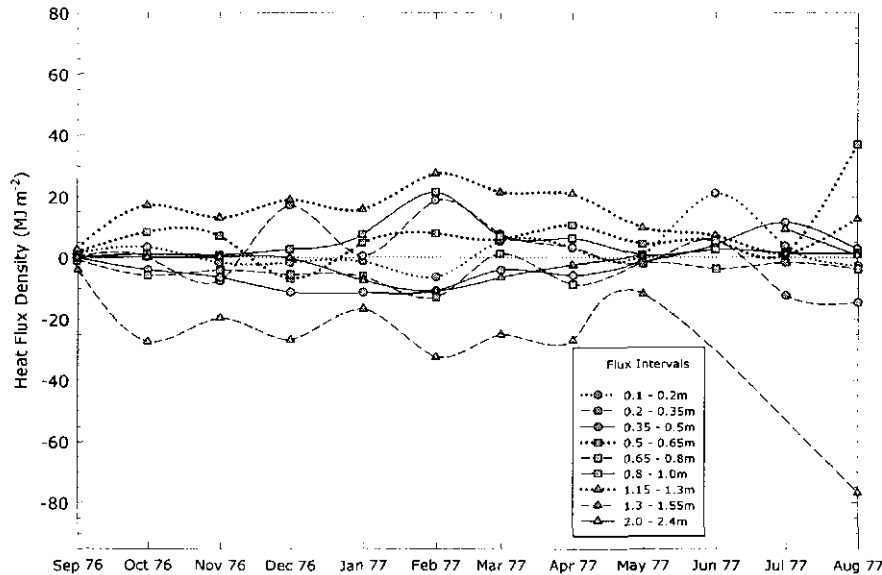


Figure 4.9. Monthly heat flux estimates for the Palsa A southern peripheral monitoring location. Lateral heat flux and other boundary conditions near the permafrost margin resulted in characteristically different heat flow patterns. Note the predominance of negative heat flow at the 1.3–1.55 m flux interval where peatland gas was present.

4.44 Palsa Recurrence

Since palsas may be present in various phases of development at the same location, the emergence of palsas within host wetlands is a continually cyclic process, which reflects no appreciable climatic influence as long as local environmental parameters remain within favorable thermodynamic and hydrogeologic process boundaries. The re-emergence of these landforms at the

site of a former palsa is predicated upon the subsequent re-establishment of a saturated peat layer at least 1.5-m thick (near the distal limit of discontinuous permafrost; less under colder conditions) to: (a) support sufficient peatland gas production and accumulation at depth, (b) accommodate shrinkage upon exposure to the elements, and (c) provide over time a sufficiently thick unsaturated active layer favoring permafrost aggradation. Palsa re-emergence at such sites will only occur after sufficient peat deposition, peatland gas production and accumulation once again create site conditions conducive to the onset of antecedent ice nucleation and continued permafrost aggradation.

4.5 Discussion and Conclusions

The dynamic interaction between palsa materials, local environmental factors (*i.e.*, climatic, geologic, etc.), and geomorphologic processes determines the pattern of palsa development. Recognition of the critical roles played by all palsa materials —peat, water, ice, air, and peatland gas— in palsa geomorphology enables a deeper understanding of when, where, how, and why these unique landforms evolve.

The evolving thermodynamic, geochemical, and structural properties of palsa materials strongly influence palsa genesis, emergence, aggradation, decline, and recurrence. Water retention hysteresis in peat is a key factor in establishing localized site conditions conducive to palsa genesis and emergence. Peatland gas pockets promote antecedent peat-layer ice nucleation and permafrost mass preservation necessary for palsa emergence and growth. Given its non-conductive nature, peatland gas trapped beneath nascent peat-layer ice lenses helps preserve permafrost mass throughout all phases of palsa development.

Peatland gas migration from beneath central palsa permafrost zones toward peripheral zones of mature palsas supports lateral permafrost protrusions into surrounding wetlands. Differential uplift and deformation facilitated by peatland gas present at the palsa periphery contributes to a complex permafrost fabric in palsas and helps explain why palsa ramparts persist above the water table after the central palsa permafrost core has degraded and subsided below the wetland surface.

The semi-confining peat layer, which entraps peatland gas, in wetlands preferentially regulates thermodynamic and hydrogeologic flow through this boreal wetland. The peat layer optimizes conditions suitable for opportunistic ice nucleation by perpetuating the year-round presence of static water column and isothermal aqueous temperatures near 0 °C in the lower water-bearing zone. Such conditions minimize the energy needed for ice nucleation, and optimize conditions suitable for continued ice aggradation and preservation in palsas.

Palsa development is predicated upon the existence of a sufficiently thick saturated peat layer that accommodates shrinkage upon exposure to the elements, supports development of an unsaturated active layer favorable to permafrost aggradation, and enables sufficient peatland gas production and accumulation at depth. Palsa re-emergence within boreal peatlands only occurs after sufficient peat deposition, gas production, and gas accumulation once again create site conditions conducive to the onset of antecedent ice nucleation and continued permafrost aggradation.

Since palsas may be present in various phases of development at the same location, the emergence of palsas within host wetlands is a continually cyclic process, which reflects no appreciable climatic influence as long as local

environmental parameters remain within favorable thermodynamic and hydrogeologic process boundaries. Further investigation of changing palsa material properties, peatland gas distribution within boreal peatlands, and hydrogeologic controls will yield valuable insights into palsa genesis, development, decline, and recurrence.

Acknowledgements

We thank F.H. Nicholson for the original opportunity to conduct palsa geomorphologic studies at McGill University and the McGill Subarctic Research Station (MSARS). Along with many MSARS summer interns, Richard Cossette provided exceptionally dedicated support during the field research program. We also thank Tim Moore and Hardy Granberg for providing ongoing support, Garry Werren for conducting the plant assessments, and Michael Przybyla for drafting the site maps and plans. This research was funded by Iron Ore Company of Canada and Environment Canada grants, and various McGill University research assistantships, fellowships, and stipends.

Chapter 5:

Research Summary, Thesis Conclusions, and Future Research

5.1 Introduction

Existing palsa research has not adequately delved into the complexities of palsa geomorphologic systems. This thesis explores the dynamic nature of geomorphologic processes, earth material behaviors, and the resulting feedback/response systems that are central to palsa emergence, development, decline, and recurrence.

The preoccupation by certain periglacial scientists with a morphocentric approach at the expense of a more complete understanding of key underlying palsa geomorphologic processes has deflected attention away from important matters and postponed scientific progress. By not appreciating the equifinality of geomorphologic processes, the morphocentric approach risks misinterpretation of field observations when investigators fail to realize that different earth surface processes may manifest in apparently similar landform expressions (Chorley and Kennedy, 1971). This prevailing condition underscores the need for long-term year-round study of permafrost landforms to avoid misinterpreting unrelated landforms as palsas.

This research investigated palsa geomorphology through a systematic analysis of seasonally changing thermodynamic patterns. This study sought to begin filling several significant data gaps including:

- What are the character and behavior of palsa materials (*i.e.*, peat, water, ice, peatland gas, and air)?

- What are the underlying physical and chemical processes affecting heat transfer within palsas?
- How do earth materials and processes within palsas interact?, and
- How do these earth materials and processes change over time to cumulatively affect the evolution of palsa geomorphologic systems near Schefferville, Québec?

5.2 Research Summary and Thesis Conclusions

This section confirms or refutes each of the hypotheses proposed in Chapter 1 (ref. Section 1.8) in light of the lines of evidence established by this study. Based on the facts and conclusions presented in Chapters 2–4, the hypotheses that have driven the research effort at the Boundary Ridge site are evaluated as follows:

5.21 Hypothesis No. 1

This hypothesis asserts that palsa heat budget estimates are indices of whether palsas are aggrading or degrading in the vicinity of Schefferville, Québec. The lines of evidence that confirm or refute this hypothesis include the following:

- The heat flux (Q_H) estimates detailed in Chapter 3 (ref. Sections 3.42–3.43) indicate that the mature-phase Palsa A and young-phase Palsa B generally were experiencing frozen mass degradation from 1976–1977. Annual net Q_H for Palsa A ranged from $22.0 \pm 0.1 \text{ MJ m}^{-2}$ (at its periphery) to $45.6 \pm 0.2 \text{ MJ m}^{-2}$ (at its center). Averaging more than $3\frac{1}{2}$ times the annual net heat flux observed at Palsa A, annual net heat flux for Palsa B was $125.77 \pm 0.04 \text{ MJ m}^{-2}$.

- The heat budget estimate for Palsa A's peripheral location was less than half that observed at its center. This difference was due in part to an anomalous annual net loss of at least $-268.5 \pm 0.1 \text{ MJ m}^{-2}$ within the 1.3–1.55 m depth interval (ref. Table 3.4), which was absent at Palsa A's central thermal monitoring location. Under-estimation of the gaseous fraction within this stratum may have resulted in an over-estimation of Q_H .
- Excluding other heat sinks and sources, annual net Q_H was $45.6 \pm 0.2 \text{ MJ m}^{-2}$ at Palsa A's center, $22.0 \pm 0.1 \text{ MJ m}^{-2}$ at Palsa A's periphery, and $125.77 \pm 0.04 \text{ MJ m}^{-2}$ at Palsa B. The potential aggregate annual loss of frozen mass totaled 0.14 m^3 , 0.06 m^3 , and 0.38 m^3 at the Palsa A (central), Palsa A (peripheral), and Palsa B thermal monitoring locations, respectively. These data show a pattern of palsa frozen mass loss, which was most pronounced at Palsa B.
- As direct physical measurements, Palsa A survey data show a general correlation with annual heat flux estimates when phase lags are taken into account (cf. Figure 3.13 and Tables 3.2–3.4). Survey points near Palsa A's center lost an average of 2 cm in elevation while peripheral survey points gained an average of 4 cm in elevation. Survey elevation changes at Palsa A coincided with observed Q_H variations since this palsa's frozen mass had contacted the underlying frozen sediment substrate, which limited buoyant response to the influence of seasonal water table fluctuations.
- Palsa B survey data showed a weaker correlation with seasonal Q_H variations since it had not contacted the underlying frozen sediment substrate. As a result, Palsa B exhibited buoyant response to, and a closer relationship with, seasonal water table fluctuations.

Based on these findings, Hypothesis No. 1 is preliminarily true with qualifications. Palsas A and B appeared to be in a state of marginal decline during the study term. The Q_H estimates appear to be indices of the physical state of palsas as long as the underlying assumptions of Fourier's Law were not violated.

5.22 Hypothesis No. 2

This hypothesis contends that near-surface thermal patterns in palsas vary as palsas progress through the developmental sequence based on the changing behavioral characteristics of palsa materials. The lines of evidence that confirm or refute this hypothesis include the following:

- As discussed in Chapter 3, Figures 3.7–3.12 illustrate distinct differences in the amplitude and duration of near-surface thermal patterns evident in young-phase Palsa B and mature-phase Palsa A. This study also documents marked differences between the near-surface thermal patterns observed at the central and peripheral thermal monitoring locations within the mature-phase Palsa A (ref. Sections 3.42–3.43).
- Interrupted only by the winter frost season, permafrost-zone isothermal conditions just below 0 °C existed within Palsa A and Palsa B for approximately seven and eight months of the year, respectively. L_f released as the frost front advances and absorbed as the frost front recedes helped preserve isothermal conditions within the Boundary Ridge palsas throughout most of the year. The $\sqrt{\lambda \cdot \rho c_p}$ of palsa materials—especially peat, air, and peatland gas— influenced palsa thermodynamics by favoring heat loss during the winter frost season to heat gain during the summer thaw season. This thermodynamic characteristic of palsas is important to both young-

phase and mature-phase palsa development. The presence of insulating peatland gas beneath Palsa B's permafrost lens appears to have significantly affected Q_H and isothermal conditions at Palsa B by preserving permafrost-zone mass. These findings lend credence to the view that peatland gas is a key palsa material affecting palsa emergence and development.

- Active-layer ice growth was greater than permafrost-zone aggradation at Palsas A and B. Active-layer ice growth extended from November–March 1977, persisting through April 1977, at the Palsa A central monitoring location; while Palsa B active-layer ice growth extended from November 1976–March 1977. Permafrost-zone (basal) aggradation at Palsa A occurred from January–April 1977, exhibiting appreciable phase lag. Palsa B permafrost-zone (basal) aggradation occurred from December 1976–March 1977, showing less phase lag than Palsa A. Ice growth at the base of the active layer contributed more significantly to young-phase palsa development than ice growth within or at the base of the permafrost zone.
- Although Palsa A experienced heat losses of lesser amplitude than Palsa B, these heat losses lasted longer resulting in more productive frozen mass aggradation than observed at Palsa B. The higher λ_{eff} , α_{eff} , and apparent moisture retention capacity of Palsa B's active-layer peat contributed to increased net heat gain and consequently less frozen mass aggradation than Palsa A. The presence of peatland gas beneath Palsa B's permafrost lens also may have inhibited ice front advance at the base of the permafrost zone due to the less thermally conductive character of peatland gas pockets.
- Q_H patterns observed at the Palsa A central and peripheral locations illustrated significant thermodynamic behavioral differences. Although the

amplitude of sinusoidal Q_H patterns was greater at its center than along its periphery, the duration of heat loss at the peripheral location was longer, extending from October 1976–May 1977 at the base of the active layer. At the base of the permafrost zone, heat loss lasted from December 1976–May 1977 due to phase lag. The distinct differences between annual heat flux density patterns for the Palsa A central and peripheral monitoring locations is suspected to be caused by lateral and anisotropic heat transfer resulting from both earth material heterogeneity and boundary conditions existing in proximity to the water/permafrost interface along Palsa A's margin.

- The evolving thermodynamic, biogeochemical, and structural properties of peat change with time and strongly influence palsa genesis, emergence, aggradation, and decline. Water retention hysteresis in peat is a key factor in establishing localized site conditions conducive to palsa genesis and emergence. Continued exposure to annual drying/rewetting cycles enhances the insulating qualities of the peat-constituent active layer, allowing active layer expansion to be optimized for continued mature-phase palsa growth. Subaerial weathering processes thereafter degrade peat's fabric and lead to palsa degradation and decline.
- The behavior, fate, and transport of peatland gas control the process of ice nucleation and palsa development in subarctic peatlands. Peatland gas accumulation at depth within and beneath the submerged semi-confining peat layers of boreal wetlands is believed to be central to palsa development, determining where palsa genesis and emergence will occur. Among palsa materials, peatland gas (with CH_4 as its primary constituent) is second only to air as an effective insulator (ref. Table 4.1, λ and $\sqrt{\lambda \cdot \rho c_p}$ values). Gas

pockets entrapped beneath downwardly concave nascent peat-layer ice lenses help preserve permafrost mass throughout all phases of palsa development.

- Peatland gas migration from beneath central palsa permafrost zones toward peripheral zones of mature palsas supports lateral permafrost protrusions into surrounding wetlands. Differential uplift and deformation caused by ice growth and preservation in the presence of peatland gas at the palsa periphery contributes to a complex permafrost fabric in palsas (ref. Section 3.5). Gas migration helps explain why palsa ramparts persist above the water table after the central palsa permafrost core has degraded and subsided below the wetland surface.
- Current scientific consensus contends that supra-permafrost ice aggradation and ice segregation at depth both exert significant influence over the course of palsa development (Seppälä, 1982; Harris, 1989). The Boundary Ridge data confirm that supra-permafrost ice aggradation at the base of the active layer affects young- and mature-phase palsa growth. Significant permafrost aggradation through ice segregation (cryosuction) at depth was evident within the mature-phase Palsa A and minimal within the young-phase Palsa B.

Based on these findings, Hypothesis No. 2 has been proven true. The evolving behavior, fate, and transport of palsa materials in boreal wetlands are key determinants of the course that palsa development takes.

5.23 Hypothesis No. 3

This hypothesis asserts that the submerged peat layer in bogs affects thermodynamic and hydrogeologic flow thereby facilitating aggradation of frozen

mass and preservation of permafrost mass in palsas. The lines of evidence that confirm or refute this hypothesis include the following:

- The Boundary Ridge bog's submerged semi-confining peat layer, being comprised of a tightly interwoven plant-litter fabric, partitioned hydrogeologic system flow and attenuated surface heat transfer between the overlying unconfined water-bearing zone and the lower semi-confined water-bearing zone. The amplitude and periodicity of subaerial temperature disturbances obvious in the shallow-bog surface water above the semi-confining peat layer were significantly attenuated or absent below the submerged peat layer (see Figure 3.6).

The anisotropic and heterogeneous character of the peat deposit's tightly interwoven plant-litter fabric avails dual porosity (*i.e.*, $K_h > K_v$) to the semi-confining peat layer. Restricting vertical hydraulic flow within the wetland, the semi-confining peat layer separates the upper aerobic water-bearing zone from the underlying anoxic water-bearing zone. The peat layer created a static water column beneath it, which perpetuated isothermal conditions within the lower water-bearing zone near or below $\pm 4^\circ\text{C}$ throughout much of the year and isothermal aqueous temperatures near 0°C for at least eight months of the year. These conditions created a year-round environment favoring opportunistic ice nucleation and growth at depth and requiring minimal energy exchange as frost fronts advanced. Based on these observations, the peat layer contributed significantly to creating site conditions conducive to palsa emergence and development.

- The peat layer's dual porosity, which results from the tightly interwoven plant-litter fabric, also limits vertical pneumatic flow within wetlands. The

submerged peat layer enables preferentially lateral peatland gas migration, fosters peat-layer ice lens protrusions at the palsa periphery, and facilitates continued permafrost aggradation. Within areas of peatland gas accumulation, many peatland gas/water interfaces exist where antecedent ice nucleation —the precursor of palsa emergence— randomly occurs. Peatland gas bubbles themselves impede lateral groundwater migration by reducing the amount of interconnected pore space available for liquid flow (ref. Section 4.3). Conjoining with the favorable thermodynamic conditions afforded by the submerged peat layer, peatland gas pockets promote antecedent peat-layer ice nucleation and permafrost mass preservation necessary for palsa emergence and growth.

Based on these findings, Hypothesis No. 3 has been proven true. The evolving behavior, fate, and transport of palsa materials in boreal wetlands are central to determining the course of palsa development.

5.3 Suggested Future Research

The foregoing research findings offer insights into the seasonal thermodynamic behavior and geomorphologic processes of palsas at the Boundary Ridge site. Based on year-round observational data, several conclusions were reached that contribute to a deeper understanding of how palsa materials, near-surface processes, and wetland environments influence embryonic-, young-, and mature-phase palsa geomorphology.

This study underscores the necessity for year-round research programs at other locations to fully understand the earth processes contributing to palsa inception, growth, decline, and recurrence. The foregoing investigation

findings and conclusions provide new perspectives on how the synergies between earth materials, near-surface earth processes, and time affect the thermodynamics operating upon palsas and the hydrogeology of the wetlands that host them. In its attempt to fill significant data gaps in our understanding of palsa geomorphology, this research uncovered new areas of scientific interest including:

- The need to investigate the year-round behavior, fate, and transport of CH_4 and other peatland gas constituents as key agents in palsa and related permafrost-induced landform development. Much attention has been given to document CH_4 emissions from boreal wetlands, but very little to ascertain the nature, distribution, and seasonal variability of peatland gas occurrence within and beneath submerged peat layers within palsa bogs. Thermal data from the Palsa A peripheral monitoring location, where peatland gas presence is believed to have produced anomalous results, call for more focused and intensive study. These study findings suggest that CH_4 may assume properties under pressurized and extremely cold winter conditions similar to near-surface clathrates reported in Canadian Arctic permafrost.
- The need for further investigations into how boreal wetland hydrogeology and biogeochemistry control palsa, and related permafrost-induced landform, genesis and development. Although beyond the scope of this thesis, further detailed assessment of the distribution, fate, and transport of organic (*i.e.*, CH_4 , humic gels, and other humic substances) and inorganic (*e.g.*, Fe^- , Ca^+ , etc.) compounds in boreal wetlands may offer valuable insights into ice/permafrost aggradational and degradational processes.

References

- Åhman, R. 1976. The structure and morphology of palsas in northern Norway. *Biuletyn Peryglacjalny*. 26:25-31.
- Åhman, R. 1977. Palsas in northern Norway. In The Royal University of Lund, Sweden, Department of Geography Publication No. 78. 165 pp.
- Åkerman, H.J. 1982. Observations of palsas within the continuous permafrost zone in eastern Siberia and in Svalbard. *Geografisk Tidskrift*. 82:45-51.
- Åkerman, H.J., and B. Malmström. 1986. Permafrost mounds in the Abisko area, northern Sweden. *Geografiska Annaler Series A (Physical Geography)*. 68:155-165.
- Allard, M., and L. Rousseau. 1999. The internal structure of a palsa and a peat plateau in the Riviere Boniface region, Québec: inferences on the formation of ice segregation mounds. *Geographie physique et Quaternaire*. 53:373-387.
- Allard, M., M.K. Seguin, and R. Lévesque. 1986. Palsas and mineral permafrost mounds in northern Québec. In *International Geomorphology, Part II*. V. Gardiner, editor. J. Wiley and Sons Ltd, Chichester. 285-309.
- Allington, K.R. 1961. The bogs of central Labrador-Ungava: an examination of their physical characteristics. *Geografiska Annaler Series A (Physical Geography)*. 43:401-417.
- An, W., and M. Allard. 1995. A mathematical approach to modeling palsa formation: insights on processes and growth conditions. *Cold Regions Science and Technology*. 23:231-244.
- Baird, A.J., and S. Waldron. 2003. Shallow horizontal groundwater flow in peatlands is reduced by bacteriogenic gas production. *Geophysical Research Letters*. 30(20):2043, doi:10.1029/2003GL018233.
- Baranov, I.Y. 1959. Geographical distribution of seasonally frozen ground and permafrost. In *Principles of Geocryology: Part I, General Geocryology*. P.F. Švetsov, editor. Academy of Sciences of the USSR, V.A. Obruchev Institute of Permafrost Studies, Moscow.
- Barr, D.R., and R.K. Wright. 1981. Selected climatological data, 1955-1980 for the Schefferville (A) Station. *McGill Subarctic Research Paper*. 32:117-134.
- Basiliko, N., and J.B. Yavitt. 2001. Influence of Ni, Co, Fe, and Na additions on methane production in *Sphagnum*-dominated Northern American peatlands. *Biogeochemistry*. 52:133-153.

- Baženova, A.P. 1953. Thermal insulation effect on water migration in freezing ground. In *Materialy po Laboratornym Issledovaniyam Merzlykh Gruntov*. Izdatel'stvo Akademii Nauk SSSR. Vol. 1, Moscow.
- Beckwith, C.W., A.J. Baird, and A.L. Heathwaite. 2003. Anisotropy and depth-related heterogeneity of hydraulic conductivity in a bog peat. I: Laboratory experiments. *Hydrological Processes*. 17:89-101.
- Beckwith, C.W., A.J. Baird, and A.L. Heathwaite. 2003. Anisotropy and depth-related heterogeneity of hydraulic conductivity in a bog peat. II: Modeling the effects on groundwater flow. *Hydrological Processes*. 17:103-113.
- Beskow, G. 1935. Soil freezing and frost heaving with special application to roads and railroads. Technological Institute, Northwestern University. 196 pp.
- Beswick, K.M., T.W. Simpson, D. Fowler, T.W. Choularton, M.W. Gallagher, K.J. Hargreaves, M.A. Sutton, and A. Kayes. 1998. Methane emissions on large scales. *Atmospheric Environment*. 32:3283-3291.
- Blake, W. 1974. Periglacial features and landscape evolution, central Bathurst Island, District of Franklin. In *Geological Survey of Canada Paper 74-1B*, Ottawa. 235-244.
- Blodau, C., and T.R. Moore. 2003. Micro-scale CO₂ and CH₄ dynamics in a peat soil during a water fluctuation and sulfate response. *Soil Biology & Biochemistry*. 35:535-547.
- Blyakharchuk, T.A., and L.D. Sulerzhitsky. 1999. Holocene vegetational and climatic changes in the forest zone of western Siberia according to pollen records from extrazonal palsa bog Bugristoye. *The Holocene*. 9:621-628.
- Bolz, R.E., and G.L. Tuve. 1973. CRC Handbook for Applied Engineering Science. CRC Press, Inc., Cleveland, Ohio.
- Brown, R.J.E. 1963. The relation between mean annual air and ground temperatures in the permafrost region of Canada. In *Proceedings of the International Conference on Permafrost*, Lafayette, Indiana. 241-247.
- Brown, R.J.E. 1968. Occurrence of permafrost in Canadian peatlands. In *Proceedings of the Third International Peat Conference*. National Research Council of Canada, Québec, Canada. 174-181.
- Brown, R.J.E. 1968. Permafrost investigations in northern Ontario and northeastern Manitoba. In *Division of Building Research Technical Paper No. 291*. National Research Council of Canada. 40 pp.

- Brown, R.J.E. 1973. Ground ice as an initiator of landforms in permafrost regions. *In* Research in Polar and Alpine Geomorphology, Proceedings of the 3rd Guelph Symposium on Geomorphology. B.D. Fahey and R.D. Thompson, editors. Geo Abstracts Ltd. (University of East Anglia), Norwich, GB. 25-42.
- Brown, R.J.E. 1973. Influence of climatic and terrain factors on ground temperatures at three locations in the permafrost region of Canada. *In* Permafrost: North American Contribution to the Second International Conference on Permafrost. National Academy of Sciences, Yakutsk, Siberia. 27-34.
- Brown, R.J.E. 1975. Permafrost investigations in Québec and Newfoundland (Labrador). National Research Council of Canada, Division of Building Research, Ottawa. 36 pp.
- Brown, R.J.E., and W.O. Kupsch. 1974. Permafrost terminology. 62 pp.
- Brown, R.J.E., and T.L. Péwé. 1973. Distribution of permafrost in North America and its relationship to the environment: a review, 1963-1973. *In* Permafrost: North American Contribution to the Second International Conference on Permafrost. National Academy of Sciences, Yakutsk, Siberia. 71-100.
- Carslaw, H.S., and J.C. Jaeger. 1947. General theory. *In* Conduction of Heat in Solids. Clarendon Press, Oxford. 1-49.
- Carslaw, H.S., and J.C. Jaeger. 1947. Linear heat flow: the infinite and semi-infinite solid. *In* Conduction of Heat in Solids. Clarendon Press, Oxford. 50-91.
- Chanton, J.P., J.E. Bauer, P.H. Glaser, D.I. Siegel, C.A. Kelley, S.C. Tyler, E.H. Romanowicz, and A. Lazrus. 1995. Radiocarbon evidence for the substrates supporting methane formation within northern Minnesota peatlands. *Geochimica et Cosmochimica Acta*. 59:3663-3668.
- Chorley, R.J., and B.A. Kennedy. 1971. Physical Geography: A Systems Approach. Prentice-Hall International Inc., London. 370 pp.
- Christensen, T.R., T. Johansson, H.J. Åkerman, M. Mastepanov, N. Malmer, T. Friberg, P. Crill, and B.H. Svensson. 2004. Thawing sub-arctic permafrost: Effects on vegetation and methane emissions. *Geophysical Research Letters*. 31:L04501, doi:10.1029/2003GL018680.
- Collins, E.I., R.W. Lichvar, and E.F. Evert. 1984. Description of the only known fen-palsa in the contiguous United States. *Arctic and Alpine Research*. 16:255-258.

- Coultish, T.L., and A.G. Lewkowicz. 2003. Palsa dynamics in a subarctic mountainous environment, Wolf Creek, Yukon Territory, Canada. *In* Proceedings of the 8th International Conference on Permafrost, 21-25 July 2003. M. Phillips, S.M. Springman, and L.U. Arenson, editors. International Permafrost Association, Zurich, Switzerland. 163-168.
- Cummings, C.E., and W.H. Pollard. 1989. An investigation of palsas in the Schefferville area, Québec. *The Musk-Ox*. 37:8-18.
- Cummings, C.E., and W.H. Pollard. 1990. Cryogenic classification of peat and mineral cored palsas in the Schefferville area, Québec. *In* Permafrost, Canadian Proceedings of the Fifth Canadian Permafrost Conference. Vol. Nordicana Collection No. 54, Laval, QC. 95-102.
- Cutnell, J.D., and K.W. Johnson. 1995. Physics. J. Wiley & Sons, New York. 315 pp.
- De Vries, D.A., and A.J. Peck. 1958. On the cylindrical probe method of measuring thermal conductivity with special reference to solids, I. Extension of theory and discussion of probe characteristics. *Australian Journal of Physics*. 11:255-271.
- Delisle, G., and M. Allard. 2003. Numerical simulation of the temperature field of a palsa reveals strong influence of convective heat transport by groundwater. *In* Proceedings of the 8th International Conference on Permafrost, 21-25 July 2003. M. Phillips, S.M. Springman, and L.U. Arenson, editors. International Permafrost Association, Zurich, Switzerland. 181-186.
- Delisle, G., M. Allard, R. Fortier, F. Calmels, and E. Larrivee. 2003. Umiujaq, northern Québec: innovative techniques to monitor the decay of a lithalsa in response to climate change. *Permafrost and Periglacial Processes*. 14:375-385.
- Doolittle, J.A., M.A. Hardisky, and S. Black. 1992. A ground-penetrating radar study of Goodream palsas, Newfoundland, Canada. *Arctic and Alpine Research*. 24:173-178.
- Egglesmann, R. 1988. Rewetting for protection and renaturation/regeneration of peatland after or without peat winning. *In* Proceedings of the 8th International Peat Congress. Vol. 3, Leningrad. 251-260.

- Eisner, W.R., K.M. Hinkel, F.E. Nelson, and J.G. Bockheim. 2003. Late-Quaternary paleoenvironmental record from a palsa-scale frost mound in northern Alaska. *In* Proceedings of the 8th International Conference on Permafrost, 21-25 July 2003. M. Phillips, S.M. Springman, and L.U. Arenson, editors. International Permafrost Association, Zurich, Switzerland. 229-234.
- Environment Canada. 1990. Canadian Climate and Weather Information, 1948-1990, Schefferville, Québec, Ottawa, Ontario.
- Forsgren, B. 1968. Studies of palsas in Finland, Norway and Sweden, 1964-1966. *Biuletyn Peryglacjalny*. 17:117-123.
- French, H.M. 2003. The development of periglacial geomorphology: 1- up to 1965. *Permafrost and Periglacial Processes*. 14:29-60.
- Friberg, T., T.R. Christensen, and H. Sogaard. 1997. Rapid response of greenhouse gas emission to early spring thaw in a subarctic mire as shown by micrometeorological techniques. *Geophysical Research Letters*. 24:3061-3064.
- Friedman, J.D., C.E. Johansson, N. Oskarsson, H. Svensson, S. Thorarinsson, and R.S. Williams. 1971. Observations on Icelandic polygon surfaces and palsa areas: photo-interpretation and field studies. *Geografiska Annaler Series A (Physical Geography)*. 53:115-145.
- Fries, T., and E. Bergström. 1910. Några iakttagelser öfver palsar och deras förekomst inordligaste Sverige. *Geologiska Foreningens i Stockholm Forhandlingar*. 32:195-205.
- Fritton, D.D., W.J. Busscher, and J.E. Alpert. 1974. An inexpensive but durable thermal conductivity probe for field use. *In* Soil Science Society of America Proceedings. Vol. 38. 854-855.
- Fuchsman, C.H. 1986. Peat and water: aspects of water retention and dewatering in peat. Elsevier, London. 374 pp.
- Gold, L.W., G.H. Johnston, W.A. Slusarchuk, and L.E. Goodrich. 1972. Thermal effects in permafrost. *In* Proceedings of the Canadian Northern Pipeline Research Conference. National Research Council of Canada, Associate Committee on Geotechnical Research, Ottawa. 25-45.
- Gold, L.W., and A.H. Lachenbruch. 1973. Thermal conditions in permafrost - a review of North American literature. *In* Permafrost, North American Contribution to the Second International Conference, Yakutsk, Siberia. 3-25.
- Gorbunov, A.P. 1969. La region periglaciaire du Tian-Chan. *Biuletyn Peryglacjalny*. 19:151-174.

- Granberg, H.B. 1973. Indirect mapping of snow cover for permafrost prediction at Schefferville, Québec, Canada. *In* Permafrost: The North American Contribution to the Second International Conference. National Academy of Sciences, National Academy of Engineering National Research Council, Washington, D.C., Yakutsk.
- Granberg, H.B. 2004. Personal communication about snow distribution effects in the Schefferville, Québec region, Sherbrooke, Québec.
- Gurney, S.D. 2001. Aspects of the genesis, geomorphology and terminology of palsas: perennial cryogenic mounds. *Progress in Physical Geography*. 25:249-260.
- Harris, S.A. 1982. Identification of permafrost zones using selected permafrost landforms. *In* Proceedings of the Fourth Canadian Permafrost Conference. 49-58.
- Harris, S.A. 1989. Landforms and ground ice as evidence of the source of H₂O in permafrost. *Progress in Physical Geography*. 13:367-390.
- Harris, S.A. 1993. Palsa-like mounds in a mineral substrate, Fox Lake, Yukon Territory. *In* Proceedings 6th International Conference on Permafrost. Vol. 1. Wushan Gvangzhou: South China University Press, Beijing, China. 238-243.
- Harris, S.A., and D. Nyrose. 1992. Palsa formation in floating peat and related vegetation cover as illustrated by a fen bog in the Macmillan Pass, Yukon Territory, Canada. *Geografiska Annaler Series A (Physical Geography)*. 74:349-362.
- Hustich, I. 1957. On the phytogeography of the subarctic Hudson Bay Lowland. *Acta Geographica Fennica*. 16:1-48.
- Jahn, A. 1976. Geomorphologic modeling and nature protection in arctic and subarctic environments. *Geoforum*. 7:121-137.
- Jahn, A. 1976. Pagorki mrozowe typu palsa (Palsa-type frost mounds). *Studia Societatis Scientiarum Torunensis (Geographia et Geologia)*. VIII:123-139.
- Jahn, A., and H.J. Walker. 1983. The active layer and climate. *Zeitschrift fur Geomorphologie*. 47:97-108.
- Jessop, A.M. 1972. Terrestrial heat flow in permafrost. *In* Technical Memorandum 108. NRC Associate Committee on Geotechnical Research. 51-59.
- Judge, A.S. 1972. Ground temperature measurements using thermistors. *In* Technical Memorandum 108. NRC Associate Committee on Geotechnical Research. 13-25.

- Judge, A.S., and A.M. Jessop. 1978. Heat flow north of 60°N. *In Arctic Geophysical Review*. Vol. 45. J.F. Sweeney, editor. Earth Physics Branch of Energy, Mines, and Resources Canada, Ottawa. 25-33.
- Kachurin, S.P. 1959. Cryogenic physico-geological phenomena in permafrost regions. *In Principles of Geocryology: Part I, General Geocryology*. P.F. Švetsov, editor. Academy of Sciences of the USSR, V.A. Obruchev Institute of Permafrost Studies, Moscow. 365-398.
- Kellner, E., J.S. Price, and J.M. Waddington. 2004. Pressure variations in peat as a result of gas bubble dynamics. *Hydrological Processes*. 18:2599-2605.
- Kershaw, G.P. 2003. Permafrost landform degradation over more than half a century, Macmillan/Caribou Pass region, NWT/Yukon, Canada. *In Proceedings of the 8th International Conference on Permafrost*, 21-25 July 2003. M. Phillips, S.M. Springman, and L.U. Arenson, editors. International Permafrost Association, Zurich, Switzerland. 543-548.
- Kershaw, G.P., and D. Gill. 1979. Growth and decay of palsas and peat plateau in the Macmillan Pass-Tsichu River area, Northwest Territories, Canada. *Canadian Journal of Earth Sciences*. 16:1362-1374.
- Krishnan, T.K. 1976. Structural studies of the Schefferville mining district, Québec-Labrador. *In Unpublished Ph.D. Thesis*, Department of Geology. UCLA, Los Angeles.
- Kudryavtsev, V.A. 1959. Temperature, thickness, and discontinuity of permafrost. *In Principles of Geocryology: Part I, General Geocryology*. P.F. Švetsov, editor. Academy of Sciences of the USSR, V.A. Obruchev Institute of Permafrost Studies, Moscow. 219-273.
- Kullman, L. 1989. Geoecological aspects of episodic permafrost expansion in north Sweden. *Geografiska Annaler Series A (Physical Geography)*. 71:255-262.
- Lagarec, D. 1982. Cryogenetic mounds as indicators of permafrost conditions, northern Québec. *In Proceedings of the Fourth Canadian Permafrost Conference*. H.M. French, editor. Associate Committee on Geotechnical Research, National Research Council of Canada, Calgary, AB. 43-48.
- Lagerbäck, R., and L. Rodhe. 1986. Pingos and palsas in northernmost Sweden - preliminary notes on recent investigations. *Geografiska Annaler Series A (Physical Geography)*. 68:149-154.

- Langford, C.H., T. Todoruk, M. Litvina, and A. Kantzas. 2002. Wetting cycles of air dried and "hydrophobic" soils studied by NMR relaxometry - the role of humic substances. *In* 20th Anniversary Conference of the International Humic Substances Society. E.A. Ghabbour and G. Davies, editors. Northeastern University, Boston, Massachusetts. 434-436.
- Lindqvist, S., and J.O. Mattsson. 1965. Studies on the thermal structure of a pals. *Svensk Geografiska Arsbok*. 41:38-49.
- Lu, Y., and J. Pignatello. 2002. Demonstration of the "conditioning effect" in soil organic matter and support for a pore deformation mechanism for sorption hysteresis. *In* 20th Anniversary Conference of the International Humic Substances Society. E.A. Ghabbour and G. Davies, editors. Northeastern University, Boston, Massachusetts. 395-398.
- Lundqvist, G. 1951. En palsmyr sydost om Kebnekaise. *Geologiska Foreningens i Stockholm Forhandlingar*. 73:209-225.
- Lundqvist, G. 1953. Tillag till palsfragan. *Geologiska Foreningens i Stockholm Forhandlingar*. 75:149-154.
- Lundqvist, J. 1961. Patterned ground and related frost phenomena in Sweden. *Sveriges Geologiska Undersokn Arsbok*. Series C:1-101.
- Luoto, M., and M. Seppälä. 2002. Modeling the distribution of palsas in Finnish Lapland with logistic regression and GIS. *Permafrost and Periglacial Processes*. 13:17-28.
- Luoto, M., and M. Seppälä. 2003. Thermokarst ponds as indicators of the former distribution of palsas in Finnish Lapland. *Permafrost and Periglacial Processes*. 14:19-27.
- MacFarlane, I.C. 1959. Muskeg Research: Canadian approach. *In* Technical Paper No. 83. National Research Council of Canada, Division of Building Research, Ottawa. 638-650.
- Makeev, O.W., and A.S. Keržentsev. 1974. Cryogenic processes in the soils of northern Asia. *Geoderma*. 12:101-110.
- Martynov, G.A. 1959. Heat and moisture transfer in freezing and thawing soils. *In* Principles of Geocryology: Part I, General Geocryology. P.F. Švetsov, editor. Academy of Sciences of the USSR, V.A. Obruchev Institute of Permafrost Studies, Moscow. 153-192.
- Matthews, J.A., S.-O. Dahl, M.S. Berrisford, and A. Nesje. 1997. Cyclic development and thermokarst degradation of palsas in the mid-alpine zone at Leirpullan, Dovrefjell, Southern Norway. *Permafrost and Periglacial Processes*. 8:107-122.

- Melloh, R.A., and P.M. Crill. 1996. Winter methane dynamics in a temperate peatland. *Global Biogeochemical Cycles*. 10:247-254.
- Mooney, S.J. 2003. Using micromorphology to understand the rewetting mechanisms in milled peat. *Catena*. 54:665-678.
- Moore, T.R. 1987. Thermal regime of peatlands in subarctic eastern Canada. *Canadian Journal of Earth Sciences*. 24:1352-1359.
- Moore, T.R., N.T. Roulet, and J.M. Waddington. 1998. Uncertainty in predicting the effect of climatic change on the carbon cycling of Canadian peatlands. *Climatic Change*. 40:229-245.
- Neimant-Verdriet, D., and K. Krishnamurty. 1973. 200 SC Photo Mapping, 1965/1971, Plate No. 12-12. J. Dagenais, editor. Iron Ore Company of Canada, Schefferville, Québec.
- Nelson, F.E., K.M. Hinkel, and S.I. Outcalt. 1992. Palsa-scale frost mounds. In *Periglacial Geomorphology: Proceedings of the 22nd Annual Binghamton Symposium on Geomorphology*. J.C. Dixon and A.D. Abrahams, editors. John Wiley & Sons Ltd. 305-325.
- Nicholson, F.H. 1976. Permafrost thermal amelioration tests near Schefferville, Québec. *Canadian Journal of Earth Sciences*. 13:1694-1705.
- Nihlén, T. 2000. Palsas in Härjedalen, Sweden: 1910 and 1998 compared. *Geografiska Annaler Series A (Physical Geography)*. 82:39-44.
- Nykänen, H., J.E.P. Heikkinen, L. Pirinen, K. Tiilikainen, and P.J. Martikainen. 2003. Annual CO₂ exchange and CH₄ fluxes on a subarctic palsa mire during climatically different years. *Global Biogeochemical Cycles*. 17:1018.
- Ours, D.P., D.I. Siegel, and P.H. Glaser. 1997. Chemical dilation and the dual porosity of humified bog peat. *Journal of Hydrology*. 196:348-360.
- Outcalt, S.I., F.E. Nelson, K.M. Hinkel, and G.D. Martin. 1986. Hydrostatic-system palsas at Tooli Lake, Alaska: field observations and simulations. *Earth Surface Processes & Landforms*. 11:79-94.
- P'yavchenko, K.I. 1955. Peat mounds. Izdatel'stvo Akademii Nauk SSSR, Moscow.
- Payette, S., H. Samson, and D. Lagarec. 1976. The evolution of permafrost in the taiga and in the forest-tundra, western Québec-Labrador Peninsula. *Canadian Journal of Forest Research*. 6:203-220.
- Péwé, T.L. 1975. Quaternary geology of Alaska. In US Geological Survey Professional Paper 835, Washington, DC. 145 pp.

- Pissart, A. 2000. Remnants of lithalsas of the Hautes Fagnes, Belgium: a summary of present-day knowledge. *Permafrost and Periglacial Processes*. 11:327-355.
- Pissart, A. 2002. Palsas, lithalsas and remnants of these periglacial mounds: a progress report. *Progress in Physical Geography*. 26:605-621.
- Pissart, A. 2003. The remnants of Younger Dryas lithalsas on the Hautes Fagnes Plateau in Belgium and elsewhere in the world. *Geomorphology*. 52:5-38.
- Pollard, W.H. 1988. Seasonal frost mounds. In *Advances in Periglacial Geomorphology*. M.J. Clark, editor. John Wiley & Sons Ltd, London. 201-229.
- Pollard, W.H. 1991. Seasonal frost mounds. *Canadian Geographer*. 35:208-218.
- Pollard, W.H., and H.M. French. 1983. Seasonal frost mound occurrence, North Fork Pass, Ogilvie Mountains, northern Yukon. In *Fourth International Conference on Permafrost*. National Academy Press, Washington. 1000-1004.
- Pollard, W.H., and H.M. French. 1984. The groundwater hydraulics of seasonal frost mounds, North Fork Pass, Yukon Territory. *Canadian Journal of Earth Sciences*. 21:1073-1081.
- Pollard, W.H., and H.M. French. 1985. The internal structure and ice crystallography of seasonal frost mounds. *Journal of Glaciology*. 31:157-162.
- Pollard, W.H., and R.O. van Everdingen. 1992. Formation of seasonal ice bodies. In *Permafrost Geomorphology, Proceedings of the 22nd Annual Symposium in Geomorphology*. J.C. Dixon and A.D. Abrahams, editors. John Wiley & Sons. 281-304.
- Price, J.S., and S.M. Schlotzhauer. 1999. Importance of shrinkage and compression in determining water storage changes in peat: the case of mined peatland. *Hydrological Processes*. 13:2591-2601.
- Price, J.S., and J.M. Waddington. 2000. Advances in Canadian wetland hydrology and biogeochemistry. *Hydrological Processes*. 14:1579-1589.
- Railton, J.B., and J.H. Sparling. 1973. Preliminary studies on the ecology of palsa mounds in northern Ontario. *Canadian Journal of Botany*. 51:1037-1044.
- Rapp, A., and S. Rudberg. 1960. Recent periglacial phenomena in Sweden. *Biuletyn Peryglacjalny*. 8:143-154.
- Reeve, A.S., D.I. Siegel, and P.H. Glaser. 2000. Simulating vertical flow in large peatlands. *Journal of Hydrology*. 227:207-217.
- Reeves, P. 1972. 200 SC Photo Mapping, 1965/1971, Plate No. 13-12. J. Orth, editor. Iron Ore Company of Canada, Schefferville, Québec.

- Romanov, V.V. 1968. Hydrophysics of bogs. Israel Program for Scientific Translations, Jerusalem. 299 pp.
- Romanowicz, E.A., D.I. Siegel, J.P. Chanton, and P.H. Glaser. 1995. Temporal variations in dissolved methane deep in the Lake Agassiz peatlands, Minnesota. *Global Biogeochemical Cycles*. 9:197-212.
- Romanowicz, E.A., D.I. Siegel, and P.H. Glaser. 1993. Hydraulic reversals and episodic methane emissions during drought cycles in mires. *Geology*. 21:231-234.
- Rönkkö, M., and M. Seppälä. 2003. Surface characteristics affecting active layer formation in palsas, Finnish Lapland. In Proceedings of the 8th International Conference on Permafrost, 21-25 July 2003. M. Phillips, S.M. Springman, and L.U. Arenson, editors. International Permafrost Association, Zurich, Switzerland. 995-1000.
- Salmi, M. 1970. Investigations on palsas in Finnish Lapland. In Ecology of the Subarctic Regions, Proceedings of the Helsinki Symposium, 1966. UNESCO, Paris. 143-153.
- Salmi, M. 1972. Present developmental stages of palsas in Finland. In Proceedings of the Fourth International Peat Conference. Vol. 1, Helsinki. 121-141.
- Salvigsen, O. 1977. An observation of palsa-like forms in Nordaustlandet, Svalbard. *Norsk Polarinstitut Arbok*. 1976:364-367.
- Schaumann, G.E., J. Hurrass, S. Berger, K. Sieg, J. Weber, H. Stoffregen, M. Mueller, and W. Rotard. 2002. Swelling of soil organic matter in humic soil samples: methods and relevance. In 20th Anniversary Conference of the International Humic Substances Society. E.A. Ghabbour and G. Davies, editors. Northeastern University, Boston, Massachusetts. 437-439.
- Seppälä, M. 1972. Peat at the top of Ruohittir Fell, Finnish Lapland. In Annales Universitatis Turkuensis. Vol. Series A. Universitatis Turkuensis, Turku. 6pp.
- Seppälä, M. 1972. The term 'palsa'. *Zeitschrift fur Geomorphologie*. 16:463.
- Seppälä, M. 1976. Seasonal thawing of a palsa at Enontekiö, Finnish Lapland in 1974. *Biuletyn Peryglacjalny*. 26:17-26.
- Seppälä, M. 1980. Stratigraphy of a silt-cored palsa, Atlin Region, British Columbia, Canada. *Arctic*. 33:357-365.
- Seppälä, M. 1982. An experimental study of the formation of palsas. In Fourth Canadian Permafrost Conference. National Research Council Canada. 36-42.

- Seppälä, M. 1986. The origin of palsas. *Geografiska Annaler, Series A (Physical Geography)*. 68:141-147.
- Seppälä, M. 1990. Depth of snow and frost on a palsa mire, Finnish Lapland. *Geografiska Annaler, Series A (Physical Geography)*. 72:191-201.
- Seppälä, M. 1994. Snow depth controls palsa growth. *Permafrost and Periglacial Processes*. 5:283-288.
- Seppälä, M. 2003. An experimental climate change study of the effect of increasing snow cover on active layer formation of a palsa, Finnish Lapland. In *Proceedings of the 8th International Conference on Permafrost, 21-25 July 2003*. M. Phillips, S.M. Springman, and L.U. Arenson, editors. International Permafrost Association, Zurich, Switzerland. 1013-1016.
- Seppälä, M. 2003. Surface abrasion of palsas by wind action in Finnish Lapland. *Geomorphology*. 52:141-148.
- Siegel, D.I., J.P. Chanton, P.H. Glaser, L.S. Chasar, and D.O. Rosenberry. 2001. Estimating methane production rates in bogs and landfills by deuterium enrichment of pore water. *Global Biogeochemical Cycles*. 15:967-975.
- Sjörs, H. 1961. Forest and peatlands at Hawley Lake, northern Ontario. *National Museum of Canada Bulletin*. 171:1-31.
- Sollid, J.L., and L. Sørbel. 1974. Palsa bogs at Haugtjørn, Dovrefjell, South Norway. *Norsk Geografisk Tidsskrift*. 28:53-60.
- Sollid, J.L., and L. Sørbel. 1998. Palsa bogs as climatic indicators - examples from Dovrefjell, southern Norway. *Ambio*. 27:287-291.
- Solov'ev, P.A. 1973. Thermokarst phenomena and landforms due to frost heaving in central Yakutia. *Biuletyn Peryglacjalny*. 23:135-155.
- Špolanskaya, N.A., and V.P. Evseyev. 1973. Domed-hummocky peatbogs of the northern taiga in western Siberia. *Biuletyn Peryglacjalny*. 22:271-283.
- Strahler, A.N. 1954. Statistical analysis in geomorphic research. *Journal of Geology*. 62:1-25.
- Svensson, H. 1964. Structural observations in the minerogenic core of a palsa. *Svensk Geografiska Arsbok*. 40:137-142.
- Svensson, H. 1969. A type of circular lake in northernmost Norway. *Geografiska Annaler Series A (Physical Geography)*. 51:1-12.
- Svensson, H. 1970. Frozen-ground morphology of northeasternmost Norway. In *Ecology of the Subarctic Regions, Proceedings of the Helsinki Symposium*. UNESCO, Helsinki. 161-168.
- Svensson, H. 1986. Permafrost: Some morphoclimatic aspects of periglacial features of northern Scandinavia. *Geografiska Annaler Series A (Physical Geography)*. 68:123-130.

- Švetsov, P.F. 1959. General mechanisms of the formation and development of permafrost. *In Principles of Geocryology, Part I: General Geocryology.* P.F. Švetsov, editor. Academy of Sciences of the USSR, V.A. Obruchev Institute of Permafrost Studies, Moscow. 77-107.
- Taber, S. 1929. Frost heaving. *Journal of Geology.* 37:428-461.
- Taber, S. 1930. The mechanics of frost heaving. *Journal of Geology.* 38:303-317.
- Takahashi, N., and T. Sone. 1988. Palsas in the Daisetsuzan Mountains, central Hokkaido, Japan. *Geographical Review of Japan.* 61 (Series A):665-684.
- Thorarinsson, S. 1951. Notes on patterned ground in Iceland with particular reference to the Icelandic "flas". *Geografiska Annaler.* 33:144-156.
- Thorhallsdottir, T.E. 1994. Effects of changes in groundwater level on palsas in central Iceland. *Geografiska Annaler, Series A (Physical Geography).* 76:161-167.
- Tsyтович, N.A. 1963. Phase transformations of water in soils and the nature of migration and heaving. *In Proceedings of the International Conference on Permafrost, Lafayette, IN.* 234-239.
- Tyrtikov, A.P. 1959. Perennially frozen ground and vegetation. *In Principles of Geocryology: Part I, General Geocryology.* P.F. Švetsov, editor. Academy of Sciences of the USSR, V.A. Obruchev Institute of Permafrost Studies, Moscow. 399-421.
- V.A. Obruchev Institute of Permafrost Studies. 1961. Part I: Geocryological Surveys. *In Permafrost Investigations in the Field.* Academy of Sciences of the USSR, Moscow. 189-201.
- van Everdingen, R.O. 1978. Frost mounds Bear Rock near Fort Norman, Northwest Territories, 1975-1976. *Canadian Journal of Earth Sciences.* 15:263-276.
- van Everdingen, R.O. 1982. Frost blisters of the Bear Rock Spring area near Fort Norman, NWT. *Arctic.* 35:243-265.
- Washburn, A.L. 1979. Permafrost features as evidence of climatic change. *Earth-Science Reviews.* 15:327-402.
- Washburn, A.L. 1983. Palsas and continuous permafrost. *In Proceedings of the Fourth International Conference on Permafrost, Fairbanks, AK.*
- Washburn, A.L. 1983. What is a palsa? *In Mesoformen des Reliefs im heutigen Periglazialraum (Geomorphologisches Symposium).* Vol. 35. H. Poser and E. Schunke, editors. Akademie der Wissenschaften, Mathematisch-Physikalische Klasse Dritte Folge, Gottingen. 34-47.

- Wenner, C.-G. 1947. Pollen diagrams from Labrador. *Geografiska Annaler*. 29:137-374.
- Westin, B., and F.S. Zuidhoff. 2001. Ground thermal conditions in a frost-crack polygon, a palsa and a mineral palsa (lithalsa) in the discontinuous permafrost zone, northern Sweden. *Permafrost and Periglacial Processes*. 12:325-335.
- Wetzel, H., H. Fleige, and R. Horn. 2003. Chemical and physical properties of palsas - degradation of palsas in the region of northern Norway. In *Proceedings of the 8th International Conference on Permafrost*, 21-25 July 2003. M. Phillips, S.M. Springman, and L.U. Arenson, editors. International Permafrost Association, Zurich, Switzerland. 1235-1240.
- White, S.E., G.M. Clark, and A. Rapp. 1969. Palsa localities in Padjelanta National Park, Swedish Lapland. *Geografiska Annaler Series A (Physical Geography)*. 51:97-103.
- Williams, G.P. 1968. The thermal regime of a sphagnum peat bog. In *Third International Peat Congress*. National Research Council of Canada, Québec, Canada. 195-200.
- Wramner, P. 1965. Fynd av palsar med mineraljordkarna i Sverige. *Geologiska Foreningens i Stockholm Forhandlingar*. 86:498-499.
- Wramner, P. 1973. Palsa bogs in Taavavuoma, Swedish Lapland (in Swedish). In *Goteborgs Universitet Naturgeografiska Institutionen, GUNI Rapport 3*. 140 pp.
- Zajac, I.S. 1974. The stratigraphy and mineralogy of the Sokoman Iron Formation in the Knob Lake area, Québec and Newfoundland. In *Geological Survey of Canada, Bulletin 220*. 159 pp.
- Zoltai, S.C. 1971. Southern limit of permafrost features in peat landforms, Manitoba and Saskatchewan. In *Geological Association of Canada Special Paper No. 9*. 305-310.
- Zoltai, S.C. 1972. Palsas and peat plateaus in central Manitoba and Saskatchewan. *Canadian Journal of Forest Research*. 2:291-302.
- Zoltai, S.C. 1993. Cyclic development of permafrost in the peatlands of northwestern Alberta, Canada. *Arctic and Alpine Research*. 25:240-246.
- Zoltai, S.C., and C. Tarnocai. 1971. Properties of a wooded palsa in northern Manitoba. *Arctic and Alpine Research*. 3:115-129.
- Zoltai, S.C., and C. Tarnocai. 1975. Perennial frozen peatlands in the western Arctic and Subarctic of Canada. *Canadian Journal of Earth Sciences*. 12:28-43.

- Zuidhoff, F.S. 2002. Recent decay of a single palsa in relation to weather conditions between 1996 and 2000 in Laivadalen, northern Sweden. *Geografiska Annaler, Series A (Physical Geography)*. 84A:103-111.
- Zuidhoff, F.S. 2003. Physical properties of the surface peat layer and the influence on thermal conditions during the development of palsas. *In* Proceedings of the 8th International Conference on Permafrost, 21-25 July 2003. M. Phillips, S.M. Springman, and L.U. Arenson, editors. International Permafrost Association, Zurich, Switzerland. 1313-1317.
- Zuidhoff, F.S., and E. Kolstrup. 2000. Changes in palsa distribution in relation to climate change in Laivadalen, northern Sweden, especially 1960-1997. *Permafrost and Periglacial Processes*. 11:55-69.

